Title
The role of aromatase in sexually dimorphic behaviors

Author
Unger, Elizabeth Kaye

Publication Date
2015

The role of aromatase in sexually dimorphic behaviors

by

Elizabeth K. Unger

DISSERTATION

Submitted in partial satisfaction of the requirements for the degree of

DOCTOR OF PHILOSOPHY

in

Biomedical Sciences

in the

GRADUATE DIVISION

of the

UNIVERSITY OF CALIFORNIA, SAN FRANCISCO

DEDICATION AND ACKNOWLEDGEMENTS

I want to thank all those who helped me through this gruelling but rewarding process, and especially Allison Doupe who served as the chair of my committee before her tragic passing. She provided me with valuable insight and guidance, as I know she did for many others like me, and served as a role model and source of inspiration.

ABSTRACT

All sexually reproducing animals display sex differences in social behaviors. These dimorphic behaviors are a consequence of molecular, cellular and circuit-level sex differences in the brain. In mice, these differences arise as a result of masculinization (or not) during the perinatal critical period. My lab has shown explicitly that perinatal exposure to estrogen is the key to masculinization of the brain. A male-specific surge of testosterone is then converted to estrogen by the enzyme aromatase, which is expressed locally in the brain. Estrogen then initiates a cascade of events that permanently alter the brain and prime it for male-typical behaviors. Females, in contrast, have no perinatal sex hormone surge. Estrogen, however, also acts in the adult brain, in both males and females, though its actions have not yet been delineated. My thesis addresses both the developmental and adult roles for estrogen and aromatase, as well as the neurons within the brain that express aromatase. I first examine the role of aromatase in the process of feminization of the brain. I find that absence of aromatase is both necessary and sufficient to produce a feminized brain and that feminization does appear to be the default state of the brain. I then examine the role of estrogen in adulthood and show that loss of aromatase function in males has no behavioral consequences for any of the behaviors I assayed. Because aromatase appears to be playing a minimal role in adulthood, its continued expression within the adult brain remains a mystery. I next explored the role of the neurons expressing aromatase, specifically within the medial amygdala (MeA), because the MeA has been shown to be important for sex-specific behaviors. Using an aromatase-Cre mouse, I show that ablation or inactivation of aromatase-expressing neurons in the MeA results in a mild deficit in aggression, but has no effect on mating behavior. All together, my findings show that presence or absence of aromatase dictates masculinization or feminization of the brain, and in adulthood, marks neurons within the brain that are necessary for sex-specific behaviors.

TABLE OF CONTENTS

LIST OF FIGURES

LIST OF TABLES

Chapter 1

Introduction

All sexually reproducing animals display sexually dimorphic behaviors. These behaviors are innate and require no training or experience in order to be displayed, thus these behaviors must be hardwired into the brain. However, behavior programs are vastly different between males and females; for example males mark and defend their territory and seek out and attempt to mate with females, while females produce offspring and mammalian females even nurse and act as the primary caregivers for their young.

It has long been known, and my lab has shown explicitly, that perinatal estrogen is the key to masculinization of the brain. This process occurs specifically in males because the gene Sry on the y chromosome triggers the development of testes and these testes produce a perinatal surge of testosterone. This testosterone is converted to estrogen by aromatase expressed locally in the brain. Estrogen then initiates a series of events including region-specific cell survival and long term chromatin modifications that permanently alter the function of the brain and gene expression patterns. Females, in contrast, have no perinatal hormone surge as their ovaries are quiescent until puberty.

Because estrogen appears to be the key player in this process, and aromatase is the enzyme that catalyzes the final step in its synthesis pathway, this means that aromatase expression is likely to be extremely important for sexually dimorphic behaviors. Indeed aromatase null animals have already been shown to have altered behavior patterns. In this thesis I will explore the role of aromatase in sex-specific behaviors.

I first explore the process of feminization in the brain in chapter 2. In order to determine the default state of the brain I genetically eliminate both aromatase and androgen receptor to remove all estrogen and testosterone signaling. In this way I hoped to produce an animal whose brain is in the default state, and then compare its behaviors and gene expression to those of a female in order to identify elements of feminization. What I find

is that the hormoneless brain is indistinguishable from the female brain in both female-specific behaviors and also female-typical gene expression patterns. Furthermore, I find that absence of estrogen--and not testosterone--signaling is necessary and sufficient to produce a feminized brain, further underlining the importance of aromatase.

It is now quite clear that estrogen is responsible for developmental masculinization of the brain, however its role in adult behaviors has not yet been explored. In chapter 3 I address this question. To do so my lab generated a mouse line wherein I can disrupt the function of the aromatase gene in any cell type, at any time. These studies are ongoing, but preliminary findings suggest that aromatase, while highly significant during development, is no longer necessary in the adult male brain.

However, aromatase continues to be expressed in defined populations throughout the brain. Presumably its function is still necessary in some capacity to justify its continued expression. However, in chapter 3 I show that disruption of the gene itself does not alter behavior. So this raises the question of whether or not the neurons marked by the expression of aromatase are functional in sexually dimorphic behaviors. In chapters 4 and 5 I present published work first describing a new tool developed, and then its application for elucidating the function of aromatase expressing neurons in a brain region important for sex-specific behaviors, the medial amygdala (MeA). I find that aromatase positive neurons in the MeA are indeed necessary, but only for a small subset of behaviors, primarily the initiation and intensity of aggression behavior in both males and females. This is particularly interesting because expression of aromatase in the female brain seems unnecessary at best, given that the ovaries produce much of the body's estrogen and there is very little circulating testosterone in females. Nonetheless, aromatase expression marks neurons in the MeA that are necessary for maternal aggression.

Given that maternal aggression and intermale aggression are executed in a very different manner, yet the contribution of the MeA to these two behaviors appears to be similar, I next wanted to explore the circuit downstream of the MeA. Again, these studies are ongoing, but I find that there are two main outputs of the MeA originating from anatomically distinct subregions within the MeA, and I speculate on the possible functions of these two outputs.

Overall, I find that aromatase is essential during development for creating a masculinized brain capable of producing male-typical behaviors, while in adulthood aromatase function is less important and it seems to mark neurons necessary for sex-specific behaviors.

Chapter 2

Loss of aromatase is necessary and sufficient for female-like behavior and gene expression in the brain

Elizabeth K. Unger, Melody V Wu, Nirao M. Shah

ABSTRACT

All sexually reproducing animals display sex differences in social behaviors. These dimorphic behaviors are a consequence of molecular, cellular and circuit-level sex differences in the brain. In mice, these differences arise as a result of masculinization (or not) during the perinatal critical period. My lab has shown explicitly that perinatal exposure to estrogen is the key to masculinization of the brain. During the perinatal period male-specific surge of testosterone is converted to estrogen by the enzyme aromatase, which is expressed locally within the brain. Estrogen then initiates a cascade of events that permanently alter the brain and prime it for male-typical behaviors. Females, in contrast, have no perinatal sex hormone surge, and thus lack this estrogen-mediated masculinization. However this does not indicate whether there is a similar process of feminization and what factor may mediate that. I find that in the absence of estrogen and testosterone signaling, the brain develops into something capable of producing female-specific behaviors and gene expression. Thus presence or absence of estrogen dictates the masculinization or feminization of the brain respectively. In the absence of sex hormones, the default state of the brain is female.

INTRODUCTION

It has long been known that estrogen plays an essential role in the masculinization of the brain. The presence of a functional aromatase (or exogenous estrogen administration) is required during the critical period for masculinization (Breedlove and Arnold, 1985; Beatty, 1979; Beyer, 1999; Simerly, 2002; Wu et al. 2009). This will be discussed further in chapter 3. This masculinization is necessary for the display of male-typical social behaviors. However females also display a repertoire of behaviors that are unique to them. For example, lordosis (assuming a receptive sexual position to allow intromission by a male) is specific to females and never seen in males (Powers, 1970; Young, 1941). I therefore posed the question of whether there is an equal process of feminization that is

necessary in order to elicit these female-typical behaviors.

Females are not sexually receptive all the time. It is only while they are in estrus that they allow males to mate with them. Female mice ovulate once every 4-5 days, and are receptive only during the following 8-12h period (Edwards, 1970; Ring, 1944; Whalen, 1974). At all other times they will reject male sexual advances by running away, sitting down to prevent access to the genitalia, struggling, or kicking the male in the face (Yang et al., 2013). During their receptive period they will stay still, arch their back and lift their tail to allow the male to intromit (lordosis, Yang et al., 2013).

Because females are only receptive during the brief period surrounding ovulation, and this is entirely controlled dynamically by hormones, but it also requires a non-masculinized brain. Males can be castrated and given female levels of hormones, but will never show this behavior (Lustig et al., 1989). This raises the question of whether is it necessary to have a feminized brain, ready to perform this behavior, waiting for the right combination of hormones, or just simply a non-masculinized brain. How would the brain develop in the absence of hormones, and could female-typical behaviors be elicited from this animal? In this study I have genetically eliminated estrogen and testosterone signaling during development in order to reduce the brain to its asexual default state. In fact, I find that loss of aromatase is sufficient to demasculinize the brain, and that this process of demasculinization is equivalent to feminization. Essentially the default state of the brain is female.

RESULTS

Female-typical sexual behavior

In order to create an animal lacking or unresponsive to hormones, I crossed the androgen receptor (AR) null mouse (ARKO, Goldstein and Wilson, 1972) to the aromatase null mouse

(aroKO, Honda, 1998). This mouse produces testosterone but is unable to respond to it, and cannot convert that testosterone to estrogen, thereby eliminating all testosterone and estrogen signaling. Because estrogen is necessary to elicit female receptive behaviors (Bakker et al., 2002; Parsons et al., 1984), the aroKO mouse has the added benefit over the ERα null mouse in that in this mouse all estrogen signaling is intact, through all the various estrogen receptors (ERα, ERβ, GPR30), but endogenous estrogen is absent and can be provided exogenously just before behavior testing. Mice lacking AR signaling develop feminized secondary sex characteristics (Ono et al., 1974), however because estrogen masculinizes the brain, the prediction is that AR single mutant mice will have a masculinized brain and will not display feminized behaviors. Conversely the aroKO mouse, which develops a masculinized body, should develop a demasculinized brain because it lacks the perinatal estrogen necessary for masculinization. The test is whether AR-Aro double mutant mice, which do not display any male-typical behaviors (see chapter 3), will display any female-typical behaviors, or simply no dimorphic behaviors at all. If they do show female-typical behaviors this indicates that the default state of the brain is indeed the same as a feminized brain and there is no additional process of feminization.

It should also be noted that in Chapter 3 I will show that aroKO mice rarely attack males, but in fact when they do, it is usually in response to being investigated or mounted by the intruder male. Females who are not in estrus will sometimes reject male mating attempts by physically pushing the male away or twisting around attack the front of the male (Heinrichs et al., 1997; Yang et al., 2013). It is possible that the few attacks I see in those assays are actually rejection of mating attempts rather than an aberrant form of intermale aggression. AroKO mice are known to have extremely high testosterone levels (Toda et al., 2012), which may be contributing to their aggressive behaviors.

The mice tested for male behaviors in chapter 3 have intact gonads. Thus in order to test female behaviors in these mice I removed their gonads and treated them with estrogen

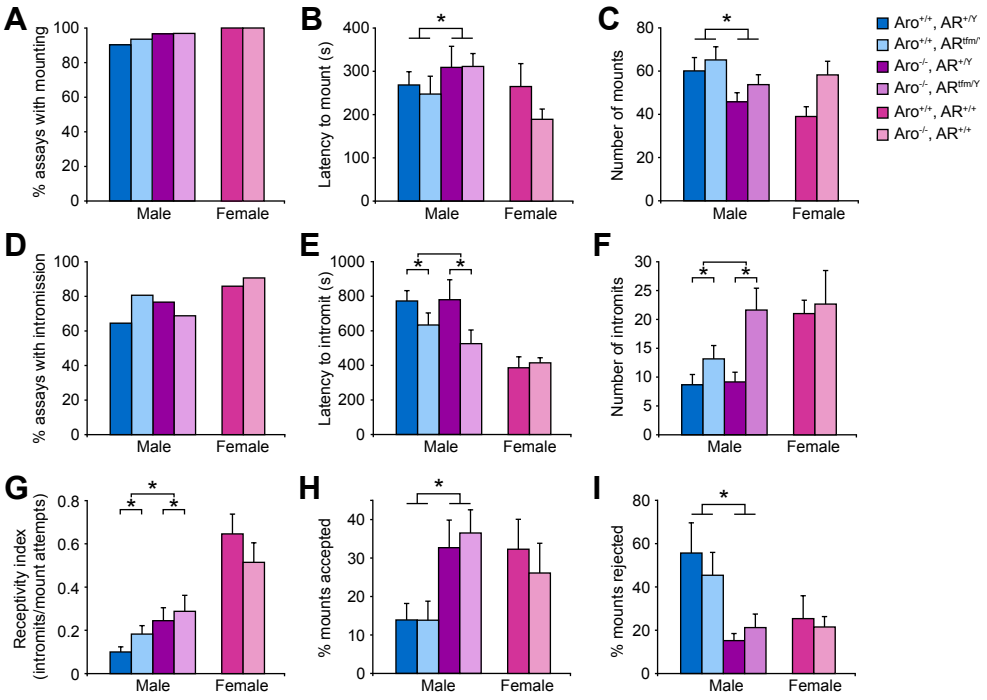

Figure 2.1: Loss of aromatase in males leads to female-like sexual behavior.

Group housed male mice either wildtype or null for either AR, aromatase or both, and group housed female mice either wildtype or null for aromatase were gonadectomized and given >1 week to recover. They were then primed with estrogen and progesterone before placing them in the home cage of a sexually experienced (stud) male for 30 mins. All studs attempted mounts in all assays. n > 10. Error bars represent SEM. * $p < 0.05$ by 2-way ANOVA (aromatase vs. AR - males only). Graphs in B, C, I and J showed a significant effect of aromatase loss. Graphs in E and F showed a significant effect of AR loss. H showed significant effects of both aromatase and AR, but no interaction between the two.

and progesterone at doses that elicit sexual receptivity in ovariectomized wildtype females (Edwards, 1970; Ring, 1944; Whalen, 1974). I then introduced them into the cage of a sexually experienced male mouse (stud) for 30 minutes. In fact, I am able to elicit similar levels of sexual receptivity in aroKO and ARKO/aroKO mice, suggesting that absence of estrogen is all that is necessary for a feminized brain (Figure 2.1). I do not see receptivity in AR single KO mice, suggesting that loss of AR does not produce a feminized brain, despite having feminized secondary sex characteristics. This is consistant with the current understanding of how the brain is masculinized.

For statistical purposes, I analyzed this data using a 2-way ANOVA, so that I could measure the effect of each of the genetic mutations separately. I see an effect of aromatase on mounting behavior (Figure 2.1B,C), and an effect of AR on intromission behavior (Figure 2.1E,F). Not surprisingly these effects are additive when combining the two behaviors to obtain the receptivity index (the number of mount attempts that the mountee allows to proceed to intromission, Figure 2.1G). However, as mentioned previously, ARKO mice have feminized secondary sex characteristics, whereas aroKO mice have masculinized secondary sex charateristics. Thus there may be simple physical limitations to intromission that are not actually dependent on the masculinization or feminization of the brain. Indeed I observe that the stud males have difficulty intromitting in these assays as compared to when they are presented with wildtype female intruders. Also of note, the stud males have more difficulty intromitting the ARKO mice as compared to wildtype females. Presumably this is due to the fact that while the ARKO mice have a vaginal canal, it is both shorter and narrower than that of a wildtype female (Drews, 2007). Nonetheless, stud males are able to intromit and ejaculate with ARKO and aroKO mice, and even castrated wildtype males.

Because of these physical limitations, and the fact that a sexually experienced male can achieve intromission even when the experimental animal is not showing signs of receptivity, the most relevant parameters to analyze are the behavioral responses to being mounted (mounts accepted vs. mounts rejected, Figure 2.1H,I). A mount is considered to be accepted if the animal stayed still and did not struggle, while a mount is considered to be rejected if the animal struggled, sat down or ran away. Some mounts showed a mix of both receptive and unreceptive behavior, and thus did not fall into either category. Using these parameters, it is clear that the lack of aromatase is sufficient to elicit female-like sexual receptivity.

For comparison I also performed these assays on wildtype and aroKO females (Figure 2.1). It was not possible to generate ARKO females because AR is located on the X

chromosome and ARKO males are infertile for the reasons discussed earlier–both physical and behavioral.

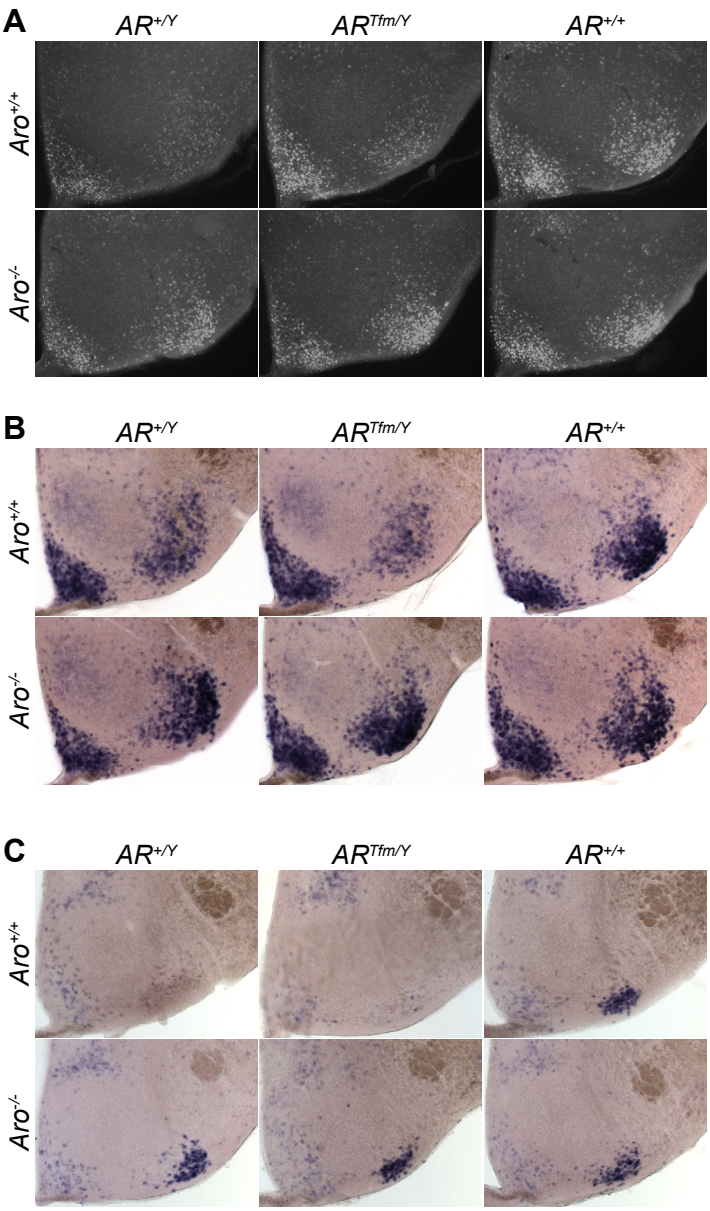

Figure 2.2 Loss of aromatase leads to female-like gene expression patterns in the VMH

Male and female mice either wildtype or lacking aromatase or AR or both were gonadectomized and given >4 weeks to recover and for hormone levels to subside. They were then primed with estrogen and progesterone before perfusing them and staining for ERα (A), PR mRNA (B) and Cckar mRNA (C).

I find that there is no additional enhancement or deficit in sexual receptivity for females lacking aromatase (Figure 2.1) despite the fact that aroKO females are infertile. This infertility is likely due to impaired ovary function rather than insufficient mating behavior.

Gene expression

I next wanted to analyze the brains of these mice for markers of masculinization and feminization. The ventromedial hypothalamus (VMH) is a sexually dimorphic region that has been shown by my lab and others to play a role in sexual receptivity (Kendrick et al., 1995; Leedy and Hart, 1985; Mathews and Edwards, 1977; Robarts and Baum, 2007; Yang et al., 2013). Our lab has also shown that there are several genes that are expressed in this region that are highly sexually

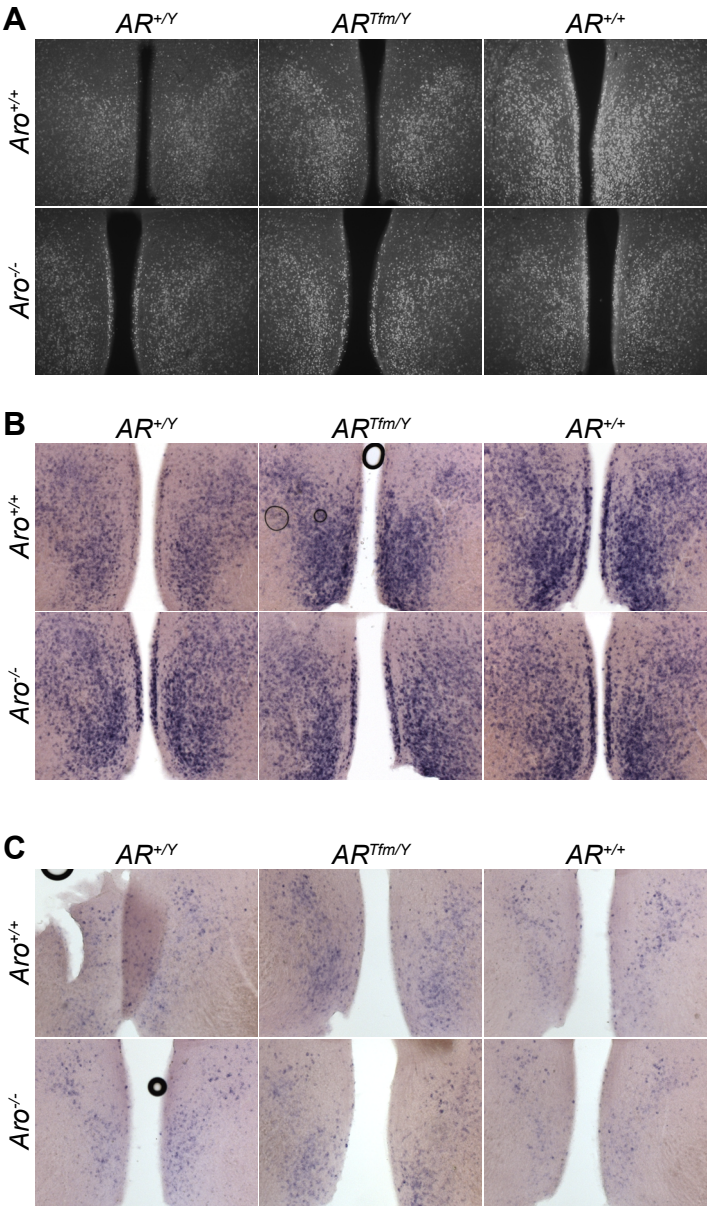

Figure 2.3 Loss of aromatase leads to female-like gene expression patterns in the POA/AVPV

Male and female mice either wildtype or lacking aromatase or AR or both were gonadectomized and given >4 weeks to recover and for hormone levels to subside. They were then primed with estrogen and progesterone before perfusing them and staining for ERα (A), PR mRNA (B) and Cckar mRNA (C).

dimorphic and directly linked to sexual receptivity in females: *Esr1* (ERα), *Pr* (progesterone receptor), and *Cckar* (Cholecystokinin receptor a) (Xu et al. 2012, Yang et al. 2013). I therefore compared the expression of these genes in the VMH of gonadectomized and hormone primed control and mutant males and females.

Indeed I find that gene expression patterns are consistent with sexual receptivity: aroKO and ARKO/aroKO males show similar patterns as wildtype females and ARKO males show similar patterns as wildtype males (Figure 2.2). Interestingly, just as with mounting response, there is no gross alteration in gene expression for females lacking aromatase as compared to wildtype females.

The pre-optic area (POA) and the anteroventral periventricular nucleus (AVPV) have also been shown to play a role in reproductive behaviors, particularly ovulation (Nance et al., 1977; Ohkura et al., 2009; Radovick et al., 2012; Simerly and

Swanson, 1987; Vida et al. 2010). Females show a prominent AVPV stripe that is heavily innervated by PR expressing neurons in the VMH (Yang et al., 2013), that is not present in males. However, it is possible that because my mutant males do not ovulate, the POA/ AVPV will show altered gene expression. In fact I find that the expression of ERα, *Pr* and *Cckar* is consistent with VMH expression and behavioral responses, with aroKO and ARKO/aroKO males showing similar patterns as wildtype females and ARKO mice showing a similar pattern as wildtype males, and no obvious deficits in aroKO females (Figure 2.3).

Another brain region associated with sexually dimorphic behaviors is the bed nucleus of the stria terminalis (BNST). There is some speculation that the size and shape of the BNST is correlated with gender identity in humans (Arai, 2004; Zhou et al., 1995). Those who identify as male tend to have a larger, wider BNST, while those who identify as female have a smaller, narrower BNST (Zhou et al., 1995). If this is true, and can be extended to mice, the shape, size and gene expression patterns of the BNST should serve as a surrogate for the gender identity of the mouse. I therefore assessed the shape expression of ERα, *Pr* and *Cckar* in the BNST (Figure 2.4). Indeed I find that the patterns of expression in the BNST matches that of the VMH and POA, as well

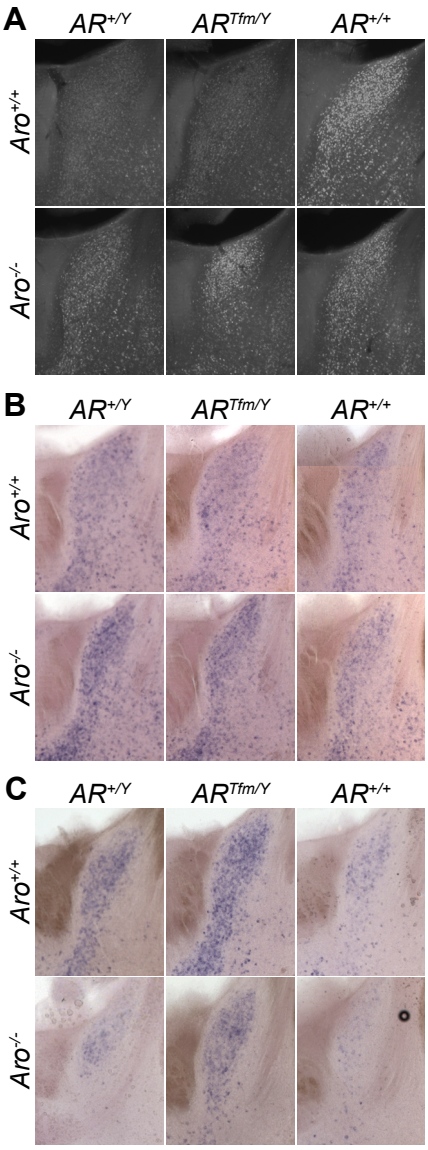

Figure 2.4 Loss of aromatase leads to female-like gene expression patterns in the BNST

Male and female mice either wildtype or lacking aromatase or AR or both were gonadectomized and given >4 weeks to recover and for hormone levels to subside. They were then primed with estrogen and progesterone before perfusing them and staining for ERα (A), PR mRNA (B) and Cckar mRNA (C).

as the behavioral response. In addition the mice who showed receptive behaviors have a smaller narrower BNST, and those who showed rejection behavior have a larger wider BNST, consistent with the human data (Figure 2.4, most apparent in B).

Interestingly I see a pronounced increase in *Pr* expression in mice lacking aromatase. One possible explanation is that they have never seen estrogen in their lifetime and so have compensated and are now more sensitive to it. Estrogen can induce expression of *Pr* (Guerra-Araiza et al., 2009; MacLusky and McEwen, 1978), therefore when I inject estrogen, they would have a greater increase in *Pr* expression. I also see an increase in *Cckar* expression in mice lacking AR as compared to their genetic controls, as well as a decrease in mice lacking aromatase. This suggests that *Cckar* expression is suppressed by testosterone and weakly induced by estrogen. I see this type of expression regulation in the POA as well, which is not surprising as the two regions are close together and highly interconnected. However, I do not see these patterns in the VMH suggesting that this regulation is region-specific. This is consistent with previous work from the lab (Xu et al. 2012). Likewise I do not see differences in expression of *Cckar* in the PVN, a region not known to be sexually dimorphic (data not shown). Similar results as those seen in the BNST were observed in the medial amygdala (data not shown).

DISCUSSION

The brains of aroKO and ARKO/aroKO mice appear to be feminized. In addition, these mice perform behaviors that can only be elicited by females. Not only are they demasculinized, but they are also definitely feminized, suggesting that the two are the same. There is no hormonal requirement for developing a feminized brain primed for female-specific behaviors, although acute hormone regulation is necessary to produce female-specific behaviors.

However, it should also be noted that these mice do not behave entirely female. As

will be presented in chapter 3, aroKO mice will attack female intruders in about ⅓ of assays. This is a behavior never seen in males or females and so aroKO mice cannot be considered truly feminized. This behavior, however, is not seen in ARKO/aroKO mice despite the fact that they are occasionally mounted by the female intruders, suggesting that this propensity to attack females arises from the presence of AR. The ARKO/aroKO mice display no male-specific behaviors, no aberrant social behaviors and are receptive to male mating attempts, and thus could be considered to be effectively feminized. Nonetheless, absence of aromatase (and not AR) is necessary and sufficient to eliminate male-specific behaviors and elicit female-specific behaviors, as well as female-specific gene expression in the brain.

The fact that in the absence of estrogen and testosterone the brain develops into something resembling a female brain is surprising because that also means there is no additional hormonal requirement during puberty. This is in contrast to previous reports showing that pubertal hormones are necessary for feminization (Bakker et al., 2002; Brock et al., 2010; Brock et al., 2011). The female's ovaries are quiescent during development, so it is not surprising that lack of hormones during this period will produce a demasculinized brain. However, during puberty the ovaries begin producing estrogen causing multiple changes in gene expression throughout the brain. It is surprising that simply giving hormone supplements (not during puberty) is sufficient to elicit female-specific reproductive behaviors.

METHODS

Animals

Adult mice 10–24 weeks of age were used in all studies. Mice were housed in a UCSF barrier facility with a 12:12 hr light:dark cycle, and food and water were available *ad libitum*. Experimental mice and their genetic control siblings were used for behavioral studies and

histology. Animals were group-housed by (genetic) sex after weaning at 3 weeks of age. All studies with animals were done in accordance with UCSF IACUC protocols.

Behavior

All behavioral testing was initiated ≥ 1 hr after onset of the dark cycle, and recorded and analyzed as described previously (Juntti et al., 2010; Wu et al., 2009; Xu et al., 2012; Yang et al. 2013). There were always ≥ 7 days between behavioral tests to allow hormone levels to subside to baseline levels prior to estrus induction for the next assay, and experimental animals were always exposed to a novel stud male. All tests were scored by an experimenter blind to the genotype of the mice, using a software package we developed in MATLAB (Wu et al., 2009). Following behavior testing, some animals were perfused for histological analysis.

Mice were group housed throughout behavioral testing. Mice were gonadectomized and allowed >2 weeks to recover, then primed with estrogen and progesterone prior to receptivity assays as previously described (Yang et al. 2013) and placed with a sexually experienced singly housed male for 30 min. Mice were tested 3 times for receptivity.

Histology

Animals were perfused with 4% PFA as previously described (Wu et al., 2009, Juntti et al., 2010, Yang et al., 2013) and sectioned at 65 μm (immunofluorescence) or 100 μm (*in situ* hybridization, ISH) using a vibrating microtome (Leica).

Immunolabeling was performed using previously published protocols (Shah et al., 2004; Wu et al., 2009). The primary antiserum used was: rabbit anti-ERα (Millipore, 1:6,000). The fluorophore conjugated secondary antiserum was: Cy3 donkey anti-rabbit, (Jackson ImmunoResearch, 1:800). Sections were imaged using an upright epifluorescent

microscope (Zeiss).

Pr and Cckar probes for ISH were generated from subcloned RT-PCR products. The ISH was performed as described previously (Xu et al., 2012). Briefly, mice were perfused with 4% paraformaldehyde (PFA), and the brains were dissected, post-fixed, and sectioned at 100 μm with a vibrating microtome (Leica). Sections were treated with proteinase K (10 μg/mL, Roche) and fixed at room temperature. Sections were then acetylated and equilibrated to hybridization solution for 2-5 hr at 65°C, followed by incubation at 65°C overnight in hybridization buffer containing 0.5 μg/mL digoxygenin-labeled RNA probe. The sections were then washed in high stringency buffers and incubated overnight at 4°C in buffer containing alkaline phosphatase-conjugated sheep anti-digoxygenin antibody (Roche, 1:2000). The sections were then incubated for 4-6 hr at 37°C in staining solution containing nitro blue tetrazolium and 5-bromo-4-chloro-3-indolyl-phosphate (NBT and BCIP, respectively; Roche). Finally, sections were washed, post-fixed, and mounted on glass slides as described previously (Xu *et al.*, 2012).

REFERENCES

Arai, Y. (2004). [Sex differentiation of central nervous system--brain of man and woman]. Nippon Rinsho 62, 281–292.

Bakker, J., Honda, S.-I., Harada, N., and Balthazart, J. (2002). The Aromatase Knock-Out Mouse Provides New Evidence That Estradiol Is Required during Development in the Female for the Expression of Sociosexual Behaviors in Adulthood. J. Neurosci. 22, 9104–9112.

Beatty, W.W. (1979). Gonadal hormones and sex differences in nonreproductive behaviors in rodents: Organizational and activational influences. Hormones and Behavior 12, 112–163.

Beyer, C. (1999). Estrogen and the developing mammalian brain. Anat Embryol 199, 379–390.

Breedlove, S.M., and Arnold, A.P. (1980). Hormone accumulation in a sexually dimorphic motor nucleus of the rat spinal cord. Science 210, 564–566.

Brock, O., Douhard, Q., Baum, M.J., and Bakker, J. (2010). Reduced prepubertal expression of progesterone receptor in the hypothalamus of female aromatase knockout mice. Endocrinology 151, 1814–1821.

Brock, O., Baum, M.J., and Bakker, J. (2011). THE DEVELOPMENT OF FEMALE SEXUAL BEHAVIOR REQUIRES PREPUBERTAL ESTRADIOL. J Neurosci 31, 5574–5578.

Drews, U. (2007). Helper function of the Wolffian ducts and role of androgens in the development of the vagina. Sex Dev 1, 100–110.

Edwards, D.A. (1970). Induction of estrus in female mice: Estrogen-progesterone interactions. Hormones and Behavior 1, 299–304.

Goldstein, J.L., and Wilson, J.D. (1972). Studies on the pathogenesis of the pseudohermaphroditism in the mouse with testicular feminization. J. Clin. Invest. 51, 1647–1658.

Guerra-Araiza, C., Gómora-Arrati, P., García-Juárez, M., Armengual-Villegas, A., Miranda-Martínez, A., Lima-Hernández, F.J., Camacho-Arroyo, I., and González-Flores, O. (2009). Role of progesterone receptor isoforms in female sexual behavior induced by progestins in rats. Neuroendocrinology 90, 73–81.

Heinrichs, S.C., Min, H., Tamraz, S., Carmouché, M., Boehme, S.A., and Vale, W.W. (1997). Anti-sexual and anxiogenic behavioral consequences of corticotropin-releasing factor overexpression are centrally mediated. Psychoneuroendocrinology 22, 215–224.

Honda, S., Harada, N., Ito, S., Takagi, Y., and Maeda, S. (1998). Disruption of sexual behavior in male aromatase-deficient mice lacking exons 1 and 2 of the cyp19 gene. Biochem Biophys Res Commun 252, 445–449.

Juntti, S.A., Tollkuhn, J., Wu, M.V., Fraser, E.J., Soderborg, T., Tan, S., Honda, S.-I., Harada, N., and Shah, N.M. (2010). The Androgen Receptor Governs the Execution, but Not Programming, of Male Sexual and Territorial Behaviors. Neuron 66, 260–272.

Kendrick, A.M., Rand, M.S., and Crews, D. (1995). Electrolytic lesions to the ventromedial hypothalamus abolish receptivity in female whiptail lizards, Cnemidophorus uniparens. Brain Res. 680, 226–228.

Leedy, M.G., and Hart, B.L. (1985). Female and male sexual responses in female cats with ventromedial hypothalamic lesions. Behav. Neurosci. 99, 936–941.

Lustig, R.H., Mobbs, C.V., Pfaff, D.W., and Fishman, J. (1989). Temporal actions of 16 alpha-hydroxyestrone in the rat: comparisons of lordosis dynamics with other estrogen metabolites and between sexes. J. Steroid Biochem. 33, 417–421.

MacLusky, N.J., and McEwen, B.S. (1978). Oestrogen modulates progestin receptor concentrations in some rat brain regions but not in others. Nature 274, 276–278.

Mathews, D., and Edwards, D.A. (1977). Involvement of the ventromedial and anterior hypothalamic nuclei in the hormonal induction of receptivity in the female rat.

Physiol. Behav. 19, 319–326.

Ohkura, S., Uenoyama, Y., Yamada, S., Homma, T., Takase, K., Inoue, N., Maeda, K.-I., and Tsukamura, H. (2009). Physiological role of metastin/kisspeptin in regulating gonadotropin-releasing hormone (GnRH) secretion in female rats. Peptides 30, 49–56.

Ono, S., Geller, L.N., and Lai, E.V. (1974). TfM mutation and masculinization versus feminization of the mouse central nervous system. Cell 3, 235–242.

Parsons, B., Rainbow, T.C., and McEWEN, B.S. (1984). Organizational Effects of Testosterone via Aromatization on Feminine Reproductive Behavior and Neural Progestin Receptors in Rat Brain. Endocrinology 115, 1412–1417.

Powers, J.B. (1970). Hormonal control of sexual receptivity during the estrous cycle of the rat. Physiol. Behav. 5, 831–835.

Radovick, S., Levine, J.E., and Wolfe, A. (2012). Estrogenic regulation of the GnRH neuron. Front Endocrinol (Lausanne) 3, 52.

Ring, J.R. (1944). Tthe estrogen-progesterone induction of sexual receptivity in the spayed female mouse. Endocrinology 34, 269–275.

Robarts, D.W., and Baum, M.J. (2007). Ventromedial hypothalamic nucleus lesions disrupt olfactory mate recognition and receptivity in female ferrets. Horm Behav 51, 104–113.

Simerly, R.B. (2002). Wired for reproduction: organization and development of sexually dimorphic circuits in the mammalian forebrain. Annu. Rev. Neurosci. 25, 507–536.

Simerly, R.B., and Swanson, L.W. (1987). The distribution of neurotransmitter-specific cells and fibers in the anteroventral periventricular nucleus: implications for the control of gonadotropin secretion in the rat. Brain Res. 400, 11–34.

Toda, K., Hayashi, Y., Ono, M., and Saibara, T. (2012). Impact of ovarian sex steroids on ovulation and ovulatory gene induction in aromatase-null mice. Endocrinology

153, 386–394.

Unger, E.K., Burke Jr., K.J., Yang, C.F., Bender, K.J., Fuller, P.M., and Shah, N.M. (2015). Medial Amygdalar Aromatase Neurons Regulate Aggression in Both Sexes. Cell Reports 10, 453–462.

Vida, B., Deli, L., Hrabovszky, E., Kalamatianos, T., Caraty, A., Coen, C.W., Liposits, Z., and Kalló, I. (2010). Evidence for suprachiasmatic vasopressin neurones innervating kisspeptin neurones in the rostral periventricular area of the mouse brain: regulation by oestrogen. J. Neuroendocrinol. 22, 1032–1039.

Whalen, R.E. (1974). Estrogen-progesterone induction of mating in female rats. Horm Behav 5, 157–162.

Wu, M.V., Manoli, D.S., Fraser, E.J., Coats, J.K., Tollkuhn, J., Honda, S.-I., Harada, N., and Shah, N.M. (2009). Estrogen masculinizes neural pathways and sex-specific behaviors. Cell 139, 61–72.

Xu, X., Coats, J.K., Yang, C.F., Wang, A., Ahmed, O.M., Alvarado, M., Izumi, T., and Shah, N.M. (2012). Modular Genetic Control of Sexually Dimorphic Behaviors. Cell 148, 596–607.

Yang, C.F., Chiang, M.C., Gray, D.C., Prabhakaran, M., Alvarado, M., Juntti, S.A., Unger, E.K., Wells, J.A., and Shah, N.M. (2013). Sexually dimorphic neurons in the ventromedial hypothalamus govern mating in both sexes and aggression in males. Cell 153, 896–909.

Young, W.C. (1941). Observations and Experiments on Mating Behavior in Female Mammals (Concluded). The Quarterly Review of Biology 16, 311–335.

Zhou, J.N., Hofman, M.A., Gooren, L.J., and Swaab, D.F. (1995). A sex difference in the human brain and its relation to transsexuality. Nature 378, 68–70.

Chapter 3

Hormonal regulation of male-typical behaviors

Elizabeth K. Unger, Scott A. Juntti, Xiaohong Xu, Nirao M. Shah

ABSTRACT

All sexually reproducing animals display sex differences in social behaviors, many of which are heavily influenced by or directly under the control of sex hormones. Aromatase, which catalyzes the conversion of testosterone into estrogen, plays an important role in regulating these behaviors, as do the receptors for these hormones: estrogen receptor (ER) and androgen receptor (AR). During development, the presence or absence of estrogen dictates the masculinization or the feminization of the brain. In this study I show that this estrogen is produced and acts locally within the male brain. When I genetically eliminate aromatase or ER alpha (ERα) specifically within the brain this results in major deficits in both mating and aggression. However, while the developmental role of aromatase is apparent, its role in adulthood is much more subtle. Although aromatase is expressed in several distinct locations throughout the brain, elimination of aromatase function produces no behavioral deficits in males, suggesting that the role of estrogen in adulthood in males is far less prominent than previously thought.

INTRODUCTION

All sexually reproducing animals display sex-specific behaviors, many of which are heavily influenced by or under the control of gonadal hormones. This influence can either occur developmentally, creating long-lasting effects, or it can be exerted in real time. Developmental effects include cell number differences, alterations in wiring or projection pattern, and long term chromatin modification (Forger, 2006; Raisman and Field, 1971). Real time changes include gene expression, firing rate or pattern, and local synaptic strength.

It has long been known that estrogen has both “organizational” (developmental) and “activational” (acute) roles in male behavior (Pheonix et al., 1959). The organizational necessity of estrogen has been demonstrated by my lab and others on several occasions (Breedlove and Arnold, 1985; Beatty, 1979; Beyer, 1999; Simerly, 2002; Wu et al. 2009).

Male mice experience a perinatal testosterone surge. This testosterone is then converted to estrogen by aromatase presumably expressed locally within the brain (Naftolin and Ryan, 1975). Through estrogen-mediated cell survival (Chung et al., 2000; Davis et al., 1996; Forger, 2006, Murakami and Arai, 1989; Nordeen et al., 1985) and estrogen-mediated chromatin modifications (Jessica Tollkuhn unpublished data), masculinized cell number, wiring, and gene expression programs are established in the male brain (Breedlove and Arnold, 1980; Dodson and Gorski 1993; Giullamon et a., 1988; Sumida et a., 1993).

In females, the ovaries are quiescent until puberty, thus they lack this estrogen-mediated masculinization (McCarthy, 2008). However, females treated with testosterone or estrogen during the critical period (P0-P4) will develop a masculinized brain and exhibit many male-typical behaviors as adults, including urine marking their territory, fighting with males, and attempting to mate with females (Wu et al., 2009). This is in spite of the fact that they have feminized bodies and normal ovary function. However, their behaviors are not exhibited at the same level as a normal male, a phenotype that can be rescued by supplementing with adult testosterone (Simon and Gandelman, 1978; Simon and Whalen, 1987; Wu et al., 2009). Thus while estrogen is needed to developmentally masculinize the brain, testosterone is needed to achieve normal levels of male-typical behaviors as adults.

This raises the question of the function of estrogen in adulthood. Females experience cycles of high estrogen as adults, but these cycles were not sufficient to elicit male-typical levels of behavior in neonatally masculinized females in the experiment above. Similarly, males castrated as adults, which cease to display nearly all male-typical behaviors (Södersten, 1973), cannot be rescued with estrogen alone (Finney and Erpino, 1976; Södersten et al., 1986). However, estrogen must play some role because these males' behavior also cannot be rescued with dihydrotestosterone (DHT, a non-aromatizable form of testosterone) alone (Feder et al., 1974; Södersten, 1973; Whalen and Luttge,

1971). Either testosterone replacement or DHT + estrogen is required to achieve normal male behaviors, suggesting that both testosterone signaling and estrogen signaling are required.

In order to understand the role of estrogen in adulthood and its precise contribution to male-typical behaviors, I have eliminated either aromatase (to eliminate all estrogen) or ERα in different tissues, at different timepoints using a genetic means. I show that estrogen signaling is indeed required during development for the diplay of normal male-typical behaviors and that this effect is specific to the brain. Furthermore, I show that manipulations induced after the critical period produce an animal capable of normal male behaviors, suggesting that the "activational" effects of estrogen play a much smaller role than previously thought.

RESULTS

Constitutive removal of hormones and hormone receptors

It has previously been shown (and discussed in chapter 2) that, estrogen is required during development to masculinize the brain (Arnold and Breedlove, 1985; Beatty, 1979; Beyer, 1999; Simerly, 2002; Wu et al. 2009). Perinatal administration of an aromatase

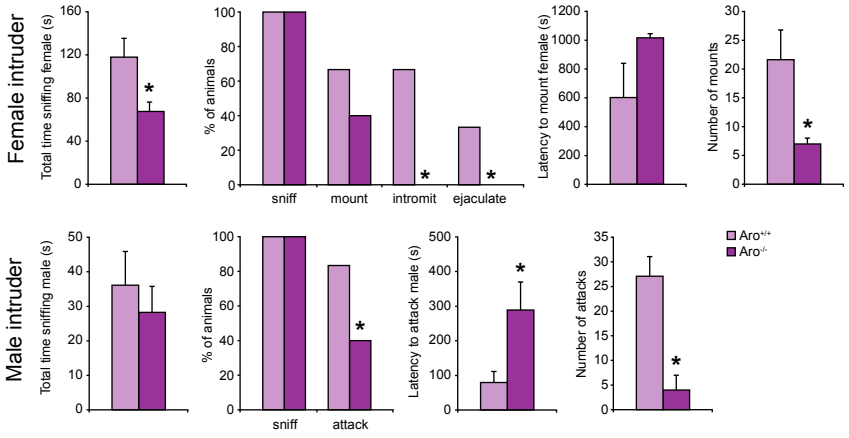

Figure 3.1: Constitutive loss of aromatase in males leads to deficits in mating and aggression

Male mice either wildtype or null for aromatase, were singly housed for 1 week then tested in assays for mating (30 mins with a primed estrus female) and aggression (15 mins with a novel intruder male). n > 5. Error bars represent SEM. * $p < 0.05$ by student's *t* test.

inhibitor is sufficient to block this effect (Ohe, 1994). However, I used a genetic strategy to completely eliminate all estrogen. I used a mouse constitutively null for aromatase such that it would be incapable of synthesizing estrogen. In this mouse exons 1 and 2 were deleted by targeted mutation (Honda et al., 1998). It has previously been shown that this mouse does not display normal male behaviors (Fisher et al., 1998; Honda et al., 1998). I was able to confirm these results (figure 3.1). Also, as shown previously, these males occasionally display aggression towards females (2/5), a behavior that is never seen in the wildtype population and is neither male-typical nor female-typical. However the pattern of attack is distinctly male (discussed in chapter 5).

The primary receptor for estrogen is ERα. While estrogen is also capable of signaling through ERβ and GPR30 (Kuiper et al., 1996; Kuiper et al., 1997; Revankar et al. 2005; Shughrue et al., 1997), it is thought that the majority of estrogen action is through ERα (Ogawa et al., 2000). Mice null for ERβ have been shown to have mostly normal male-typical behaviors with the exception of a short period during puberty where they show increased aggression (Choleris et al., 2008; Clipperton Allen et al., 2010; Krege et al., 1998; Nomura et al., 2002; Nomura et al., 2006; Ogawa et al., 1999). In addition mice null for GPR30 did not show any alterations in behavior (Revankar et al., 2005; Otto et al., 2009). In contrast, it has previously been shown that similar to *aro*$^{-/-}$ mice, mice null for ERα also

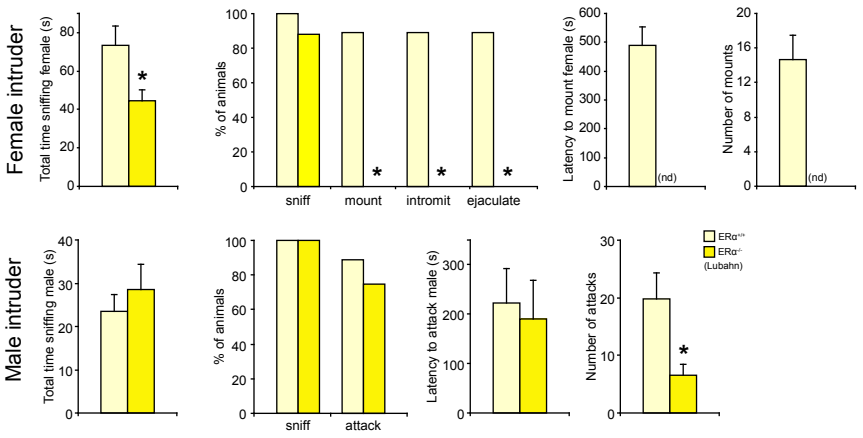

Figure 3.2: Constitutive loss of ERα in males leads to deficits in mating and aggression

Male mice either wildtype or null for ERα, were singly housed for 1 week then tested in assays for mating (30 mins with a primed estrus female) and aggression (15 mins with a novel intruder male). n > 5. Error bars represent SEM. * $p < 0.05$ by student's *t* test.

fail to display male typical behaviors. In order to confirm these results I used a mouse with a constitutive null mutation in ERα, and was able to replicate the previously published data (Figure 3.2). Like the *aro*$^{-/-}$ mice, these males occasionally display aggressive behavior towards females (5/8).

All of these manipulations involve variations surrounding estrogen. However testosterone is also essential for male-typical behaviors, even though it is not thought that testosterone is necessary for the masculinization process because AR does not begin expressing until after the start of the critical period (Juntti et al., 2010). In addition, studies have shown that perinatal treatment with DHT is not sufficient to fully masculinize the brain (Goldstein and Sengelaub, 1992; Hart, 1977; Hart 1979). Previous studies have characterized the behavior of mice constitutively null for AR (*AR*$^{tfm/Y}$, Charest et al., 1991; Goldstein and Wilson, 1972; Ono et al., 1974; Olsen, 1992; Sato et al., 2004). These studies show drastically reduced male-specific behaviors. I was able to replicate their results, showing that *AR*$^{tfm/Y}$ mice display no mating behavior and very little aggression (Figure 3.3).

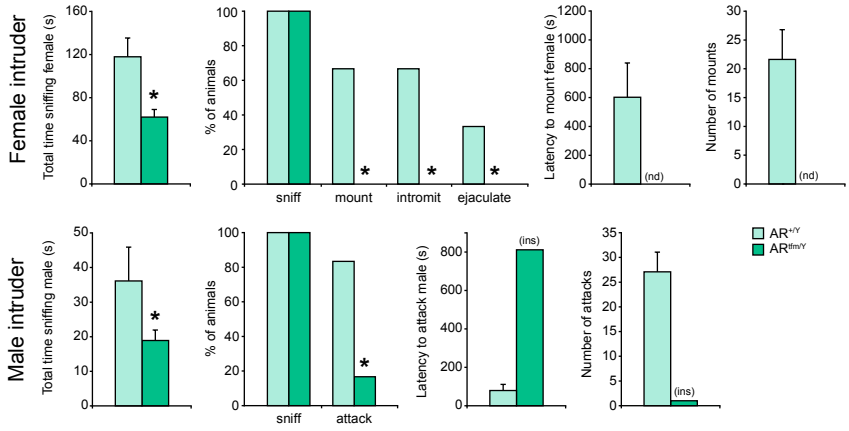

Figure 3.3: Constitutive loss of AR in males leads to deficits in mating and aggression

Male mice either wildtype or null for androgen receptor (AR), were singly housed for 1 week then tested in assays for mating (30 mins with a primed estrus female) and aggression (15 mins with a novel intruder male). n > 5. Error bars represent SEM. * $p < 0.05$ by student's *t* test. ins: insufficient data for statistical analysis.

However *AR*$^{tfm/Y}$ mice, also known as testicular feminized males (tfms), develop female secondary sex characteristics, and their testes are roughly 1/10th the size of a wildtype's and fail to descend (Goldstein and Wilson, 1972; Lyon and Hawkes, 1970). In fact the small amount of

aggression displayed may very well have been a response to the fact that *AR*$^{tfm/Y}$ mice occasionally get mounted by the intruder male and are showing defensive behavior rather than overt aggression. Indeed, in a different experiment (described in chapter 2) *AR*$^{tfm/Y}$ mice initiated attacks only after being mounted by a stud male (the resident in this study), but these attacks disappeared when the testes were removed prior to behavior testing (5/5 intact, 0/11 castrated). However, this does not mean that they failed to develop a masculinized brain. On the contrary, this would suggest that they are capable of showing male-typical behaviors, but lack the adult levels of testosterone to display them at the same intensity. In support of this idea, we have previously shown that females who received perinatal estrogen treatment developed a masculinized brain, but did not show normal male-typical levels of these behaviors until they were treated with male levels of testosterone (Wu et al., 2009). The fact that the aggression displayed by these *AR*$^{tfm/Y}$ mice resembles male-pattern attack behavior and goes away completely when the testes are removed suggests that despite the lack of normal male-typical behaviors in *AR*$^{tfm/Y}$ mice they do indeed have a masculinized brain, but lack the adult testosterone to properly display these behaviors. I did not perform a testosterone supplementation experiment to confirm this hypothesis, however.

So far all of these manipulations involve removing one single hormone or signaling pathway. However what would the outcome be if all hormone

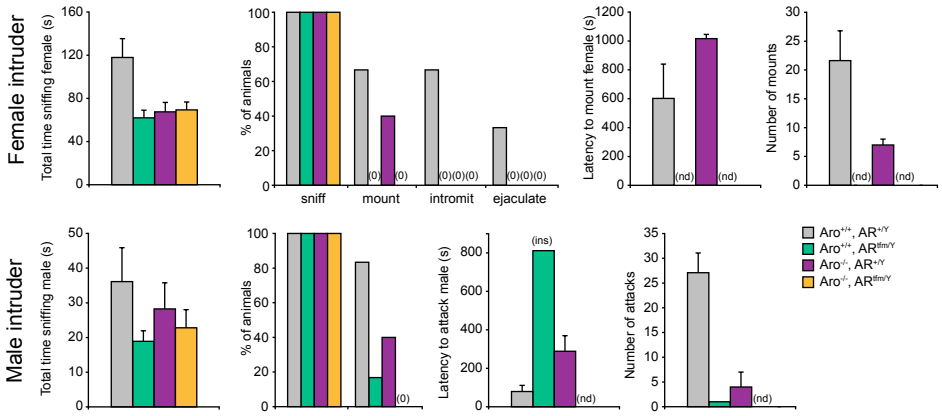

Figure 3.4: Constitutive loss of both AR and aromatase in males leads to complete loss of both mating and aggression

Male mice either wildtype or null for androgen receptor (AR), aromatase, or both were singly housed for 1 week then tested in assays for mating (30 mins with a primed estrus female) and aggression (15 mins with a novel intruder male). n > 5. Error bars represent SEM. * $p < 0.05$ by student's *t* test. ND: no data

signaling were abolished? By crossing the *AR*$^{tfm/Y}$ mouse line to the *aro*$^{-/-}$ mouse line (DKO), both testosterone and estrogen signaling would be effectively eliminated. In chapter 2 I tested he ability of these mice to display female-typical behaviors. Here, when I test them in assays for mating and aggression, I find that these mice display no male-typical behaviors at all (Figure 3.4). In fact, while I have no direct comparison in these studies, they seem to behave more or less female in my behavior assays. Similar to the *AR*$^{tfm/Y}$ mice, the DKOs occasionally get mounted by the intruder male during aggression assays (5/10), but their response is usually to run away or struggle, similar to the responses of non-estrus females (discussed in chapter 2).

Requirement of estrogen and ERα in the brain

All of the mice tested thus far are constitutively null for a hormone or hormone receptor, all of which are expressed in the brain as well as elsewhere in the body. In order to localize these effects to the brain, I used a Nestin-Cre mouse line and crossed it to floxed versions of aromatase, and ERα. Previous work from my lab has addressed the necessity of testosterone signaling in the brain using the same approach (Juntti et al,. 2010).

Because no aromatase-flox animal existed previously, we generated an aromatase flox mouse line. LoxP sites were introduced around exon 8 of aromatase (242 bp) which codes for the steroid binding domain (enzymatically active region, Bakker et al., 1986; Kumar et al., 1986) (Figure 3.5A). To ensure the deletion of exon 8 I first crossed the aroflox mouse line to an EIIa-Cre mouse line, which expresses at the 4-cell stage and will recombine in cells that contribute to the germline (Lakso et al., 1996). The EIIa-Cre was subsequently bred out of the line in order to create a mouse with a constitutive null mutation in aromatase. I then microdissected the bed nucleus of the stria terminalis (BNST) and the medial amygdala (MeA), two regions of the brain known to express aromatase, from a mouse heterozygous for the mutation. PCR amplification from the extracted RNA using primers

located in exon 7 and exon 9 yielded two bands in the heterozygote that were the predicted size (Figure 3.5B). Sequencing results confirmed that exon 8 was indeed absent from the smaller band.

In order to localize this deletion neuroanatomically in later experiments involving cell-type specificity, I wanted to perform in situ hybridization for the deleted transcript. However, the published probe for aromatase detects exons 1-7 (Lien et al., 2007; Wu et al., 2009), and because the transcript continues to be produced, despite a non-functional protein

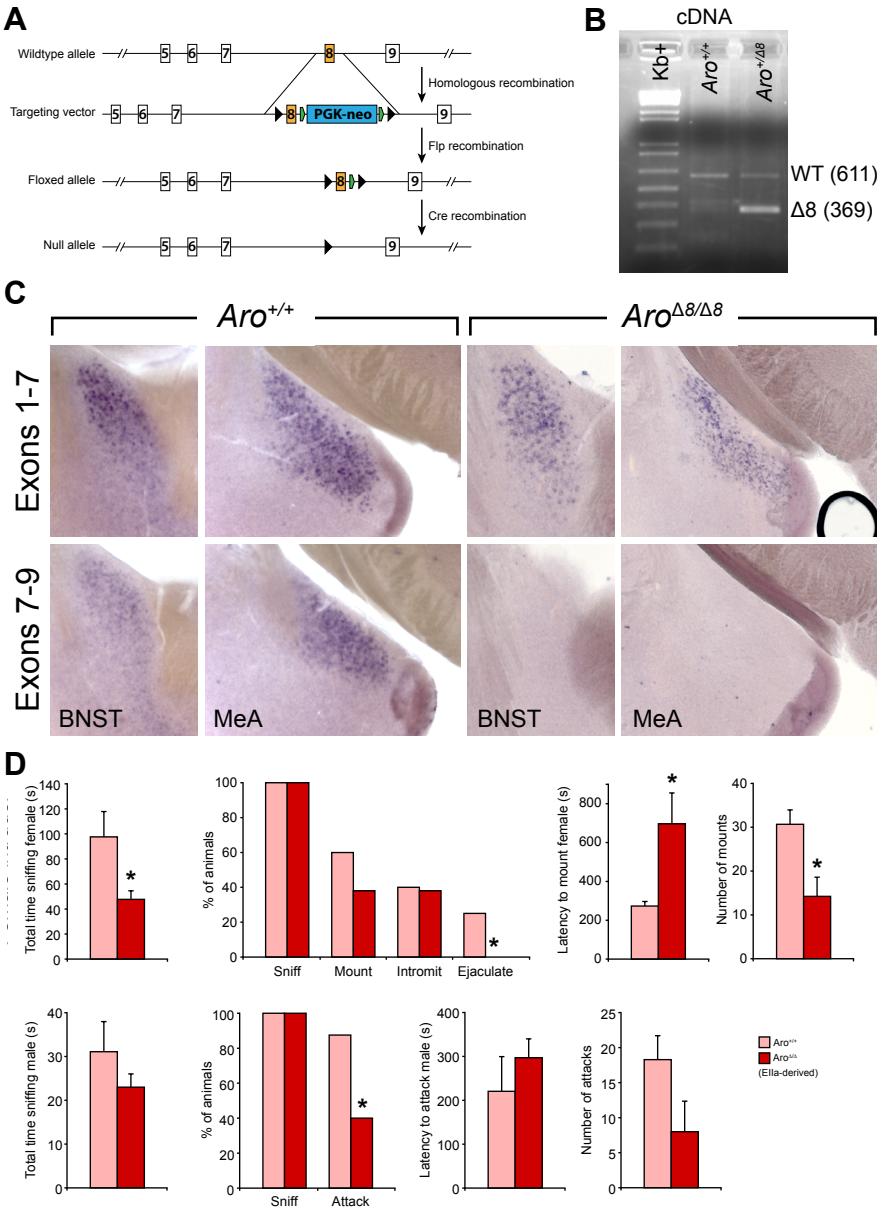

Figure 3.5: Generation of a floxed aromatase allele

A) Strategy to generate the floxed aromatase allele. (Not drawn to scale.) B) cDNA from microdissected BNST and MeA of a wildtype male and male heterozygous for the recombined aromatase allele was PCR amplified using primers located in exons 7 and 9. C) In situ hybridization was perfromed using a probe for exons 1-7 and exons 7-9 in a wildtype male and a male homozygous for the recombined aromatase allele. D) Male mice either wildtype or homozygous for the recombined aromatase allele were singly housed for 1 week then tested in assays for mating (30 mins with a primed estrus female) and aggression (15 mins with a novel intruder male). n > 5. Error bars represent SEM. * $p < 0.05$ by student's *t* test. BNST: bed nucleus of the stria terminalis, MeA: medial amygdala.

(Figure 3.5B), this would not be useful in localizing loss of exon 8. Therefore I designed a short probe to detect exons 7-9. In the wildtype animal detection of exons 7-9 is similar to that of exons 1-7, while in an *aro*$^{\Delta 8/\Delta 8}$ animals exons 1-7 are detected while the probe for exons 7-9 does not have sufficient binding affinity to be detected (Figure 3.5C). In addition, the BNST and MeA, which are regions that are sexually dimorphic, with 30% fewer cells and a narrower shape in females (Allen and Gorski, 1990), appear to be feminized in the *aro*$^{\Delta 8/\Delta 8}$ male, suggesting that aromatase is indeed non-functional (also see chapter 2). In order to confirm this result, I tested these animals for male-typical behaviors. These studies are ongoing, but preliminary results match the previously published and previously tested animals (Figure 3.1, 3.5D, Bakker et al., 2004; Honda et al., 1998; Matsumoto et al., 2003a; Matsumoto et al., 2003b;

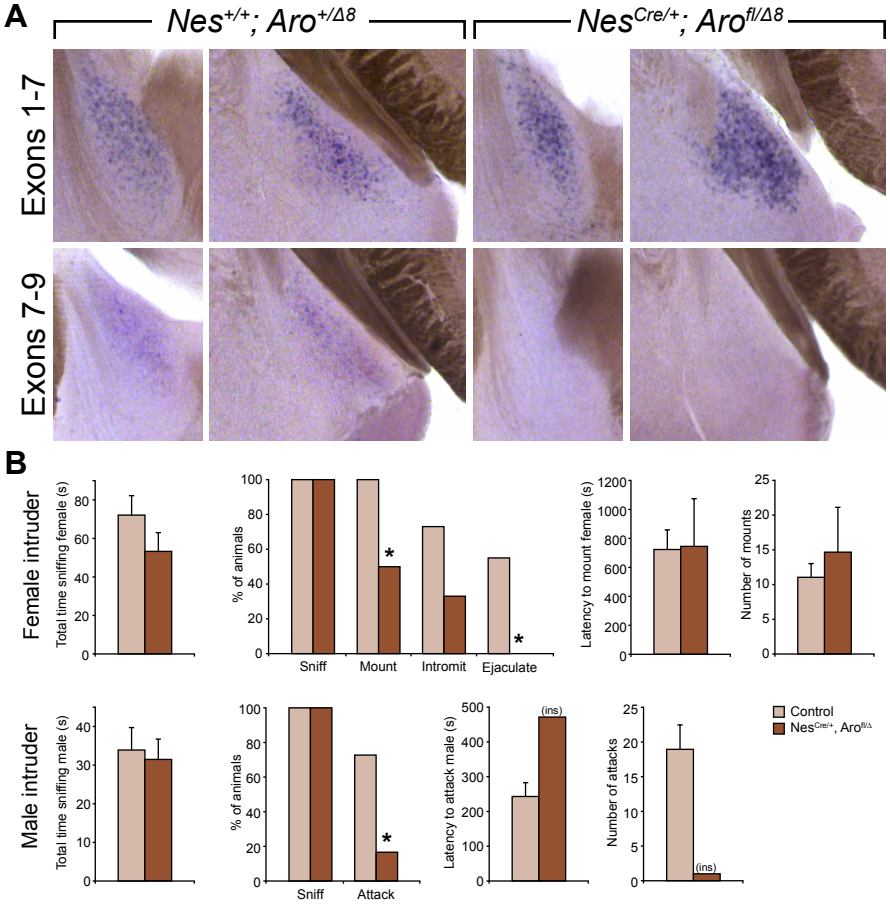

Figure 3.6: Loss of aromatase specifically in the brain leads to deficits in mating

A) In situ hybridization was performed using a probe for exons 1-7 and exons 7-9 in control and mutant nestin-Cre, aromatase-flox males to demonstrate deletion of aromatase exon 8. B) Male mice carrying a Nestin-Cre allele and doubly heterozygous for a floxed aromatase allele, and a recombined aromatase allele, and their control littermates were singly housed for 1 week then tested in assays for mating (30 mins with a primed estrus female) and aggression (15 mins with a novel intruder male). n > 5. Error bars represent SEM. * $p < 0.05$ by student's *t* test. ins: insufficient data for statistical analysis.

Robertson et al., 2001; Toda et al., 2001), including the propensity to attack females (5/8), however in this case, I saw both mounting and aggression in the same assays (4/5).

While it is assumed that estrogen synthesized locally within the brain is necessary to create male-type wiring, it has yet to be proven that this is true. In order to prove aromatase is only required within the nervous system to masculinize male-typical behaviors, I crossed the aro-flox line to a Nestin-Cre (Nes-Aroflox, and performed the same behavioral tests. Nestin-Cre expresses within neural precursors, thus affecting nearly all nervous tissue (Tronche et al., 1999). Nes-Aroflox mice showed a less severe phenotype than *aro*$^{-/-}$ mice, but showed many of the same phenotypes including decreased aggression and mating, and failure to ever ejaculate. Also similar to *aro*$^{-/-}$ mice, they sometimes attack females (1/3). This supports the previously held assumption that locally expressed aromatase is responsible for masculinization of the brain. Interestingly, when I tested Nes-Aroflox females for fertility, I found that all plugged within the first 5 days of being paired with a stud male and all gave litters of normal size and frequency (4/4) suggesting that brain-derived estrogen is not necessary in females for normal fertility.

Another widely held, but never proven assumption is that estrogen made locally in the brain acts on ERα within the brain to create this male-type wiring. In order to test this hypothesis my lab obtained an ERα-flox mouse line (Geiske et al., 2008) in which loxP sites have been introduced around exon 3 of ERα. Similar to the aro-flox mice I wanted to ensure that this deletion was comparable to the published deletion, so I crossed the line to the Ella-Cre to induce germline recombination. Ella-Cre was subsequently bred out of the line prior to behavior testing. My results were similar between the two lines (Figure 3.7), including the propensity to attack females (1/7), confirming that the recombined ERα-flox produces a nonfunctional ERα similar to the currently published studies. It should be noted that the Lubahn mice were maintained on their original 129 background and the EIIa-derived mice were backcrossed several generations to a B6 background. Strain differences exist

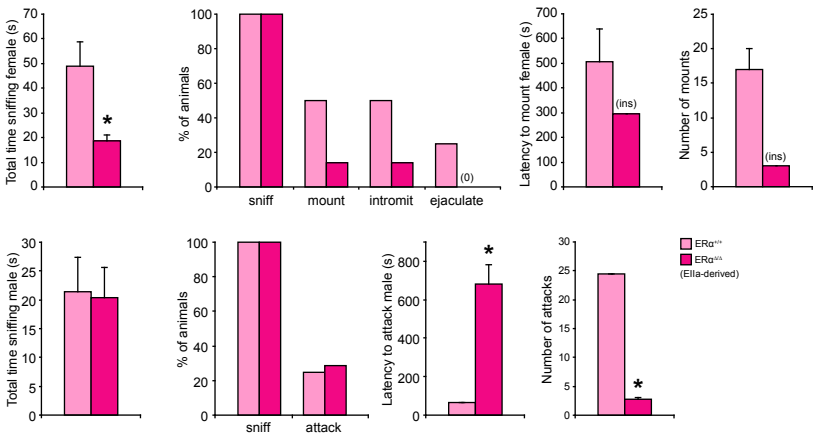

Figure 3.7: Recombined ERα allele is similar to the targeted knockout

Male mice either wildtype or homozygous for a recombined allele for ERα, were singly housed for 1 week then tested in assays for mating (30 mins with a primed estrus female) and aggression (15 mins with a novel intruder male). n > 5. Error bars represent SEM. * $p < 0.05$ by student's *t* test.

and can affect behaviors enormously (Ginsberg and Allee, 1942). This may account for some of the differences I see in the wildtype behavior.

In order to prove that ERα is only required within the nervous system to masculinize male-typical behaviors, I crossed the ERα-flox line to a Nestin-Cre (Nes-ERαflox), and performed the same behavioral tests. Nes-ERαflox mice showed a less severe phenotype than ERα$^{-/-}$ mice, but had many of the same characteristics including decreased aggression, decreased mating and failure to ever ejaculate (Figure 3.8). Indeed, Nes-ERαflox males also occasionally attack females (1/19). Interestingly, when I tested Nes-ERαflox females for fertility, I found that unlike the Nes-Aroflox females, none plugged within the first 5 days of being paired with a stud male, and none gave litters in the following 2 month period (0/3). It is clear that repoduction in females is dependent on estrogen signaling, but that this estrogen is not produced within the brain (likely it is derived from the ovaries).

Juntti et al. published a paper demonstrating the effects of removing androgen receptor specifically from the nervous system (AR Ns-del). These mice differ from the *AR$^{tfm/Y}$* mice in that they develop male-typical secondary sex characteristics, including external genetalia. They showed that AR Ns-del mice display greatly decreased aggression and mating behavior, despite having a masculinized brain (Juntti et al., 2010). This is consistent with with the idea testosterone signaling dictates the intensity with which male behaviors

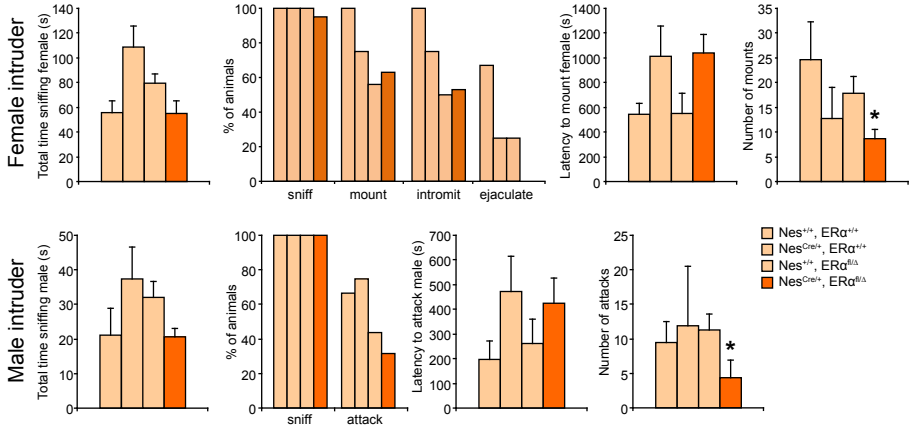

Figure 3.8: Loss of ERα specifically in the brain leads to deficits in aggression

Male mice carrying a Nestin-Cre allele and doubly heterozygous for a floxed ERα allele, and a recombined α allele, and their control littermates were singly housed for 1 week then tested in assays for mating (30 mins with a primed estrus female) and aggression (15 mins with a novel intruder male). n > 5. Error bars represent SEM. * p < 0.05 by student's *t* test.

are executed, and also consistent with the idea that testosterone signaling within the brain is the most important for this.

Temporal requirement of estrogen and ERα

The above data indicates that estrogen production and signaling in males is localized to the brain. However, All of these manipulations occur before the critical period for masculinization of the brain. This means that so far I have only explored the developmental necessity of these hormones and hormone receptors. The developmental necessity of estrogen and ERα has previously been shown (Baum et al., 1990; De Vries and Simerly, 2002), but this does not answer the question of its role in adulthood. To address this, I crossed the aro-flox line to a new AR-Cre mouse line, such that all cells that express AR would have a non-functional aromatase. Nearly all of aromatase neurons express AR (in males) such that aromatase would be effectively deleted everywhere in the nervous system. However AR does not begin expressing until P4 (Juntti et al., 2010), which is during the critical period rather than before. Assuming that Cre action is not immediate, these mice should have normal aromatase function during the critical period and develop normally masculinized brains, but lack aromatase as adults. While results are still preliminary, I find that these mice show normal male-typical behaviors in all parameters tested (Figure 3.9) and also do not attack females (0/4). This suggests that aromatase is either not necessary in the adult male

for normal male-typical behaviors, or sufficient estrogen is being synthesized in non-AR+ cells.

ERα is expressed in many different places in the brain. Indeed it is expressed in far more cells and in far more regions than aromatase is expressed, suggesting that estrogen may diffuse or be transported to these cells or ERα may be functioning independent of estrogen. To test the adult necessity of ERα

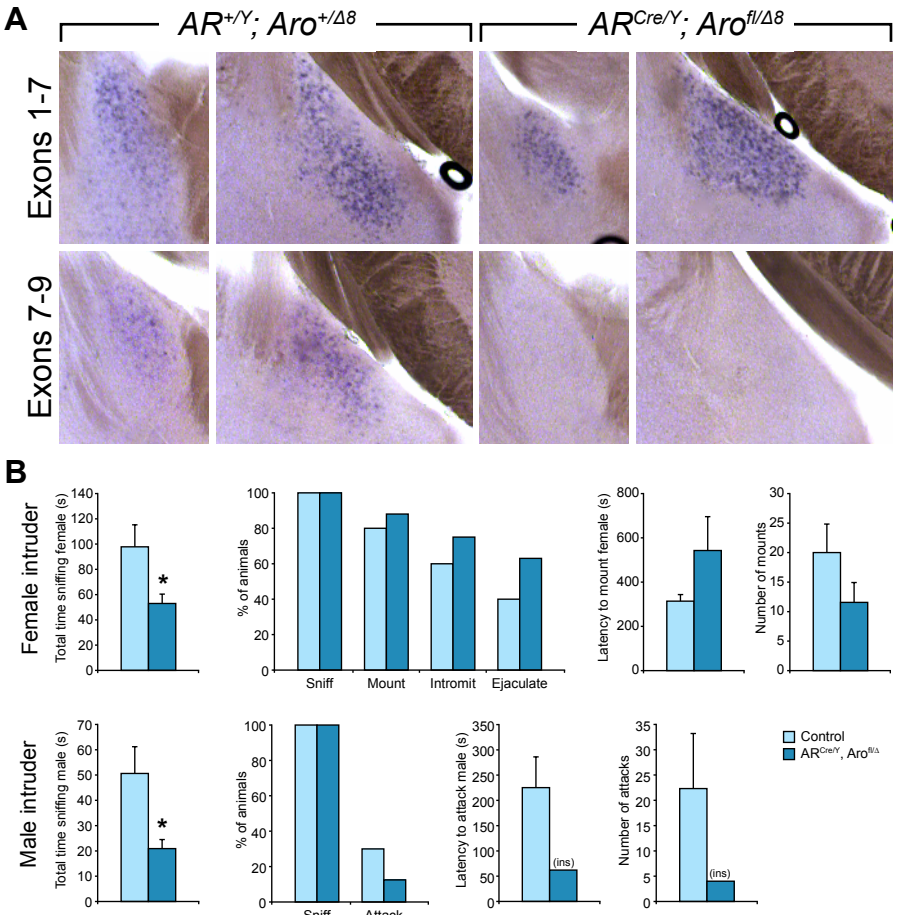

Figure 3.9: Loss of aromatase in AR cells has no behavioral effect

A) In situ hybridization was performed using a probe for exons 1-7 and exons 7-9 in control and mutant AR-Cre, aromatase-flox males to demonstrate deletion of aromatase exon 8. B) Male mice carrying a AR-Cre allele and doubly heterozygous for a floxed aromatase allele, and a recombined aromatase allele, and their control littermates were singly housed for 1 week then tested in assays for mating (30 mins with a primed estrus female) and aggression (15 mins with a novel intruder male). n > 4. Error bars represent SEM. ins: insufficient data for statistical analysis.

I crossed the ERα-flox mouse line to the AR-Cre line. About 95% of ERα expressing cells in the brain also express AR (unpublished data), such that ERα would be essentially lost in all cells. However, because AR does not begin expressing until P4, these mice should have normal ERα function during the critical period and thus develop normally masculinized brains, but lose ERα function in adulthood. Again these studies are ongoing,

and insufficient data has been generated to make any conclusions.

Given that aromatase-expressing neurons are the primary source for estrogen in males, I next wanted to test the necessity for ERα in aromatase-expressing neurons. While ERα is not the only receptor for estrogen, it is considered the primary receptor, and presumably cells that produce estrogen need a means of sensing it as well, in order to titer the amount. Therefore, I crossed the ERα-flox line to an aromatase-Cre mouse line generated in the lab (Unger et al., 2015; see chapter 5). Mutant mice were behaviorally indistinguishable from their control genotypes (Figure 3.10A), indicating that either cell-autonomous estrogen signaling is not necessary for normal male behaviors or this effect is mediated by another estrogen receptor. Given that ERβ cannot compensate for the loss of ERα in ERα$^{-/-}$ mice, it is unlikely, although still possible, that ERβ is compensating completely for the loss of ERα in these neurons. It is also possible that upregulation of ERα in other regions could compensate for the loss of ERα in the small number of aromatase+ neurons. It should also be noted that aromatase expression begins in utero, and is present by P0 (Wu et al., 2009). It is nonetheless possible, though not yet confirmed, that ERα expression is present long enough to masculinize the brain. It should also be noted that expression of aromatase during development is much more widespread than in adulthood, thus loss of ERα is occurring in many more cells and many more brain regions than the small number seen in adulthood (Figure 3.10B,C, Wu et al. 2009).

In order to truly eliminate estrogen production in adulthood, without any possibility of developmental compensation, I used a slightly different strategy. Instead of crossing the aroflox line to a Cre line, I instead injected a Cre virus directly into the MeA, which is one of the few regions that expresses aromatase. In this way I am able to determine the precise contribution of estrogen produced in the MeA to male-specific behaviors. While aromatase is also expressed elsewhere in the brain, and can potentially compensate for loss of aromatase in the MeA, this strategy allows me to parse the contribution of each

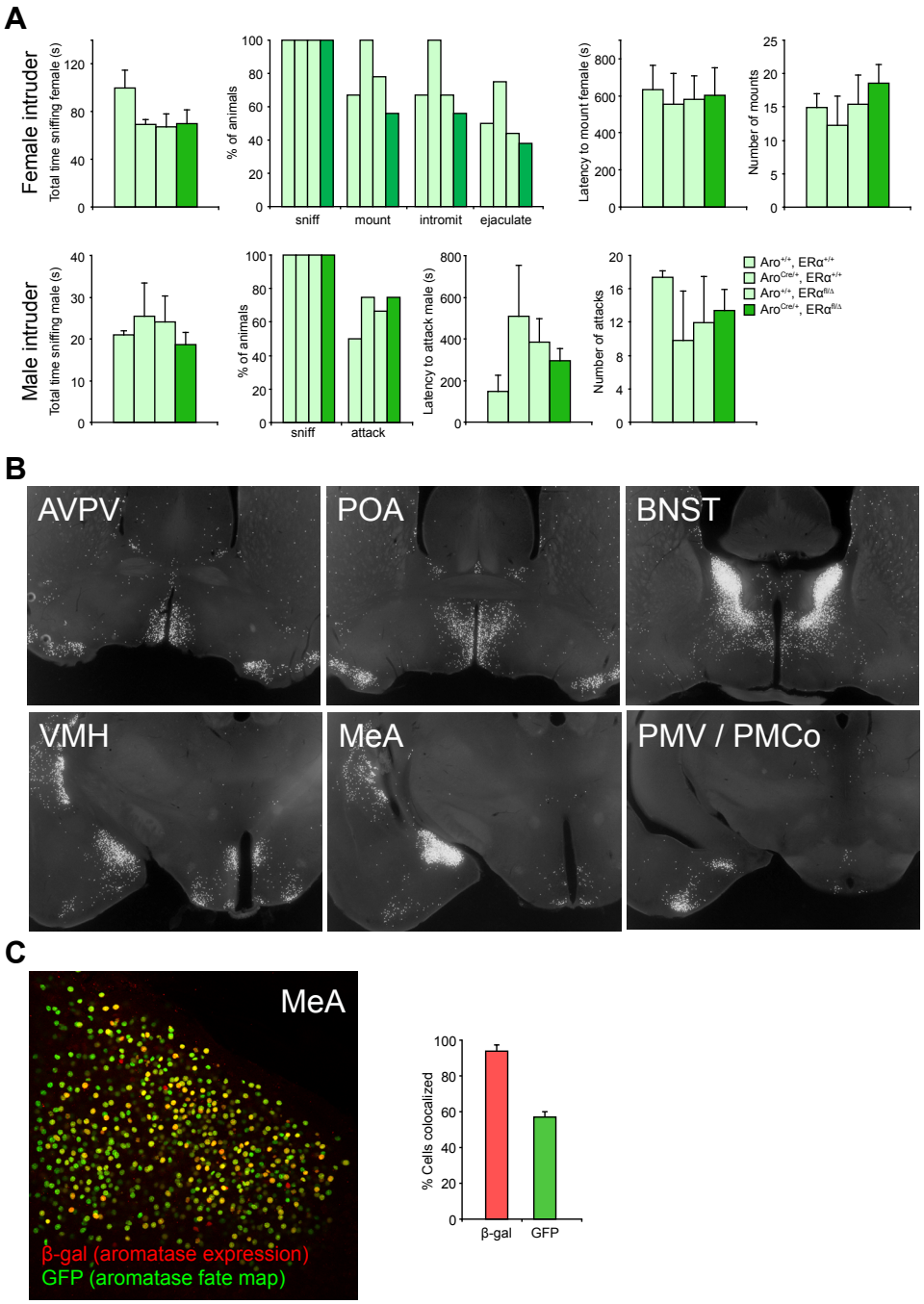

Figure 3.10: Loss of ERα specifically in the aromatase neurons has no effect

A) Male mice carrying an aromatase-Cre allele and doubly heterozygous for a floxed ERα allele, and a recombined ERα allele, and their control littermates were singly housed for 1 week then tested in assays for mating (30 mins with a primed estrus female) and aggression (15 mins with a novel intruder male). B) An aromatase-Cre line was crossed to a Rosa26-floxed-H2B-GFP reporter line to fate map aromatase expression. C) The same section as in B, now showing colocalization with an aromatase reporter, and quantification of colocalization. The MeA shows higher colocalization than many other regions, such as the PMCo, in which aromatase in not expressed in adulthood. n = 3-9. Error bars represent SEM.

separate brain region, to the overall behavior. In addition, when I inject an adeno associated virus (AAV) that expresses Cre into the MeA I do not see a compensatory increase in aromatase expression in the BNST (Figure 3.11A). It should be noted here that the probe for exons 7-9 of aromatase shares 20% homology with Cre, thus cross-reactivity is difficult to avoid when Cre is expressed at such high levels. When I assay for male-typical behaviors, I find no deficits or alterations in any of the behaviors tested (Figure 3.11B). This clearly shows that aromatase is not necessary in the MeA for male-typical behaviors. This suggests two possibilities: either there is compensation from other brain regions, which is unlikely given that other brain regions such as the BNST do not show increased aromatase expression (Figure 3.11A), or aromatase itself is not necessary for male-typical behaviors. Taken together with the results of the AR-Aroflox experiment, it

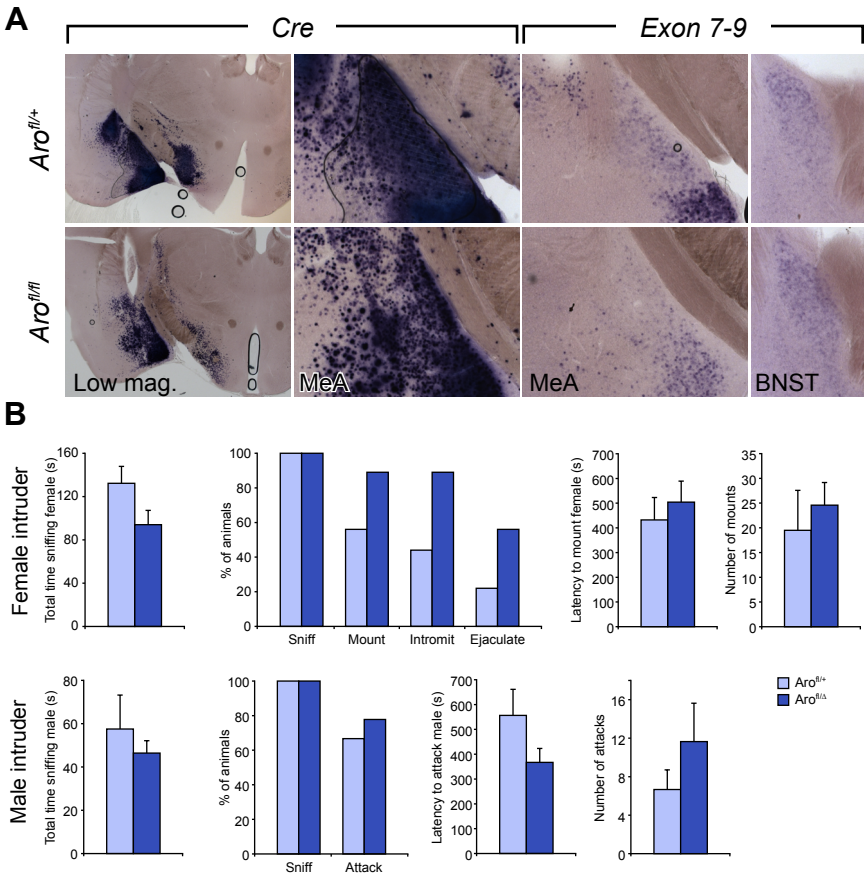

Figure 3.11: Loss of aromatase in the medial amygdala has no behavioral effect

Male mice either heterozygous or homozygous for the floxed aromatase allele were injected with an AAV-CMV-Cre-GFP into the medial amygdala. A) In situ hybridization in serial sections for Cre mRNA and aromatase exons 7-9 mRNA. Some contamination occurred during the staining process. Better sections will be prepared. B) Mice were allowed 3 weeks to recover from surgery, then singly housed for 1 week then tested in assays for mating (30 mins with a primed estrus female) and aggression (15 mins with a novel intruder male). n > 4. Error bars represent SEM.

is possible that the role of aromatase in male-typical behaviors is not as prominent as previously believed. However, the MeA has been implicated in many of these behaviors, which raises the question of the role of aromatase+ cells in the MeA in regulating male-typical behavior (discussed in chapter 5).

DISCUSSION

All of these manipulations involve removing a hormone receptor or ligand, many of which show some sort of deficit in social behaviors. Taken together, there are several patterns that emerge (Table 3.1).

Estrogen production and signaling in males is localized to the brain

First and foremost, the pattern that emerges in that the constitutive null is behaviorally similar to its corresponding floxed allele crossed to the Nestin-Cre. It is true that the Nestin-Cre mutants often have a milder phenotype than their constitutive null counterparts, and this may be due to incomplete recombination within neural precursors leading to continued expression of aromatase or ERα, or it may be due to the contribution of aromatase or estrogen signaling that occurs outside the brain. Nonetheless, this suggests that the majority of estrogen synthesis and signalling in males occurs within the brain. This is not terribly surprising, given that male levels of estrogen in the bloodstream are undetectably low, and it was previously assumed that the masculinization process occurred via local conversion of testosterone within the brain. These results support that notion.

Adult estrogen synthesis in the brain is not necessary for male-typical behaviors

The next pattern that emerges is the difference between manipulations that occur before the critical period and those that occur after the critical period. Manipulations before the critical period produce an array of different behavioral deficits, while manipulations that occur after the critical period produce animals that are indistinguishable from their control

		Constitutive null						Nestin Cre			AR Cre		Aro Cre		MeA	Female¥		
	Wildtype	Aro (Honda)	Aro (flox)	ERα (Lubahn)	ERα (flox)	AR	AR/Aro	Aro-flox	ERα-flox	AR-flox†	Aro-flox	ERα-flox	ERα-flox	AR-flox	Aro-flox	Wildtype	NE	NE + AOT
Sniff female	100	↓	↓	↓	↓	↓	↓	-	-	ND	↓	ND	-	-	-			
Fraction mount	0.7	-‡	-§	0‡	↓‡	0*	0*	↓‡	-‡	-	-	ND	-	-	-	↓	↓	ND
Latency to mount	500	-	↑		-			↓	-	ND	-	ND	-	-	-	↑	ND	ND
Number mounts	15	↓	↓		↓			-	↓	↓	-	ND	-	-	↑	↓	ND	ND
Fraction intromit	0.6	0	-		↓			-	↓	↓	-	ND	-	-	↑	↓	ND	ND
Fraction ejaculate	0.3		0		0			0	0	↓	-	ND	-	-	-			
Sniff male	40	-	-	-	-	↓	-	-	-	ND	↓	ND	-	-	-			
Fraction attack	0.6	↓*	↓	-	-	↓*	0*	↓	-	↓	-	ND	-	-	-	0*	-*	-*
Latency to attack	250	↑	-	↑	-	Ins.		Ins.	-	ND	Ins.	ND	-	-	-		ND	ND
Number attacks	15	↓	-	↓	↓	Ins.		Ins.	↓	↓	Ins.	ND	-	-	-		↓	-

Table 3.1 Summary of behavior results

‡ Attack females (no assays with both), § Attack females (assays with both), Ins. Insufficient data for statistics ND No data

† Juntti et al. 2010, ¥ Wu et al. 2009, purple text represents preliminary data

littermates. Clearly the critical period is acting to masculinize the brain, but it is surprising that estrogen is not necessary in adulthood in order to perform normal male-typical behaviors at wildtype levels. Wu et al. showed that perinatal estrogen was sufficient masculinize behavior in females, but that in order to display these behaviors at wildtype male levels, testosterone supplementation was required. However, these experiments were done in regularly cycling females where estrogen was present, and thus its contribution could not be evaluated. My results suggest that there is no adult necessity for estrogen in males. This then begs to question as to why aromatase continues to be expressed in the male brain. What is the purpose of this aromatase, assuming that no protein synthesis is wasted energy (discussed further in chapter 5)?

Differences in the regulation of aggression and mating

Aggression appears to be a more robust behavior than mating. Some manipulations affect

both mating and aggression, and in these cases mating is typically affected more severely, and shows greater deficits in more different parameters than aggression. In addition, there are cases where mating is completely abolished, while aggression is only slightly affected. This is counterintuitive because from a biological perspective, reproduction is the measure of evolutionary success, and thus the single most important behavior to preserve beyond basic survival is mating. Furthermore, aggression is more energetically costly and risky, as there is the possibility of fatal injury. These are however, very large perturbation in major signaling pathways and most of these mice are infertile anyway. Interestingly, I paired several Nestin-ERα/flox females and Nestin-Aroflox/flox females with stud males for one month. None of the Nestin-ERαflox/flox females produced litters or showed signs of pregnancy, while all of the Nesting-Aroflox/flox females plugged within the first 5 days and produced litters within the first month (0/3 and 4/4 respectively). This suggests that while estrogen signaling within the brain is necessary for pregnancy, aromatase is not.

In addition to the notion that aggression is a more robust behavior than mating, the parameter that most often shows a deficit is the number of mounts or attacks, rather than the fraction of animals performing the behavior or the latency to do so. This gives some insight into the circuitry as the decision whether or not to perform a behavior, as well as how long it takes to make that decision are both separable from the intensity with which the behavior is performed.

Aberrant aggression towards females

Without estrogen signalling through ERα, males sometimes attack females. The incidence of this behavior is low (about ⅓ of animals), however, it is a behavior that is never seen in the wildtype population. This suggests that either the aggression circuitry is present, but directed towards the wrong sex, or that the mating circuitry has been miswired to

produce aggression instead. Approximately ⅓ of males mount, ⅓ attack and the other ⅓ simply sniff the female, whereas in the wildtype population, approximately ⅔ mount and ⅓ simply sniff. Because attacks are never seen in the same assays or from the same mice as those that mount females (with the exception of the EIIa-derived *aro*$^{\Delta 8/\Delta 8}$ mice, and because the proportion of males that do one or the other matches that of the proportion that mount in the wildtype population, it is more likely that mating circuitry has been rewired to produce aggression. In the case of the EIIa-derived *aro*$^{\Delta 8/\Delta 8}$ mice, the proportion of males that mounted remained the similar to wildtype, while some of those mice also attacked the females. It is still possible that the mating circuit has been rewired, but in an incomplete way. This also raises the question of what causes a male to decide to mount or not, however, that will not be addressed in this thesis.

METHODS

Animals

Adult mice 10–24 weeks of age were used in all studies. Mice were housed in an UCSF barrier facility with a 12:12 hr light:dark cycle, and food and water were available ad libitum. Experimental mice and their control same-sex siblings were used for behavioral studies. Animals were group-housed by sex after weaning at 3 weeks of age. All studies with animals were done in accordance with UCSF IACUC protocols.

Generation of reagents

The aro-flox mouse was created by homologous recombination similar to the mouse line described in chapter 5. Neomycin was used as a selection cassette in ES cells and subsequently removed by crossing the resulting mouse to the flippase mouse line. As I was not personally involved in the generation of this mouse line, I will not describe the procedure here. Future publications will detail the methods used and characterize the mouse line properly.

The AR-Cre mouse was created by homologous recombination similar to the mouse line described in chapter 5. As I was not personally involved in the generation of this mouse line, I will not describe the procedure here. Future publications will detail the methods used and characterize the mouse line properly.

Sterotaxic surgery

Stereotaxic surgery was performed as described previously (Morgan et al., 2014). Briefly, a mouse was placed in a stereotaxic frame (Kopf Instruments) under anesthesia (0.5-2% isofluorane), the skull was exposed with a midline scalp incision, and the stereotaxic frame was aligned at bregma using visual landmarks. The drill (drill bit #85; ~279 μm diameter) on the stereotaxic frame was placed over the skull at coordinates corresponding to the MeA (rostrocaudal, −1.6 mm; mediolateral, ± 2.2 mm), and a hole was drilled through the skull bone to expose the brain. A 33 gauge steel needle connected via PE20 tubing to a Hamilton syringe was loaded with virus, aligned at bregma (including in the z-axis) and slowly lowered to a depth of 5.15 mm. Virus was delivered bilaterally at 100 nL/min with a Hamilton syringe using a micropump (Harvard Apparatus). The needle was left in place for an additional 5 min to allow diffusion of the virus and then was slowly withdrawn. The wound was then closed using vetbond (3M). Mice were weighed and allowed to recover on a heating pad before being returned to their home cage.

Histology

Animals were perfused with 4% PFA as previously described (Juntti et al., 2010; Wu et al., 2009; Xu et al., 2012; Yang et al., 2013) and sectioned at 65 μm (immunofluorescence) or 100 μm (*in situ* hybridization, ISH) using a vibrating microtome (Leica).

Immunolabeling was performed using previously published protocols (Shah et al., 2004; Wu et al., 2009). The primary antiserum used was: rabbit anti-ERα (Millipore, 1:6,000).

The fluorophore conjugated secondary antiserum was: Cy3 donkey anti-rabbit, (Jackson ImmunoResearch, 1:800). Sections were imaged using an upright epifluorescent microscope (Zeiss).

Pr and Cckar probes for ISH were generated from subcloned RT-PCR products. The ISH was performed as described previously (Xu et al., 2012). Briefly, mice were perfused with 4% paraformaldehyde (PFA), and the brains were dissected, post-fixed, and sectioned at 100 μm with a vibrating microtome (Leica). Sections were treated with proteinase K (10 μg/mL, Roche) and fixed at room temperature. Sections were then acetylated and equilibrated to hybridization solution for 2-5 hr at 65°C, followed by incubation at 65°C overnight in hybridization buffer containing 0.5 μg/mL digoxygenin-labeled RNA probe. The sections were then washed in high stringency buffers and incubated overnight at 4°C in buffer containing alkaline phosphatase-conjugated sheep anti-digoxygenin antibody (Roche, 1:2000). The sections were then incubated for 4-6 hr at 37°C in staining solution containing nitro blue tetrazolium and 5-bromo-4-chloro-3-indolyl-phosphate (NBT and BCIP, respectively; Roche). Finally, sections were washed, post-fixed, and mounted on glass slides as described previously (Xu et al., 2012).

Behavior

All behavioral testing was initiated ≥ 1 hr after onset of the dark cycle, and recorded and analyzed as described previously (Juntti et al., 2010; Wu et al., 2009; Xu et al., 2012; Yang et al. 2013). There were always ≥ 2 days between behavioral tests, and residents were always exposed to a novel intruder. All tests were scored by an experimenter blind to the genotype of the mice, using a software package we developed in MATLAB (Wu et al., 2009). Following behavior testing, some animals were perfused for histological analysis and blood was collected to determine serum hormone levels as previously described.

Male mice were singly housed ≥ 7 days prior to behavior testing. Males were tested twice for mating (30 min with an estrus female), then tested once for territory marking (1h in a fresh cage lined with watman paper), then tested twice for aggression (15 min with a group housed intruder male), then tested once for ultrasonic vocalization (3 min with a male intruder, followed by 3 min with female intruder).

REFERENCES

Allen, L.S., and Gorski, R.A. (1990). Sex difference in the bed nucleus of the stria terminalis of the human brain. J. Comp. Neurol. 302, 697–706.

Baker, M.E. (1986). Computer-based search for steroid and DNA binding sites on estrogen and glucocorticoid receptors. Biochem. Biophys. Res. Commun. 139, 281–286.

Bakker, J., Honda, S., Harada, N., and Balthazart, J. (2004). Restoration of male sexual behavior by adult exogenous estrogens in male aromatase knockout mice. Horm Behav 46, 1–10.

Baum MJ, Carroll RS, Cherrv JA, Tobet SA. Steroidal control of behavioural, neuroendocrine and brain sexual differentiation: studies in a carnivore, the ferret. J Neuroendocrinol. 1990;2:401–418.

Beatty, W.W. (1979). Gonadal hormones and sex differences in nonreproductive behaviors in rodents: Organizational and activational influences. Hormones and Behavior 12, 112–163.

Beyer, C. (1999). Estrogen and the developing mammalian brain. Anat Embryol 199, 379–390.

Breedlove, S.M., and Arnold, A.P. (1980). Hormone accumulation in a sexually dimorphic motor nucleus of the rat spinal cord. Science 210, 564–566.

Charest, N.J., Zhou, Z.X., Lubahn, D.B., Olsen, K.L., Wilson, E.M., and French, F.S. (1991). A frameshift mutation destabilizes androgen receptor messenger RNA in the Tfm mouse. Mol. Endocrinol. 5, 573–581.

Choleris, E., Clipperton, A.E., Phan, A., and Kavaliers, M. (2008). Estrogen receptor beta agonists in neurobehavioral investigations. Curr Opin Investig Drugs 9, 760–773.

Chung, W.C., Swaab, D.F., and De Vries, G.J. (2000). Apoptosis during sexual differentiation of the bed nucleus of the stria terminalis in the rat brain. J.

Neurobiol. 43, 234–243.

Clipperton Allen, A.E., Cragg, C.L., Wood, A.J., Pfaff, D.W., and Choleris, E. (2010). Agonistic behavior in males and females: effects of an estrogen receptor beta agonist in gonadectomized and gonadally intact mice. Psychoneuroendocrinology 35, 1008–1022.

Davis, E.C., Popper, P., and Gorski, R.A. (1996). The role of apoptosis in sexual differentiation of the rat sexually dimorphic nucleus of the preoptic area. Brain Res. 734, 10–18.

De Vries GJ, Simerly RB. Anatomy, development, and function of sexually dimorphic neural circuits in the mammalian brain. In: Pfaff DWea., editor. Hormones, Brain and Behavior. Amsterdam: Academic Press; 2002. pp. 137–191.

Dodson, R.E., and Gorski, R.A. (1993). Testosterone propionate administration prevents the loss of neurons within the central part of the medial preoptic nucleus. J. Neurobiol. 24, 80–88.

Feder, H.H., Naftolin, F., and Ryan, K.J. (1974). Male and female sexual responses in male rats given estradiol benzoate and 5 alpha-androstan-17 beta-ol-3-one propionate. Endocrinology 94, 136–141.

Fisher CR, Graves KH, Parlow AF, Simpson ER. Characterization of mice deficient in aromatase (ArKO) because of targeted disruption of the cyp19 gene. Proc Natl Acad Sci U S A. 1998;95:6965–6970.

Finney, H.C., and Erpino, M.J. (1976). Synergistic effect of estradiol benzoate and dihydrotestosterone on aggression in mice. Horm Behav 7, 391–400.

Forger, N.G. (2006). Cell death and sexual differentiation of the nervous system. Neuroscience 138, 929–938.

Gieske, M.C., Kim, H.J., Legan, S.J., Koo, Y., Krust, A., Chambon, P., and Ko, C. (2008). Pituitary Gonadotroph Estrogen Receptor-α Is Necessary for Fertility in Females. Endocrinology 149, 20–27.

Ginsburg, B., and Allee, W.C. (1942). Some Effects of Conditioning on Social Dominance and Subordination in Inbred Strains of Mice. Physiological Zoology 15, 485–506.

Goldstein, J.L., and Wilson, J.D. (1972). Studies on the pathogenesis of the pseudohermaphroditism in the mouse with testicular feminization. J. Clin. Invest. 51, 1647–1658.

Goldstein, L.A., and Sengelaub, D.R. (1992). Timing and duration of dihydrotestosterone treatment affect the development of motoneuron number and morphology in a sexually dimorphic rat spinal nucleus. J. Comp. Neurol. 326, 147–157.

Guillamón, A., Segovia, S., and del Abril, A. (1988). Early effects of gonadal steroids on the neuron number in the medial posterior region and the lateral division of the bed nucleus of the stria terminalis in the rat. Brain Res. Dev. Brain Res. 44, 281–290.

Hart, B.L. (1977). Neonatal dihydrotestosterone and estrogen stimulation: effects on sexual behavior of male rats. Horm Behav 8, 193–200.

Hart, B.L. (1979). Sexual behavior and penile reflexes of neonatally castrated male rats treated in infancy with estrogen and dihydrotestosterone. Horm Behav 13, 256–268.

Honda, S., Harada, N., Ito, S., Takagi, Y., and Maeda, S. (1998). Disruption of sexual behavior in male aromatase-deficient mice lacking exons 1 and 2 of the cyp19 gene. Biochem Biophys Res Commun 252, 445–449.

Juntti, S.A., Tollkuhn, J., Wu, M.V., Fraser, E.J., Soderborg, T., Tan, S., Honda, S.-I., Harada, N., and Shah, N.M. (2010). The Androgen Receptor Governs the Execution, but Not Programming, of Male Sexual and Territorial Behaviors. Neuron 66, 260–272.

Krege, J.H., Hodgin, J.B., Couse, J.F., Enmark, E., Warner, M., Mahler, J.F., Sar, M., Korach, K.S., Gustafsson, J.-Å., and Smithies, O. (1998). Generation and

reproductive phenotypes of mice lacking estrogen receptor β. PNAS 95, 15677–15682.

Kuiper, G.G., Enmark, E., Pelto-Huikko, M., Nilsson, S., and Gustafsson, J.A. (1996). Cloning of a novel receptor expressed in rat prostate and ovary. PNAS 93, 5925–5930.

Kuiper, G.G.J.M., Carlsson, B., Grandien, K., Enmark, E., Häggblad, J., Nilsson, S., and Gustafsson, J.-Å. (1997). Comparison of the Ligand Binding Specificity and Transcript Tissue Distribution of Estrogen Receptors α and β. Endocrinology 138, 863–870.

Kumar, V., Green, S., Staub, A., and Chambon, P. (1986). Localisation of the oestradiol-binding and putative DNA-binding domains of the human oestrogen receptor. EMBO J. 5, 2231–2236.

Lakso, M., Pichel, J.G., Gorman, J.R., Sauer, B., Okamoto, Y., Lee, E., Alt, F.W., and Westphal, H. (1996). Efficient in vivo manipulation of mouse genomic sequences at the zygote stage. Proc Natl Acad Sci U S A 93, 5860–5865.

Lein, E.S., Hawrylycz, M.J., Ao, N., Ayres, M., Bensinger, A., Bernard, A., Boe, A.F., Boguski, M.S., Brockway, K.S., Byrnes, E.J., et al. (2007). Genome-wide atlas of gene expression in the adult mouse brain. Nature 445, 168–176.

Lyon, M.F., and Hawkes, S.G. (1970). X-linked gene for testicular feminization in the mouse. Nature 227, 1217–1219.

Matsumoto, T., Honda, S., and Harada, N. (2003a). Alteration in sex-specific behaviors in male mice lacking the aromatase gene. Neuroendocrinology 77, 416–424

Matsumoto, T., Honda, S., and Harada, N. (2003b). Neurological effects of aromatase deficiency in the mouse. J. Steroid Biochem. Mol. Biol. 86, 357–365.

McCarthy, M.M. (2008). Estradiol and the Developing Brain. Physiol Rev 88, 91–124.

Murakami, S., and Arai, Y. (1989). Neuronal death in the developing sexually dimorphic periventricular nucleus of the preoptic area in the female rat: effect of neonatal

androgen treatment. Neurosci. Lett. 102, 185–190.

Naftolin, F., and Ryan, K.J. (1975). The metabolism of androgens in central neuroendocrine tissues. J. Steroid Biochem. 6, 993–997.

Nomura, M., Durbak, L., Chan, J., Smithies, O., Gustafsson, J.-A., Korach, K.S., Pfaff, D.W., and Ogawa, S. (2002). Genotype/age interactions on aggressive behavior in gonadally intact estrogen receptor beta knockout (betaERKO) male mice. Horm Behav 41, 288–296.

Nomura, M., Andersson, S., Korach, K.S., Gustafsson, J.-A., Pfaff, D.W., and Ogawa, S. (2006). Estrogen receptor-beta gene disruption potentiates estrogen-inducible aggression but not sexual behaviour in male mice. Eur. J. Neurosci. 23, 1860–1868.

Nordeen, E.J., Nordeen, K.W., Sengelaub, D.R., and Arnold, A.P. (1985). Androgens prevent normally occurring cell death in a sexually dimorphic spinal nucleus. Science 229, 671–673.

Ogawa, S., Chan, J., Chester, A.E., Gustafsson, J.-Å., Korach, K.S., and Pfaff, D.W. (1999). Survival of reproductive behaviors in estrogen receptor β gene-deficient (βERKO) male and female mice. PNAS 96, 12887–12892.

Ogawa, S., Chester, A.E., Hewitt, S.C., Walker, V.R., Gustafsson, J.-Å., Smithies, O., Korach, K.S., and Pfaff, D.W. (2000). Abolition of male sexual behaviors in mice lacking estrogen receptors α and β (αβERKO). PNAS 97, 14737–14741.

Ohe, E. (1994). [Effects of aromatase inhibitor on sexual differentiation of SDN-POA in rats]. Nippon Sanka Fujinka Gakkai Zasshi 46, 227–234.

Olsen, K.L. (1992). Genetic Influences on Sexual Behavior Differentiation. In Sexual Differentiation, A.A. Gerall, H. Moltz, and I.L. Ward, eds. (Springer US), pp. 1–40.

Ono, S., Geller, L.N., and Lai, E.V. (1974). TfM mutation and masculinization versus feminization of the mouse central nervous system. Cell 3, 235–242.

Otto, C., Fuchs, I., Kauselmann, G., Kern, H., Zevnik, B., Andreasen, P., Schwarz, G.,

Altmann, H., Klewer, M., Schoor, M., et al. (2009). GPR30 Does Not Mediate Estrogenic Responses in Reproductive Organs in Mice. Biol Reprod 80, 34–41.

Phoenix, C.H., Goy, R.W., Gerall, A.A., and Young, W.C. (1959). Organizing action of prenatally administered testosterone propionate on the tissues mediating mating behavior in the female guinea pig. Endocrinology 65, 369–382.

Raisman, G., and Field, P.M. (1971). Sexual dimorphism in the preoptic area of the rat. Science 173, 731–733.

Revankar, C.M., Cimino, D.F., Sklar, L.A., Arterburn, J.B., and Prossnitz, E.R. (2005). A Transmembrane Intracellular Estrogen Receptor Mediates Rapid Cell Signaling. Science 307, 1625–1630.

Robertson, K.M., Simpson, E.R., Lacham-Kaplan, O., and Jones, M.E. (2001). Characterization of the fertility of male aromatase knockout mice. J. Androl. 22, 825–830.

Sato, T., Matsumoto, T., Kawano, H., Watanabe, T., Uematsu, Y., Sekine, K., Fukuda, T., Aihara, K., Krust, A., Yamada, T., et al. (2004). Brain masculinization requires androgen receptor function. Proc. Natl. Acad. Sci. U.S.A. 101, 1673–1678.

Shughrue, P.J., Lane, M.V., and Merchenthaler, I. (1997). Comparative distribution of estrogen receptor-α and -β mRNA in the rat central nervous system. J. Comp. Neurol. 388, 507–525.

Simerly, R.B. (2002). Wired for reproduction: organization and development of sexually dimorphic circuits in the mammalian forebrain. Annu. Rev. Neurosci. 25, 507–536.

Simon, N.G., and Gandelman, R. (1978). The estrogenic arousal of aggressive behavior in female mice. Horm Behav 10, 118–127.

Simon, N.G., and Whalen, R.E. (1987). Sexual differentiation of androgen-sensitive and estrogen-sensitive regulatory systems for aggressive behavior. Horm Behav 21, 493–500.

Södersten, P. (1973). Estrogen-activated sexual behavior in male rats. Horm Behav 4, 247–256.

Södersten, P., Eneroth, P., Hansson, T., Mode, A., Johansson, D., Näslund, B., Liang, T., and Gustafsson, J.A. (1986). Activation of sexual behaviour in castrated rats: the role of oestradiol. J. Endocrinol. 111, 455–462.

Sumida, H., Nishizuka, M., Kano, Y., and Arai, Y. (1993). Sex differences in the anteroventral periventricular nucleus of the preoptic area and in the related effects of androgen in prenatal rats. Neurosci. Lett. 151, 41–44.

Toda, K., Saibara, T., Okada, T., Onishi, S., and Shizuta, Y. (2001). A loss of aggressive behaviour and its reinstatement by oestrogen in mice lacking the aromatase gene (Cyp19). J. Endocrinol. 168, 217–220.

Tronche, F., Kellendonk, C., Kretz, O., Gass, P., Anlag, K., Orban, P.C., Bock, R., Klein, R., and Schütz, G. (1999). Disruption of the glucocorticoid receptor gene in the nervous system results in reduced anxiety. Nat. Genet. 23, 99–103.

Unger, E.K., Burke Jr., K.J., Yang, C.F., Bender, K.J., Fuller, P.M., and Shah, N.M. (2015). Medial Amygdalar Aromatase Neurons Regulate Aggression in Both Sexes. Cell Reports 10, 453–462.

Whalen, R.E., and Luttge, W.G. (1971). Testosterone, androstenedione and dihydrotestosterone: Effects on mating behavior of male rats. Hormones and Behavior 2, 117–125.

Wu, M.V., Manoli, D.S., Fraser, E.J., Coats, J.K., Tollkuhn, J., Honda, S.-I., Harada, N., and Shah, N.M. (2009). Estrogen masculinizes neural pathways and sex-specific behaviors. Cell 139, 61–72.

Xu, X., Coats, J.K., Yang, C.F., Wang, A., Ahmed, O.M., Alvarado, M., Izumi, T., and Shah, N.M. (2012). Modular Genetic Control of Sexually Dimorphic Behaviors. Cell 148, 596–607.

Yang, C.F., Chiang, M.C., Gray, D.C., Prabhakaran, M., Alvarado, M., Juntti, S.A.,

Unger, E.K., Wells, J.A., and Shah, N.M. (2013). Sexually dimorphic neurons in the ventromedial hypothalamus govern mating in both sexes and aggression in males. Cell 153, 896–909.

Chapter 4

Turning ON Caspases with Genetics and Small Molecules

Elizabeth K. Unger[‡§1] Charles W. Morgan*[†1] Olivier Julien*[1], Nirao M. Shah[‡], James A. Wells*[¶]

* Department of Pharmaceutical Chemistry, University of California, San Francisco, California, USA

[†] Graduate Group in Chemistry and Chemical Biology, University of California, San Francisco, California, USA

[‡] Department of Anatomy, University of California, San Francisco, California, USA

[§] Program in Biomedical Sciences, University of California, San Francisco, California, USA

[¶] Department of Cellular and Molecular Pharmacology, University of California, San Francisco, California, USA

[1] Authors contributed equally

The text of this chapter is a reprint of material that appeared in Methods in Enzymology.

Methods Enzymol. 2014;544:179-213.

ABSTRACT

Caspases, aspartate-specific cysteine proteases, have fate-determining roles in many cellular processes including apoptosis, differentiation, neuronal remodeling, and inflammation (for review, see Yuan & Kroemer, 2010). There are a dozen caspases in humans alone, yet their individual contributions toward these phenotypes are not well understood. Thus, there has been considerable interest in activating individual caspases or using their activity to drive these processes in cells and animals. We envision that such experimental control of caspase activity can not only afford novel insights into fundamental biological problems but may also enable new models for disease and suggest possible routes to therapeutic intervention. In particular, localized, genetic, and small-molecule-controlled caspase activation has the potential to target the desired cell type in a tissue. Suppression of caspase activation is one of the hallmarks of cancer and thus there has been significant enthusiasm for generating selective small-molecule activators that could bypass upstream mutational events that prevent apoptosis. Here, we provide a practical guide that investigators have devised, using genetics or small molecules, to activate specific caspases in cells or animals. Additionally, we show genetically controlled activation of an executioner caspase to target the function of a defined group of neurons in the adult mammalian brain.

KEYWORDS

Caspase; Activation; Cell death; Apoptosis; Cre-Lox; Protease; SNIPer; Ventromedial Hypothalamus; VMHvl; Sexual Behavior; Aggression

1. USE OF CHEMICAL-INDUCED DIMERIZERS TO ACTIVATE CASPASES

1.1. Controlling protein–protein interactions leads to selective activation of caspases

The elucidation of cell signaling has been empowered by chemical genetic approaches. In

particular, protein-fragment complementation assays and chemical-induced dimerization (CID) have been very powerful approaches (Fig. 4.1A) (Fegan et al., 2010, Remy and Michnick, 2007 and Spencer et al., 1993). While the ability to control transcription-based circuits has been known for decades, only recently have signaling biologists learned to harness and engineer orthogonal circuits to selectively activate proteases. Proteolysis is an irreversible posttranslational-modification that directs the fate of cells in apoptosis, protein degradation, blood coagulation, and many other processes. Here, we

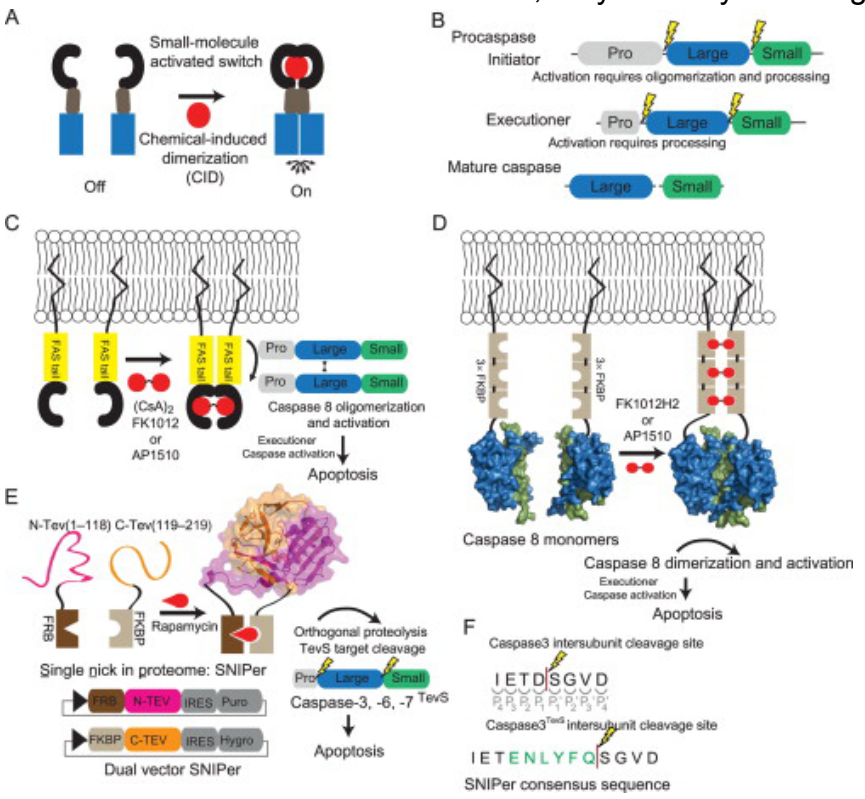

Figure 4.1. Schematic overview of chemical genetic strategies for selective caspase activation.

(A) Chemical-induced dimerization (CID) utilizes dimerization domains, dependent on cell-permeable small molecules, to control the proximity of signal transduction domains (blue). The chemical genetic strategy of CID creates an orthogonal circuit in the cell, thereby enabling the control of the ON/OFF state of signal transduction. (B) Procaspases are composed of three domains; a prodomain, a large subunit, and a small subunit. Initiators have a long prodomain and require both oligomerization and processing for activation. The executioners are predimerized and they have a short prodomain and proteolysis at the large–small domain junction is sufficient for activation. (C) Utilizing a CID-based approach, FAS tails are dimerized by the addition of the symmetric small molecule, AP1510 or FK1012, thereby reconstituting the caspase-8 (PDB ID 1QTN) activation scaffold and ultimately resulting in apoptosis. (D) Direct caspase-8 activation via CID. (E) The engineered split-tobacco etch viral (TEV) variant, single nick in proteome (SNIPer), used for inducible and selective cleavage of the executioner caspase isoforms (TEV structure PDB ID 1LVM). Each SNIPer half is expressed from a single plasmid that coexpresses an IRES-driven drug-resistance marker for stable cell line engineering. The addition of rapamycin causes the heterodimerization of FKBP and FRB, thereby rescuing TEV protease activity. (F) The TEV protease consensus sequence (green) is inserted into the caspase-processing site to generate a TevS allele, susceptible to SNIPer-mediated proteolysis.

discuss practical approaches that we and others have recently employed to selectively activate caspases using CID strategies.

There are two classes of apoptotic caspases: initiators (caspase-8, -9, -10) which are activated by oligomerization, and the primary executioners (caspase-3 and -7) that are activated by proteolysis mediated by upstream proteases (initiator caspases or granzyme B) (Fig. 4.1B). The purpose of this first section is to (1) briefly review previous approaches and research highlights that employed chemical genetic strategies used to activate caspases, primarily caspase-8, (2) summarize the progress that our laboratories have made in selectively turning on apoptosis via orthogonal executioner caspase activation, and (3) provide a detailed method for selective activation of executioner caspases employing this chemical genetic strategy.

1.2. Oligomerization strategies for selective caspase activation

1.2.1. Selective caspase-8 oligomerization and activation

The first target for CID activation of caspases was caspase-8, a classic initiator caspase involved in the extrinsic apoptosis pathway (Muzio et al., 1998 and Yang et al., 1998). CID activation of caspase-8 facilitated elegant experimentation of the induced-proximity hypothesis (Salvesen & Dixit, 1999), which is that the monomeric proenzyme is activated through dimerization. Previous studies have shown that heterologous expression of the inactive zymogens retained modest catalytic activity prior to their proteolytic processing. Initial tests of the caspase-8 cellular activation mechanism were described in two simultaneous papers that demonstrated the role of receptor oligomerization in caspase-8 activation (Belshaw et al., 1996 and Spencer et al., 1996). This work showed that it was possible to activate procaspase-8 through CID of the intracellular FAS receptors using either a homodimerization analog of FK506, FK1012, a cyclosporin derivative $(CsA)_2$ (Fig.

4.1C). A year later, the symmetric small molecule, AP1510, was used to oligomerize FAS tails (Amara et al., 1997). The CID approach was then applied directly to caspase-8. Competing caspase-8 chimeras, containing trimeric homodimerization domains demonstrated that oligomerization was sufficient for robust caspase-8 activation (Muzio et al., 1998 and Yang et al., 1998) (Fig. 4.1D). Other investigators showed that conditional dimerization of known monomeric initiator caspases-8, -9, or 10 could result in activation yet the predimerized executioner caspase-3 was not activated by oligomerization (Chen, Orozco, Spencer, & Wang, 2002). CIDs have now been applied to several caspases and together constitute a collection of artificial death switches (Steller, 1998).

Further work showed that during activation, procaspase-8 both dimerizes and undergoes proteolysis (Chang et al., 2003, Hughes et al., 2009, Kang et al., 2008, Murphy et al., 2004, Pop et al., 2007 and Sohn et al., 2005). Utilizing the unique specificity of tobacco etch viral (TEV) protease in mammalian cells and the previously described CID approaches for oligomerization, both methods of activation have been beautifully tested simultaneously (Oberst et al., 2010). Oberst et al. showed that dimerization alone in the absence of proteolysis of the intersubunit linker or prodomain failed to lead to activation, as detected by IETDase activity. Similarly, selective cleavage by TEV protease, in mutated linker regions with the TEV consensus sequences failed to activate the caspase-8. Only the combination of induced dimerization and proteolytic processing resulted in full activation of caspase-8. These experiments highlight the utility of engineered inducible and orthogonal activation strategies for the caspases, thereby permitting a more complete understanding of their function and regulation.

1.2.2. In vivo strategies for selective caspase activation

Inducible caspase activation has been utilized in several *in vivo* strategies that include conditional induction of apoptosis during development in *C. elegans*, mouse adipocytes, and a caspase-9-based artificial death switch for T-cell therapies. In order to reconstitute

Ced-3/caspase-3 activity in *C. elegans* during development, individual subunits of caspase-3 chimeras were fused to antiparallel leucine-zippers and expressed by separate promoters, and selective apoptosis was observed only when promoters overlapped in cells (Chelur & Chalfie, 2007). Pajvani and colleagues demonstrated the power in reversible CID-based approaches in mice, upon removal of the dimerizer, thereby leading to the inactivation of the caspase-8 death switch in adipocytes; mice regained weight lost during treatment (Pajvani et al., 2005). Cell-based treatments for cancer and regenerative-based medicine hold promise, yet in the event of an adverse effect, elimination of the engineered cells would be critical. Toward this end, several artificial death switches, utilizing similar CID strategies discussed above, have demonstrated their usefulness in selectively killing engineered T-cells, demonstrated in mice and later in human patients (Di Stasi et al., 2011 and Straathof et al., 2005).

1.3. Design of orthogonal and selective proteolysis for individual caspase activation

1.3.1. Inducible and selective proteolysis

We have recently shown one can selectively activate the executioner caspases through an orthogonal and selective CID approach of an initiating protease. This utilized a reengineered version of the split-TEV protease (Wehr et al., 2006), we call the SNIPer (single nick in proteome). The SNIPer was optimized by truncating the C-terminus of TEV and swapping the order of the heterodimerization domains of FKBP/FRB (Gray, Mahrus, & Wells, 2010). This new design greatly reduced background of TEV activity caused by small amounts of constitutive TEV dimer formation. The SNIPer leads to the rescue of the TEV activity by the addition of the cell-permeable small-molecule, rapamycin, which was shown using a genetically encoded TEV FRET reporter (Gray et al., 2010). Selective and exclusive proteolysis of each target caspase by TEV is achieved by inserting the TEV

consensus cleavage motif into the endogenous caspase-processing sites (Fig. 4.1E). Once each caspase is activated, it is able to process endogenous targets, including wild-type caspases, but cannot activate the TEV-sensitive caspase alleles (caspase^{TevS}) since they are missing the caspase consensus site.

TEV cleavage sequences were introduced into the two major processing sites in caspases-3, -6, and -7. Selective cleavage of the site between the prodomain and the large subunit did not lead to activation, but all three caspases were activated upon SNIPer-mediated proteolysis between the large and small subunit. When these alleles were stably transfected into human 293 cells, only activation of caspases-3 and -7 lead to apoptosis, whereas caspase-6 did not, therefore suggesting it is not a typical executioner. The executioner caspases were shown to be ubiquitinated and degraded by the ubiquitin proteasome system after activation, and proteasome inhibitors greatly accelerate SNIPer-mediated caspase^{TevS}-driven apoptosis. Interestingly, caspase-6^{TevS} activation by SNIPer is lethal in the presence of proteasome inhibitors.

1.3.2. Generating SNIPer substrates: TEVs alleles

In order to generate SNIPer-cleavable substrates, we employ an insertion strategy using standard molecular biology techniques. Briefly, we replace the P1 residue of the endogenous cleavage site with the six residues required for TEV recognition and cleavage (ENLYFQ↓). This insertion yields an orthogonal substrate (i.e., no longer cleavable by caspases) because the substrate lacks the required aspartic residue followed by a small amino acid (G/S/A). We also verify the P1′ residue as TEV prefers G/S at P1′ and depending on the endogenous sequence, this may also need to be mutated. A variety of PCR techniques can be used to insert the six residues required for TEV cleavage, such as standard overlap extension PCR or kunkel mutagenesis for simultaneous insertions (Tonikian, Zhang, Boone, & Sidhu, 2007). We always test our constructs using transient transfections prior to making stable cell lines.

1.4. Cell engineering

Direct caspase dimerization or orthogonal upstream protease activation both require substantial cellular engineering. The requirements for each strategy vary and each has its own set of advantages and disadvantages. Here, we discuss in detail our approach to cellular engineering stable cell lines that express the SNIPer and subsequent screening for caspase^{TevS}-sensitive proteolysis. It should be noted that since the SNIPer is a highly selective and orthogonal mechanism capable of inducing caspase processing, the target substrate does not need to be a caspase but the processing site needs to be accessible to TEV protease. Our first approach consisted of engineering cells to constitutively express the SNIPer using traditional MMLV retrovirus transduction (Ory, Neugeboren, & Mulligan, 1996). However, we recently have had better success using a lentiviral-based approach that enables for a wider range of engineered target cell lines (Cooray, Howe, & Thrasher, 2012).

1.4.1. Protocol for SNIPer stable cell line engineering (inducible and selective proteolysis)

Our strategy for stable expression of both halves of SNIPer has been described previously (Gray et al., 2010). The purpose of this section is to highlight some specific details, technical challenges, and potential solutions that can be anticipated during cellular engineering with the SNIPer (Fig. 4.2).

1.Culture HEK293/GPG cells in DMEM supplemented with 10% FBS, nonessential amino acids, sodium pyruvate, l-glutamine, penicillin–streptomycin, 300 μg/mL G418, 2 μg/mL puromycin, and 1 μg/mL doxycycline.

2.A modified protocol for lipofectamine2000 (Life Technologies) is used to transfect GPG cells. We find robust transfection efficiency using only ¼ of the recommended amount of lipid mixture and that the decreased amount also minimizes cellular toxicity. We co-transfect both N- and C-terminal SNIPer plasmids together to increase successful generation of double-positive clones. The media is replaced after 5 h with fresh DMEM without

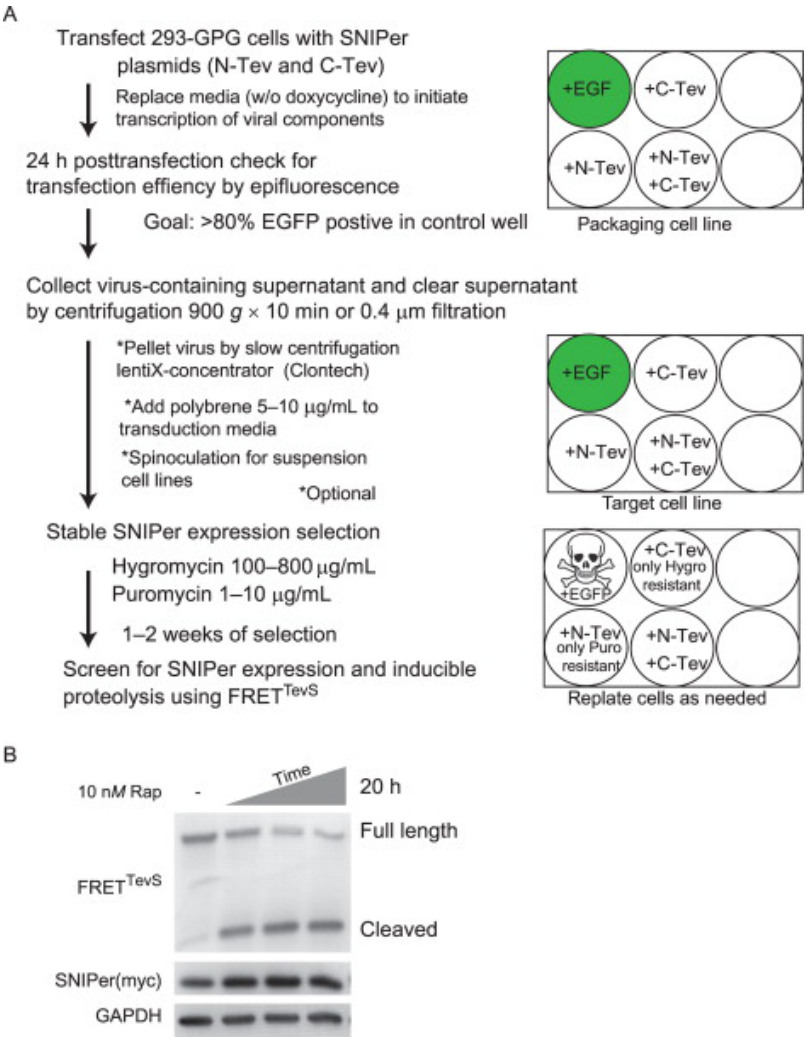

Figure 4.2. Cell engineering overview.

(A) Summary of the protocol used for virus production and stable cell line engineering of SNIPer expressing cells. (B) A representative Western immunoblot of SNIPer engineered cells, transfected with FRET^{TevS} reporter, shows selective proteolysis of the reporter over time.

doxycycline and antibiotics. Transfection efficiency is visually inspected at 24 h posttransfection by examining a control well that has been transfected in parallel with a fluorescent protein (EGFP or mCherry). We generally observe > 80% transfection efficiency.

3. Viral-containing supernatant is collected at 48 and 72 h posttransfection.

4. The viral supernatant is clarified of cellular debris by either centrifugation at 900 × *g* for 10 min or passage through a SFCA 0.4 μm filter. Optional: virus concentration by Clontech Lenti-X concentrator.

5. Cleared supernatant is added to previously plated adherent target cell lines (at 60–70% confluency) and incubated overnight. Polybrene increases effective viral titers by neutralizing the charge on the cell surface. Appropriate concentrations of polybrene should be screened on each new cell types. Typically, we use 8 μg/mL for HEK293 and HeLa cells. Standard spinoculation protocols may be employed when targeting suspension cell lines.

6. We start selection 24 h post target cell transduction. At this point, puromycin and hygromycin are simultaneously added to select for double-positive cells, those that have integrated both halves of the SNIPer. Each half of the SNIPer also coexpresses via internal ribosomal entry site (IRES)-dependent translation of an antibiotic resistance marker (Fig. 4.1E). Dual selection usually takes ~ 14 days and cells are replated as necessary.

7. Tips on successful selections

a. Adjusting the growing density of the cells aids in the successful recovery of cells difficult to transduce. Drug selection is also very dependent upon cell density and rate of cell division. We always use a nontransduced cell line treated with selection antibiotics to ensure that all nontransduced cells are eliminated.

b. In most cases, heterogeneous pools of SNIPer positive cells are sufficient for further study and transfection with caspase^{TevS} isoforms. The SNIPer positive cell line can be used as a parental cell line for further transduction with caspase^{TevS} isoforms.

c. Typical ranges for selections when using puromycin and hygromycin are 1–10 μg/mL and 100–800 μg/mL, respectively. The effective concentration is cell-type specific. To ensure proper selection, we perform serial selections, first with puromycin since it is fast acting and then with the slower acting hygromycin. When working with a new cell line, we utilize fluorescent proteins with puromycin and hygromycin resistance to get immediate and observable feedback on transduction efficiency and progression of selection.

1.4.2. Assessing SNIPer-mediated proteolysis and rapamycin side effects

In addition to binding the SNIPer, rapamycin also binds to endogenous FK506-binding protein (FKBP) forming a complex that binds the FRB domain of mTOR and results in mTOR inhibition. We, and others, have shown that this problem is reduced by minimizing the dose of rapamycin (typically 5–10 n*M* needed to activate the SNIPer) and in combination the overexpression of the FKBP and FRB from the SNIPer, acts as a buffer

to compete with endogenous FK506 binding. Nonetheless, we recommend measuring the level of mTOR inhibition by monitoring the phosphorylation state of the mTOR substrate S6 kinase via Western immunoblotting. We typically monitor this using antibodies for p70 S6 kinase and phoso-p70 S6 kinase (Cell Signaling Technology, #9202 and #9205). One should expect levels of mTOR inhibition in the presence of SNIPer to vary depending on the particular cell line used and the SNIPer expression level.

As a first screen of SNIPer function on a TevS target substrate, it is convenient to test it in transiently transfected cells. We typically use a molar ratio of 6:1 SNIPer halves to substrate^{TevS}. This ratio yields the most consistent results for substrate cleavage. Once substrate cleavage is observed to be rapamycin dependent, then one should move to stably transfected cells to ensure more homogeneity in the cell population.

Western immunoblotting is our standard technique for tracking cleavage of engineered TEV cleavage site containing-substrates and expression of the SNIPer (each half is N-terminally myc tagged). It should be noted that FRB fusions are regularly observed to be less stable than FKBP fusions (Edwards & Wandless, 2007). The kinetics of cleavage by the SNIPer varies depending on the substrate being studied and the readout. We initially test for substrate cleavage following 8 h of rapamycin treatment, but we observe rapamycin-dependent cleavage in as little as 1 h after its addition with certain substrates.

1.4.3. Considerations when employing SNIPer-mediated proteolysis

When designing a SNIPer-mediated research project, it is important to be aware of some of its limitations. As is common with any protein-engineering strategy that introduces conditional control of an enzyme, background activity, for example, TEV protease activity in the absence of rapamycin, presents a challenge and needs to be thoroughly considered when looking at the overall signaling pathway. An additional consideration is the partial loss of catalytic activity of engineered variants. It has been shown that split-TEV

constructs suffer from both constitutive background and low maximal activity level (Wehr et al., 2006 and Williams et al., 2009). The SNIPer was designed to minimize background proteolysis as this was essential for selective caspase^{TevS} activation. For other substrates, where complete cleavage of the substrate is necessary, there are additional challenges with the SNIPer. First, the endogenous substrate will compete with the function of the engineered TevS allele, thereby masking the functional consequence of substrate^{TevS} cleavage. Second, the SNIPer has only about ~ 30% the native activity of intact full-length TEV. In some cases, the transcriptional expression rate of the full-length substrate may exceed the catalytic rate of the SNIPer. If complete cleavage of the substrate is required, then other approaches may need to be considered.

1.4.4. Next-generation SNIPer-based stable cell line creation (lentiviral-based engineering and single-vector versions)

The adaptation of the SNIPer to a lentiviral-based backbone enables the creation of a wider range of cell lines with higher titers, including nondividing cells and cell lines more resistant to traditional retroviral delivery of transgenes. A single-vector version with bicistronic expression of the SNIPer has been constructed and varying iterations are currently being tested for robust and reliable inducible proteolysis. We will make these available upon request once validation is completed (C. W. Morgan & J. A. Wells unpublished).

1.5. Monitoring cell death phenotypes

Following the successful observation of rapamycin-induced cleavage of the targeted protein in cells using Western immunoblotting, the phenotype of this cleavage event can be characterized. This volume offers many detailed protocols, and in addition, Galluzzi et al. reviewed the latest techniques for monitoring cell death (Galluzzi et al., 2009). Assay selection should be matched with the specific cell line and available equipment for characterization. Often, the most convenient method for apoptosis is to measure

cell viability following activation by standard methods such as Cell Titer Glo (Promega), MTT assay, or propidium iodide staining. Depending on the cell type, concentration of rapamycin, expression levels of the split-TEV halves, caspase^{TevS} allele, the time to death, and homogeneity of the cells will need to be screened. Generally, with caspase-3^{TevS} we initially observe a decrease in viability starting at 3 h following activation. Once an initial dose response and corresponding time course have been completed, more detailed characterization of the engineered cell line is suggested using TUNEL and Annexin V staining, DNA laddering, and caspase-3 and PARP cleavage. Together, these phenotypic observations constitute hallmarks of apoptosis.

1.6. Conclusions and future questions

Harnessing CID strategies has expanded our ability to test different activation modes for apoptotic caspases, oligomerization, and processing. Previous research on selective activation on caspases has given us crucial insight into the process that cells use to dismantle themselves during apoptosis. The chemical genetic tools outlined above give researchers an unprecedented tool to selectively induce apoptosis in a controlled circuit that conveniently feeds into the endogenous apoptotic pathway. Further engineering for inducible and selective activation needs to be undertaken for the inflammatory caspases-1, -4, -5, -11, and the remaining apoptotic caspase-2. The ability to specifically control caspase signal transduction through selective activation could play important roles in future cell-based therapies in the form of death switches. The conditional control of caspase activation will certainly be important for basic science research, as we uncover more details about the role of proteolysis in controlling cell fate decisions and the cellular mechanisms that antagonizes caspase activation. The chemical genetic strategies outlined above enable researchers highly selective control to turn on caspase-mediated signaling pathways.

2. USE OF CRE-LOXP AND A SELF-ACTIVATING CASPASE-3^{TEVS} FOR CONDITIONAL APOPTOSIS OF NEURONS

2.1. Introduction

Unlike the cells in most other tissues, neurons that are born during development are primarily the same neurons that will make up the nervous system for the remainder of an organism's life. Neurons are postmitotic cells and do not readily regenerate, meaning that any lesions incurred during an organism's life will be permanent. Moreover, neurons are remarkably heterogeneous, anatomically, molecularly, and functionally. In order to meaningfully study the function of such diverse neuronal cell types in anatomically distinct regions, we need a means of performing targeted lesions and other manipulations to assess their function. We have utilized the caspase-3^{TevS} to specifically ablate progesterone receptor (PR)-expressing neurons in the ventrolateral region of the ventromedial hypothalamus (VMHvl) in mice, and showed that this region is critical for sexual behavior in both sexes and aggression in males.

2.2. Viral-mediated neuronal ablation

We have encoded the caspase-3^{TevS} described in Section 1, and a full-length TEV protease, in a single adeno-associated virus (referred to as AAV-flex-taCasp3-TEVp) such that expression of both transgenes and enzymatic activation of caspase-3^{TevS} is dependent on Cre recombinase. In this review, we refer to this virus as AAV-flex-C3-Tp. Cre-loxP is a bipartite genetic system that allows for reproducible, inducible targeting of any molecularly defined cell type. We injected this virus into the VMHvl of PR-IRES-Cre mice and were able to ablate, on average, ≥ 95% of PR neurons while leaving neighboring Cre-nonexpressing cells intact (Fig. 4.3) (Yang et al., 2013). This system is highly modular and applicable not just to PR neurons, but, in principle, any molecularly distinct neuronal population or other Cre-expressing cell type in the body. Indeed, we have successfully used this virus to ablate other distinct neuronal populations engineered to express Cre

recombinase *in vivo* (E. K. Unger & N. M. Shah unpublished observations).

2.2.1. Self-activating caspase-3^{TevS} transgene

Caspase-3 was modified to encode the TEV protease consensus recognition sequence, caspase-3^{TevS}, as described above. Our virus coexpresses caspase-3^{TevS} and TEV protease linked by a T2A sequence. T2A is a short, self-cleaving peptide that allows multiple proteins to be expressed from the same transgene (Provost, Rhee, & Leach, 2007). T2A has been shown to be more efficient than an IRES for the expression of multiple products and is effective in neurons (Tang et al., 2009). It is also smaller and thus easier to package within the AAV genome.

2.2.2. Cre-loxP

Our strategy uses the bipartite Cre-loxP system wherein Cre recombinase recognizes and recombines two short palindromic loxP sites eliminating the intervening sequence (Orban et al., 1992, Sauer, 1987 and Sauer and

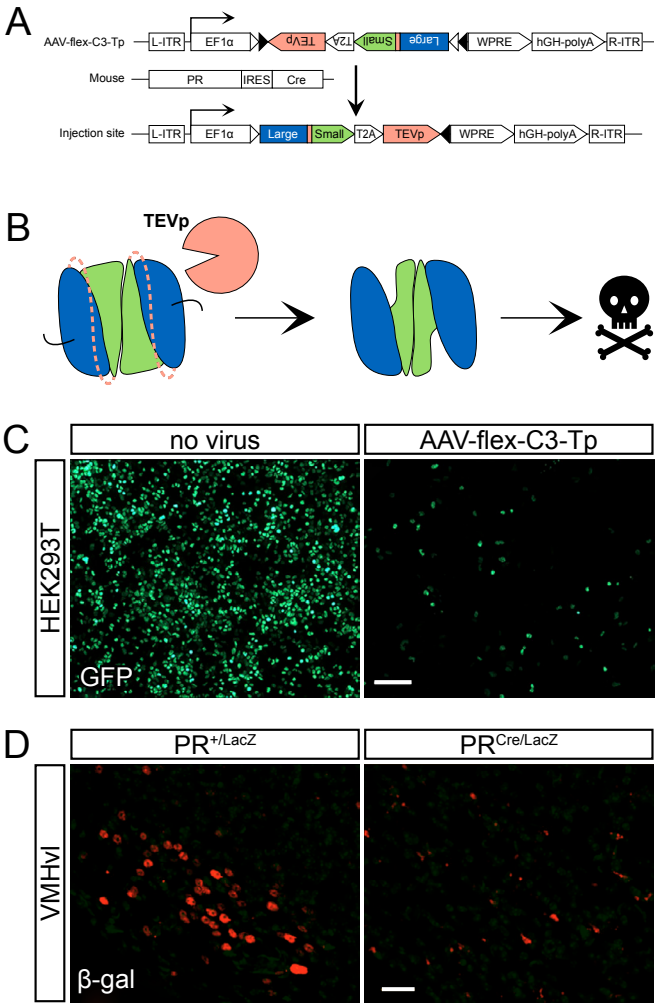

Figure 4.3. Utilizing AAV-flex-C3-Tp.

(A) Strategy to ablate PR-expressing cells *in vivo*. (B) Within Cre + cells, the TEV protease will cleave its consensus recognition sequence (dashed lines) between the large and small subunits of the caspase-3 dimer, activating it and leading to apoptosis. (C) The AAV-flex-C3-Tp encoding plasmid was transfected into HEK293T cells expressing the fusion protein Cre-GFP. Cell death was evaluated after 1 week. (D) AAV-flex-C3-Tp was stereotaxically targeted to the ventrolateral region of the VMH (VMHvl) of adult *PR$^{+/LacZ}$* and *PR$^{Cre/LacZ}$* mice which harbor the transgenes nuclear LacZ (*PR^{LacZ}* allele) or Cre recombinase (PRCre allele) inserted into the PR locus by homologous recombination. Cell death was evaluated after 4 weeks. Scale bars represent 100 μm (C) and 25 μm (D). (C) and (D) are reproduced from Yang et al. (2013).

Henderson, 1988). In our strategy, Cre has been knocked-in to the PR locus to generate the PR-IRES-Cre mouse strain, such that expression of Cre mirrors the endogenous expression of PR (Yang et al., 2013). The virally encoded caspase-3^{TevS} and TEV protease are flanked by loxP sites such that in PR-expressing cells, both proteins will be expressed and induce apoptosis. Although AAV can infect cells indiscriminately, only Cre-expressing cells will switch on functional expression of the encoded transgene, thereby enabling genetically targeted ablation of the desired cell type exclusively without bystander toxicity to Cre-nonexpressing cells.

2.2.3. Flex

Caspase-3 is an executioner caspase, and leaky expression of the enzyme even at low levels can elicit apoptosis. We therefore wished to restrict caspase-3 expression exclusively to cells expressing Cre recombinase. Accordingly, we employed a strategy (flex switch) that utilizes flanking heterologous loxP sites to encode the desired transgene, *caspase-3^{TevS}-T2A-TEV protease* in our case, in an orientation reversed to that of the promoter driving expression of the transgene (Atasoy et al., 2008, Schnütgen et al., 2003 and Sohal et al., 2009). This strategy ensures that the transgene cannot be expressed except in the presence of Cre recombinase, whose activity irreversibly switches the transgene on to the same strand as the promoter. In our case, the flex switch restricts coexpression of caspase-3^{TevS} and TEV protease to Cre-expressing cells.

2.2.4. AAV

We chose to encode the *caspase-3^{TevS}-T2A-TEV protease* transgene in an AAV because it is the best option for our *in vivo* application. First, it is not a retrovirus and thus only requires BSL-1. Second, it has extremely low immunogenicity so there is less worry of an immune response. Third, it has a very broad tropism, which can be made still broader with different serotypes—there are currently 11 in use today with “preferences” for different cell types (Taymans et al., 2007). Fourth, it can be produced at very high titer (10^{12}–10^{13}),

and there are several commercial facilities dedicated to producing high-titer AAV for a nominal fee. A potential drawback of using AAV is that its genome is small and it can only accept 4–5 kb DNA inserts. However, this was not an issue for our studies because our transgenic insert is within this range.

An alternative approach to delivering the *caspase-3^{TevS}-T2A-TEV protease* transgene would be to generate a mouse strain harboring this transgene in a Cre-dependent manner. However, promoter sequences that drive transgene expression in a spatiotemporally appropriate manner in the adult VMHvl remain to be defined, and our viral approach circumvents this caveat. Our approach does necessitate, however, that the virus must be injected manually into every experimental animal. Viruses provide the added convenience of being much faster and less resource intensive to generate, produce, and maintain than mouse lines.

2.3. Protocol: Cloning the caspase-3^{TevS}-T2A-TEVp construct and AAV plasmid expression

1. Assembling the caspase-3^{TevS}-T2A-TEVp construct

The *caspase-3^{TevS}* allele described above (see Section 1.3) was stitched to a T2A-TEVp sequence using overlapping PCR. The resulting *caspase-3^{TevS}-T2A-TEVp* transgene was cloned in an orientation reverse to that of the ubiquitous promoter, EF1α, into the pAAV-EF1α-DIO-WPRE-pA plasmid (Sohal et al., 2009). This plasmid is currently available from Addgene.

2. Tips for growing AAV plasmids

a. Subcloning in AAV vectors can be difficult because the two encoded inverted terminal repeats (ITRs) often render the plasmid unstable. It is therefore desirable to perform as many subcloning steps as possible in a standard plasmid lacking ITRs prior to moving the transgene into the AAV vector.

b. When transforming, be sure to use high-competency cells that have been

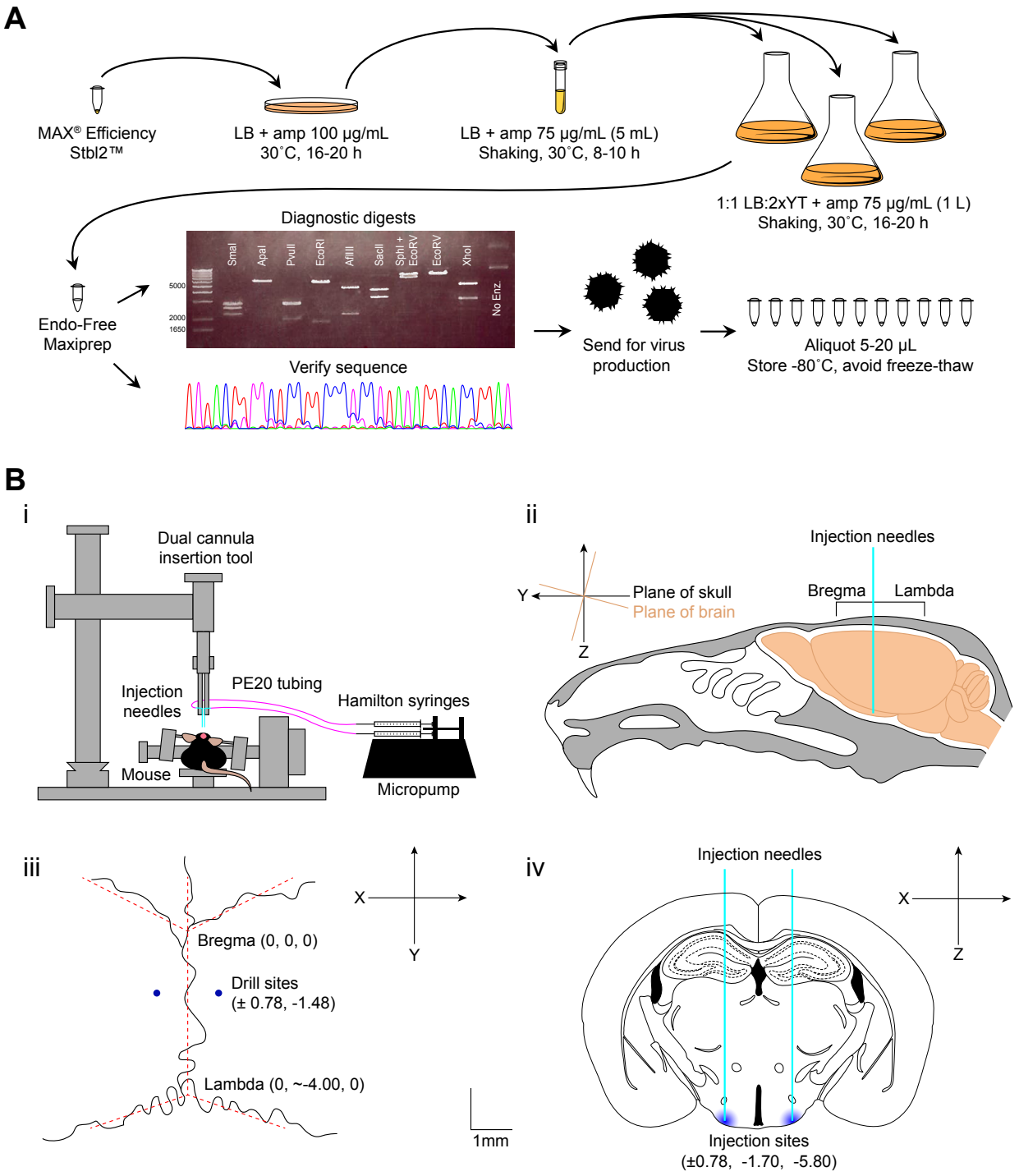

Figure 4.4. Overview of AAV virus production and injection.

(A). Summary of the protocol used for AAV plasmid growth and verification for virus production. Maxipreps originating from the same colony were pooled for diagnostics. (B) Schematic of virus injection. (i) Stereotax and micropump setup: injection needles are connected to Hamilton syringes by PE20 tubing. The syringes are depressed steadily and simultaneously by a micropump. (ii) Orientation of the brain within the cranial cavity. Note the 15° slant of the

specifically designed for unstable sequences. We use MAX Efficiency® Stbl2™ high-competency cells.

c. Plate these cells on standard LB + ampicillin (amp; 100 µg/mL) plates and grow 16–20 h at 30 °C.

d. Pick a colony for a starter culture and grow it for 8–10 h at 30 °C in LB with amp (75 µg/mL). It is best to pick several colonies from which to make starter cultures and then expand only the best growing one for the final large-scale maxi-prep culture.

e. The large-scale culture should be grown in 1:1 LB:2×YT with amp (75 µg/mL) at 30 °C for 16–20 h. Because these cells are grown at 30 °C rather than 37 °C, they will expand much more slowly. These are also low-copy number plasmids meaning that the yield will be quite low. It may be better to split the starter culture into several larger cultures rather than simply growing a single culture for a longer period of time.

f. We use the Endo-Free Plasmid Maxi Kit from Qiagen to purify the plasmid DNA. In our hands, the yield from these columns is ~ 300 µg/L culture.

g. Diagnostic digests of the purified plasmid DNA are essential to exclude recombination events triggered by the ITRs. We digested the AAV-flex-C3-Tp plasmid with eight different enzymes to ensure each element was present and of the expected size (Fig. 4.4A). Some viral cores even require specific digests before they will initiate virus production from the plasmid DNA.

h. Verifying the sequence of the plasmid is also very important, including all subcloning boundaries and the ITRs. Because of the repeats, sequencing will often fail just inside the ITRs, but it is important to verify that they are present and that

skull relative to the brain which is common in inbred strains. (iii) Cranial sutures with bregma and lambda marked. (iv) Coronal section through the VMHvl where we injected the virus. Note that the y coordinate is different from the drilling site in (iii) because of the 15° slant. Scale bar represents 1 mm (iii and iv). Figure (iv) was modified from Paxinos Brain Atlas (Paxinos & Franklin, 2004).

the flanking sequences are intact. We sequenced the AAV-flex-C3-Tp plasmid with nine different primers (Table 8.1) that each covered 700–900 bp in an overlapping manner to give the entire sequence of the insert and ITRs.

i. Most AAV's are produced in dedicated cores. Many viral cores have a minimum requirement for the plasmid you provide them, typically 300–500 μg of plasmid DNA.

j. Once the virus is made, it should be aliquoted (typically 5–20 μL) and frozen at − 80 °C. Once the aliquot is thawed, it should not be refrozen as freeze–thaw

Sequence	Orientation	Position	Reads Through
CCT CTG ACT TGA GCG TCG AT	forward	7107	Into left ITR
ACA CGA CAT CAC TTT CCC AG	reverse	314	Into left ITR
TTC TCA AGC CTC AGA CAG TGG	forward	1413	lox/lox, TEVpro, T2A, small
AAT CAT GTC CCT GCC GTC GAT C	forward	2035	T2A, small, TEV, large
AGA GGG GAT CGT TGT AGA AGT C	reverse	2766	TEV, small, T2A, TEVpro
AAA GCA GCG TAT CCA C	reverse	3393	lox/lox, large, TEV, small
TAG AAG GAC ACC TAG TCA GA	reverse	4053	pA, WPRE, lox/lox large
TCA AGC GAT TCT CCT GCC TC	forward	4282	pA, into right ITR
TAC TAT GGT TGC TTT GAC GT	reverse	4703	into right ITR

Table 4.1. List of primers used to sequence the AAV-flex-C3-Tp

cycles reduce the titer of the virus significantly. Thawed aliquots should remain on ice or at 4 °C, and we typically use each aliquot within 1 week of thawing.

2.4. Protocol: Injecting AAV-flex-C3-Tp into the adult brain

AAV particles, like other viruses and drugs, can be stereotaxically injected into a specific brain region, and the particular characteristics of the virus or chemical determine the subsequent rate and extent of diffusion within the injected area. The spread of AAV particles is limited to 0.5–2 mm from the tip of the injection needle, depending on the volume injected and the size of the needle. The timing of the surgery naturally dictates the onset of the ablation of the desired neuronal subset, offering temporal control, although expression of the virally encoded, Cre-dependent transgene is not immediate, and animals need time to recover from the surgery. Some tissue damage is unavoidable, but this can be reduced

by using a smaller needle or pulled glass pipette. There can be significant differences in the tropism of different AAV serotypes for different cell types, including different neuronal populations, and it is important to utilize a serotype that affords maximal infection of the target cells. The advantages of viral delivery—flexibility in encoding transgenes, temporal and anatomical precision—make it ideal for ablating specific cell types in specific regions.

1. Surgery

    a. Anesthetize the animal. The most common ketamine-based cocktails such as Ketamine/Xylazine/Acepromazine do not induce surgical-plane anesthesia, so addition of an inhalational anesthetic such as 0.5% isoflurane is preferable. If inhalational anesthesia is used as the primary modality of anesthesia, additional analgesics will be required.

    b. Shave and sterilize the scalp.

    c. We use a stereotaxic alignment system from Kopf (model 1900) because it allows the precision in head-angle alignment necessary for our deep brain areas. Small deviations in alignment or rotation will be exaggerated in deeper areas. A deflection of only a 100 μm will miss the target region completely. This model allows for the precise measurement and adjustment of the rotation of the skull in all planes such that variation can be accounted for between individual mice (Fig. 4.4Bi).

    d. Mount the mouse on the bite bar and secure the ear bars as indicated in the instruction manual. Many inbred strains including 129 and B6 have a 15° slant to their skull as compared to wild-caught mice and thus it is advisable to use an angled bite bar. It is also advisable to use nonrupture ear bars as these are more humane.

    e. Make an incision that is roughly 1 cm long along the top of the scalp. It should be as small as possible (to reduce pain and healing time for the animal) while still allowing for good visualization of skull landmarks (bregma and lambda) (Fig.

4.4Bii–iii).

f. Align the instrument to bregma and position and level the skull according to the instruction manual. Bregma is not always well-defined because of the nonlinear cranial sutures (Fig. 4.4Biii), and visualizing lines that most closely approximate the sutures *in situ* to construct an ideal bregma is recommended (dashed lines in Fig. 4.4Biii). To minimize variability in generating such an ideal bregma, we also recommend that the user maintain a reasonably fixed angle at the intersection of the lines that approximate the sutures. If using the double pressure gauge tool (alignment indicator tool) from Kopf Instruments to level the skull, be sure not to press too hard. The mouse skull is easily deformed, and this will lead to mistargeting.

2. Choosing coordinates

a. Mouse brain atlas-based coordinates are very accurate, with small mouse-to-mouse variability, at least for standard inbred laboratory strains that we use such as C57Bl/6J (Lein et al., 2007 and Paxinos and Franklin, 2004). However, because of how the cranial surface is angled relative to the brain, the final coordinates of the needle tip may not match the coordinates where the holes are drilled in the skull (Fig. 4.4Bii–iv). This tilt should be taken into consideration when establishing coordinates. For the VMHvl, we drill at ± 0.78, − 1.48 (*x*,*y*) and inject at ± 0.78, − 1.70, − 5.80 (*x*,*y*,*z*, bregma = 0,0,0). To ensure an accurate set of coordinates, each new region should be tested several times before injecting the experimental virus.

b. We usually establish our initial coordinates by injecting trypan blue, a dye that labels dead cells. For these studies, we euthanize the mouse with a lethal dose of anesthesia just prior to lowering the injection needles. The brain is dissected immediately, cut into slices thin enough to visualize the needle tracks, and placed in a dish of cold PBS to be viewed on a dissecting microscope.

c. These coordinates are subsequently refined by a more precise means involving the injection of a fluorescent-tagged reporter (such as cholera toxin B) or an AAV constitutively expressing a fluorescent reporter protein, and careful histological processing, to ensure accuracy. This is often a reiterative process, with the results of each stereotaxic injection trial leading to further refinement of the injection coordinates.

3. Injecting the virus

a. Assuming coordinates have been chosen, drill holes in the skull above the injection sites (Fig. 4.4Bii).

b. Lower the needles slowly (1–2 mm/min) to the correct *z* coordinate. Once there, create a space 50–100 μm above and below the target site, by moving the needles up and down a few times slowly to generate a small pocket for the virus solution to fill.

c. We use 33G needles (~ 200 μm outer diameter) coupled to Hamilton syringes via PE20 tubing. Our syringes are mounted on a micropump to maintain an even flow rate during infusion (Fig. 4.4Bi). If more precision is needed, pulled glass pipettes can be substituted for steel needles; however, glass pipettes are more fragile and are potentially deflected by fiber tracts within the brain.

d. Infuse the virus slowly, 60–100 nL/min. The volume can be anywhere from 50 to 1000 nL depending on the titer and efficacy of the virus. Larger volumes will spread farther. It is not recommended that you exceed 1 μL as this will potentially damage the target site.

e. Allow an additional 5 min for the virus to diffuse away from the needle tips before pulling the needles back up. Retract the needles at the same rate they were lowered.

4. Finishing

a. Close the wound with skin glue (vetbond, dermabond, or liquid bandaid). You

may also use sutures, but in most cases this is not necessary. Wound clips are not recommended for the scalp because the mice will pull these out.

b. Be sure to use an appropriate analgesic. If an opiate-based analgesic is used (e.g., buprenorphine) monitor the mouse's respiration until it returns to normal before administering the drug, as opiates are a respiratory depressant.

c. Wait 1–4 weeks before analyzing the mouse to allow adequate recovery time and for expression of the virus to peak. A time course should be performed for each neuronal population to establish a timepoint at which maximal cell loss has occurred. We wait 3–4 weeks after injecting AAV-flex-C3-Tp prior to behavioral testing.

2.5. The future of viral-mediated ablation in the brain

While stroke, cancer, trauma, and neurodegenerative victims have provided invaluable insights into localizing brain function, genetically targeted ablations of specific neuronal populations will enable high-resolution functional mapping of the neural circuits that encode behavior in health and disease. The electrolytic or surgical lesions of the past have offered us insight into regional functionalization of the brain, but now we have the means to determine the function of any group of adult neurons or model neurodegenerative disorders with remarkable accuracy. These genetically targeted studies will provide us with more precise understanding of the function of discrete neuronal populations and a testing ground for therapeutic interventions. As we mentioned earlier, our strategy is modular and can, in principle, be applied to any cell type in the brain or other organ system. We are also developing means of ablating even more specific neuronal populations with enhanced temporal control in the form of light- and ligand-activated caspases.

3. SMALL-MOLECULE ACTIVATORS OF CASPASES

3.1. Introduction

Allosteric modulation of enzymes with unnatural small molecules is an attractive way of modifying enzymatic activities by often offering greater selectivity over targeting conserved active sites. Allosteric control also allows the possibility to turn enzymes on, and there have been important recent discoveries in this area for kinases, deacetylases, dehydrogenases, phosphatases, and nucleases (for review, see Zorn & Wells, 2010). Upregulation of apoptotic signaling is common in precancerous cells and silencing of apoptosis is a hallmark of cancer cells. This apoptotic suppression is usually achieved by making lesions in signaling pathways upstream of the caspases, such as p53 (Lowe & Sherr, 2003). Thus, there has been a significant effort to activate executioner caspase with small molecules in hopes of differentially killing cancer cells.

The caspases are expressed as inactive proenzymes, or zymogens, and their activation is under tight regulation in cells due to their fate-determining activity. For example, the zymogenicity (defined as the mature enzyme k_{cat}/K_m divided by the proenzyme k_{cat}/K_m) of procaspase-3 is greater than 10^7, making it the most inactive protease zymogen yet reported (Pop et al., 2007, Stennicke and Salvesen, 2000 and Zorn et al., 2012). Upon proteolysis by upstream proteases, the N-terminal prodomain of the procaspase is removed, and the intersubunit linker is cut, the later being crucial to activation (Fig. 4.1B). This proteolytic activation leads to a dimer of heterodimers consisting of a large and small subunit, as illustrated by the crystal structure of mature caspase-7 (Fig. 4.5A) (Chai et al., 2001, Riedl et al., 2001 and Wei et al., 2000). In this active state, the executioner caspases exist in a conformational equilibrium between an “off” and “on” state, but predominantly in the on-state to allow substrate binding in the active site (Fig. 4.5B). Interestingly, mature caspase-1 is predominantly in the off-state until driven to the on-state by binding substrate (Gao, Sidhu, & Wells, 2009). In the “off” state, the active caspase can be trapped in a nonfunctional conformation by allosteric inhibitors that bind to the

dimer interface, as shown in previous studies of caspase-1, -5, and -7 (Gao and Wells, 2012, Hardy et al., 2004 and Scheer et al., 2006). These results also raise the question as to whether small molecules can potentially be found to activate the proenzyme (Fig. 4.5C). More recently, our group demonstrated the feasibility of activating procaspase-3 and -7. Antibody fragments were selected for binding the on-state and could stimulate procaspase-3 activity by 1000-fold (Thomsen, Koerber, & Wells, 2013). These results also highlight the enormous barrier of activation of procaspases and suggest that finding robust allosteric activators of procaspase-3 will be challenging.

3.2. Small-molecule activators of caspases

At present, four small-molecule compounds have been reported to activate procaspases *in vitro* and to induce cell death in cell culture. Neither of the binding sites for these small molecules have been structurally defined, nor have their stoichiometry of binding been determined. Interestingly, the mechanisms for the two that have been most extensively characterized are not through traditional allosteric means, that is, stoichiometric binding of a small molecule to the protein. Here, we review the discovery of each of these four compounds and provide practical suggestions for assays that may be useful for future discovery efforts.

3.2.1. PAC-1

PAC-1, or procaspase-activating compound 1, was a small molecule discovered by the Hergenrother group as being capable of activating procaspase-3 *in vitro* and inducing apoptosis in various cell lines (Fig. 4.6A) (Putt et al., 2006). This compound was discovered by performing a high-throughput screen for 20,500 diverse small molecules, and looking for procaspase-3 activation by monitoring cleavage of a peptidic substrate (acetyl Asp-Glu-Val-Asp-*p*-nitroanilide (Ac-DEVD-*p*Na) at 200 μ*M*). The compound PAC-1 activated procaspase-3 up to fourfold over background after 12 h of incubation with an EC_{50} of 0.22 and 4.7 μ*M* for procaspase-3 and -7, respectively (Peterson et al., 2009). This activation is

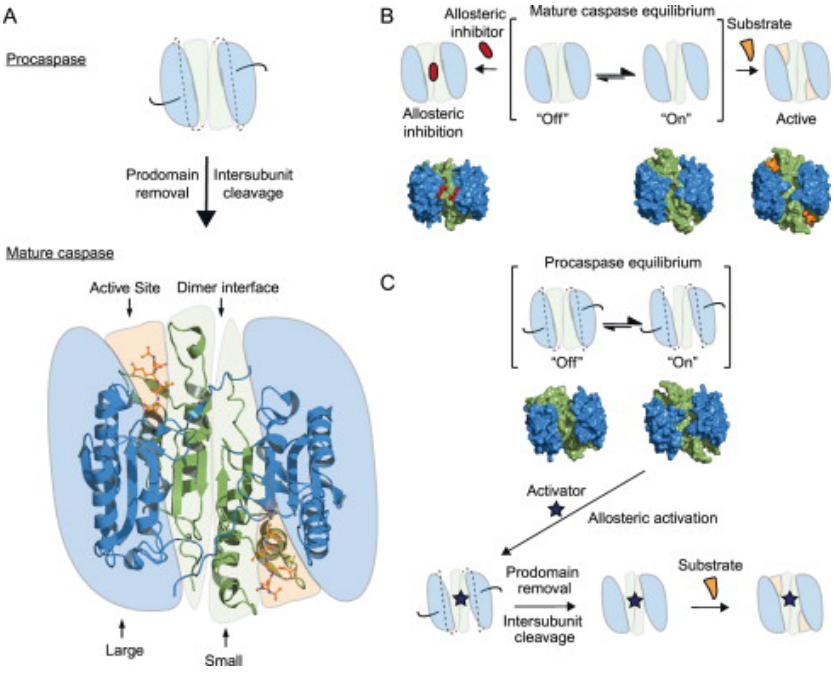

Figure 4.5. Mechanism of caspase regulation.

(A) Executioner procaspase maturation requires proteolysis of the N-terminal prodomain (black lines) and cleavage of the intersubunit linker (dashed lines) between the large and small subunits. The crystal structure of mature caspase-7 is shown (PDB ID 1F1J) highlighting the dimer interface, the large and small subunits and the Ac-DEVD-CHO peptide occupying the active site (shown in sticks). (B) Mechanism of allosteric inhibition of caspases, showing the hotspot for allosteric binding located at the dimer interface. The surface representation of experimentally determined X-ray structures of caspase-7 is shown below the cartoons. From left to right, the allosteric-site ligand-bound structure of caspase-7 complexed with DICA, the ligand-free apo caspase-7 structure in an “on” conformation, and the active-site ligand-bound structure of caspase-7 in complex with the Ac-DEVD-CHO peptide (PDB ID 1SHJ, 1K86, 1F1J, respectively). (C) Mechanism of allosteric activation of procaspases. The brackets denote the open and closed active-site equilibrium, with the surface of the X-ray structures of procaspase-3 in the “on” and “off” states (PDB ID 4JR0 and 4JQY, respectively). Upon binding of a hypothetical allosteric activator, the proenzyme is locked into an “on” conformation, allowing possible proteolytic cleavage of the prodomain and intersubunit linkers.

small considering the 10^7-fold change in activity for full activation of the proenzyme (Zorn et al., 2012). Nonetheless, PAC-1 was shown to induce cell death in several cancer cell lines in a manner proportional to the cellular concentration of procaspase-3, and was ineffective in MCF-7 cells that lack procaspase-3, although another group was unable to repeat this result (Denault et al., 2007). PAC-1 was also shown to significantly delay the progression of tumors in mice (Putt et al., 2006). The group later showed that PAC-1 is a zinc chelator agent that leads to activation of procaspase-3 by relieving the zinc inhibition of caspase-3 from their buffers that were missing EDTA (Peterson et al., 2009). These findings are consistent with previous studies

showing that zinc inhibits caspase-3 with an IC_{50} of 0.1 μ*M* (Perry et al., 1997). They also reported that the zinc-chelation mechanism was responsible for the cell death observed in cell culture leading to altered intracellular Ca^{2+} concentration, indicative of endoplasmic reticulum stress-induced apoptosis (West et al., 2012). In summary, PAC-1 may not be a direct activator of procaspase, but led to interesting discoveries about the role of metal chelation in caspase activation and initiation of cell death. Whether the cellular activity is a direct effect of chelating zinc from caspase-3 remains challenging to prove, given the many roles of zinc in cells.

3.2.2. Compound-1541

In a separate HTS of over 62,000 compounds, our lab discovered a compound called 1541 (Fig. 4.6A), that lead to specific activation of procaspases-3 and -6 *in vitro* but not procaspase-7 (Wolan et al., 2009). Compound-1541 induces rapid and complete apoptosis with an EC_{50} ~ 2 μ*M*. The apoptosis is minimally affected by deletion of caspase-8, a driver of the extrinsic pathway, and apoptosis proceeds without significant release of cytochrome *C*, a marker of the intrinsic pathway. These data were consistent with direct activation of caspase-3. Moreover, the rate of cell death is slowed in MCF-7 cells lacking caspase-3. However, we were unable to determine the structure of the compound bound to either the mature or zymogen form of caspase-3. Nor were we able to obtain clear biophysical evidence for stoichiometric binding, for example, by surface plasmon resonance (SPR) or isothermal titration calorimetry (ITC). Further characterization of the compounds by electron microcopy (EM) revealed the surprising finding that 1541 and its active analogs self-assemble into nanofibrils in solution (Fig. 4.5B) (Zorn et al., 2011). Using various biochemical and biophysical methods, we conclusively found that these nanofibrils colocalize caspase-3 with procaspase-3 and promote activation *in vitr*o (Zorn et al., 2012).

Globular aggregates of small molecules are known to act as inhibitors and can be diagnosed by testing for detergent sensitivity, β-lactamase inhibition, and sensitivity to

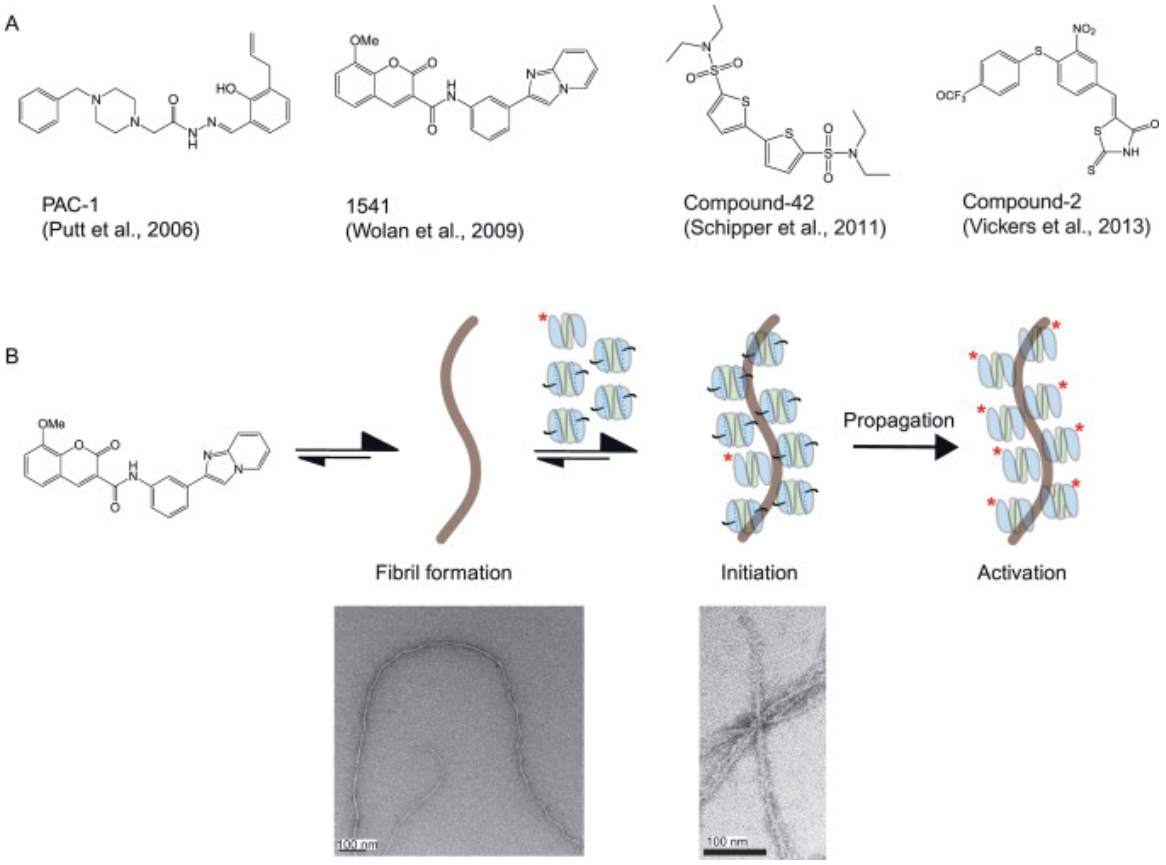

Figure 4.6. Procaspase activation by small molecules.

(A) Four small molecules have been reported to act as allosteric activators of procaspases; PAC-1 (Putt et al., 2006), 1541 (Wolan, Zorn, Gray, & Wells, 2009), compound-42 (Schipper, MacKenzie, Sharma, & Clark, 2011), and compound-2 (Vickers et al., 2013). (B) Mechanism of procaspase activation by 1541 nanofibrils. A small amount of active caspase (labeled with asterisk) is already present in *E. coli*-purified procaspase samples. The nanofibrils serve as a scaffold for colocalization of active caspase with the proenzyme, leading to activation. Figure (B) is adapted with permission from Zorn, Wille, Wolan, and Wells, (2011).

bovine serum albumin (BSA) (Coan and Shoichet, 2008, Feng et al., 2007 and Seidler et al., 2003). However, we obtained mixed results by performing these tests on 1541 (Zorn et al., 2011). For example, detergents such as Triton or CHAPS did not disrupt procaspase-3 activation, nor did 1541 inhibit β-lactamase activity. However, the addition of BSA into the assay prevented procaspase-3 activation. A careful characterization of 1541 in various conditions (e.g., buffer, temperature, concentration, etc.) led us to observe higher molecular weight species using dynamic light scattering (DLS). Spin-down assays showed coprecipitation of the nanofibrils with procaspase-3. Moreover, sequestering

procaspase-3 from the nanofibrils using a dialysis bag containing the proenzyme prevented activation. We hypothesize that unlike typical amorphous aggregates, that are in free equilibrium between monomer and aggregate, the nanofibrils have fewer ends available for monomer–nanofibrils exchange. This makes it extremely slow for the compound to reform fibrils, making it very unlikely for the compound to enter the dialysis bag and to reform fibrils on the inside of the membrane during the incubation period.

We found that activation *in vitro* depends on the presence of a small amount of active caspase to initiate proenzyme cleavage. For example, adding as little as 0.01 equivalent of the covalent caspase-3 inhibitor (Ac-DEVD-cmk) to procaspase-3 in our assays prevented procaspase activation by 1541. We believe this contaminant comes from tiny amounts of mature enzyme that is processed from the proenzyme, perhaps by endogenous *E. coli* proteases or by the procaspase itself during expression in bacteria. There is also a pronounced lag in the activation process *in vitro,* as is typical for the activation of proenzymes, in general. This lag is not due to assembly of the fibrils; we observe them forming instantly upon dilution into aqueous solution, as monitored by EM or DLS. Moreover, the inclusion of even a 1% stoichiometric amount of active caspase-3 shortens the lag period by 2.5-fold (Zorn et al., 2012). Taken together, our experiments show that 1541 nanofibrils colocalize caspase-3 with procaspase-3 *in vitro*, leading to activation of the proenzyme in a similar manner as a firecracker fuse. The spark of activation is provided by a small amount of active caspase that is colocalized to the fibril. Additional structural characterization of the nanofibrils with procaspase-3 will be important to understand the assembly and activation mechanism further.

Many questions remain to be answered regarding the cellular mechanism for 1541. How does 1541 induce apoptosis in cell culture with such potency? Our preliminary studies indicate that the fibrils are responsible for inducing apoptosis in cell culture (O. Julien & J. A. Wells, unpublished results), but the exact molecular mechanism of cell death is currently under investigation. Are the nanofibrils activating procaspases in cells in the

same way they do *in vitro*? There are some intriguing similarities, both at the functional and structural levels, between 1541 nanofibrils and some amyloid fibrils that induce apoptosis such as Aβ (Zorn et al., 2011). The ease of making 1541 and the simplicity of forming these fibrils make it a potentially important model system for understanding cell death induced by such fibril-forming molecules.

3.2.3. Compound-42

Another small molecule, named compound-42 (Fig. 4.6A), was recently discovered by the Clark group that was capable of enhancing procaspase-3 activation by 27-fold (Schipper et al., 2011). Again, this is a small change considering the zymogenicity of the procaspase-3. The compound was discovered using computational docking screen of 62 compounds that targeted the allosteric inhibitory site located at the dimer interface of procaspase-3 (Hardy et al., 2004). They hypothesized that stabilizing the same interface on procaspase-3 could lead to allosteric activation of the zymogen. Based on their docking score, 13 compounds were tested in a procaspase-3 activation assay *in vitro*. One compound, compound-42, was found to increase procaspase-3 activity by 27-fold at 400 μ*M* after 1 h incubation with the proenzyme. The authors hypothesized that compound-42 activates procaspase-3 by releasing the intersubunit linker from the dimer interface allowing the enzyme to auto-process this linker in *trans*. The group measured a K_D of 4 μ*M* for compound-42 to bind mature caspase-3 by ITC, but could not determine the binding affinity of compound-42 to procaspase-3. No cellular activity was reported.

3.2.4. Compound-2

Earlier this year, the Wolan group discovered a new compound that was capable of promoting the maturation of executioner procaspase-3 and -7 (Vickers et al., 2013). They used a clever fluorescence-polarization-based screen. This utilized a newly designed canonical DEVD-aldehyde peptide recognition motif, and a 5(6)-carboxyfluorescein at the N-terminus linked to a 3 × 6-aminohexanoic acid. The main advantage of this

new probe is that it binds and inhibits any contaminating mature caspase-3 and -7, in a reversible covalent manner that may be present or produced during the activation assay, and does not get consumed like standard caspase probes that are based on the release of a fluorophore. Using HTS, they identified a small molecule, compound-2 (Fig. 4.6A), that the activated executioner procaspases *in vitro* with an EC_{50} of ~ 1–5 μ*M*. Importantly, compound-2 and its analogs are capable of inducing apoptosis in cell culture with the same low μ*M* EC_{50}. These values are very similar to 1541. Further studies will be needed to confirm the stoichiometry and site of binding, as well as the mechanism of inducing apoptosis in cells.

3.3. A practical guide to avoid aggregating small molecules: The case of procaspase activators

3.3.1. Detergent in vitro

The use of small amounts of detergent during the high-throughput screen is the first step toward avoiding false positive results caused by small molecules (Fig. 4.7). This did not preclude the discovery of 1541 as the screen included 0.1% CHAPS to avoid standard aggregators. Vickers et al. also included some detergent in their assay buffer to discourage small-molecule aggregation. Once hits are found, it is useful to test the effect of increasing the detergent concentration on the enzymatic activity of the target of interest. If a decrease in compound potency is observed, aggregation is a strong possibility.

3.3.2. Dynamic light scattering

In our hands, the gold standard test for detecting small-molecule aggregators is DLS. If performed cautiously, this test is capable of detecting all forms of aggregation (e.g., colloid particles, micelles, fibrils, etc.). We recommend all buffer solutions to be filtered at 0.22 μm before adding the compound of interest. Measurements should be made in the same time frame used for the enzyme and cellular assays. Low and high concentration of compounds should also be tested at various temperatures. Measurements should be

performed in triplicate. Finally, it is useful to test a known aggregator as positive control (e.g., like tetra-iodophenolphthalein) and a known well-behaved small molecule as negative control (e.g., coumarins).

3.3.3. Nonspecific enzyme inhibition

Various assays can be used to detect the formation of small-molecule aggregates *in vitro*. For example, Shoichet and coworkers developed a β-lactamase inhibition assay based on the high sensitivity of this enzyme to be inhibited by colloidal particles (McGovern, Caselli, Grigorieff, & Shoichet, 2002). While useful for colloidal particles, 1541 nanofibrils did not inhibit β-lactamase. Another simple assay is to test if BSA perturbs the enzymatic activity caused by the compound of interest (Coan & Shoichet, 2007).

3.3.4. Transmission electron microscopy

Transmission electron microscopy is a powerful and relatively easy method to verify the presence of aggregators. However, it is important to remember that a negative result here does not rule out the presence of aggregation, since not all aggregators can be effectively detected using this method. This method was especially useful for observing 1541 nanofibrils.

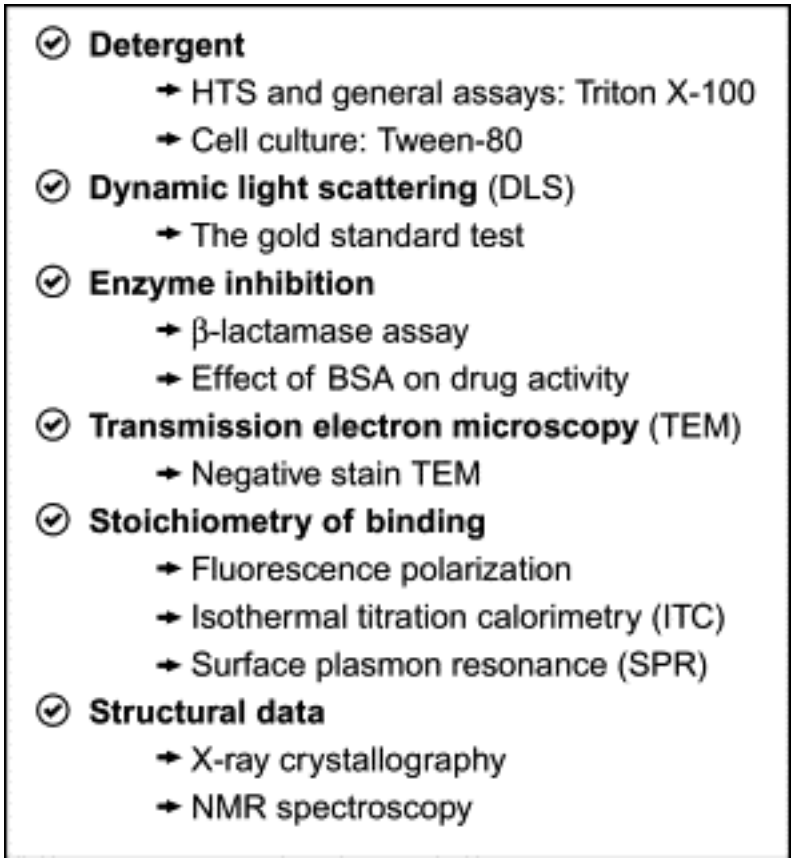

Figure 4.7. Useful tests to ensure compounds are acting through a stoichiometric binding mechanism.

3.3.5. Stoichiometry of binding

Various techniques allow the determination of the stoichiometry of binding of a compound of interest to its target. One can use ITC, X-ray crystallography, SPR, or nuclear magnetic resonance (NMR) spectroscopy. In addition, X-ray crystallography and NMR spectroscopy are powerful tools to determine the binding location of the small molecule on its target. As with EM, a single negative result does not reveal much, but one should be worried if all fails.

3.3.6. Detergent in cell culture

An easy way to test the presence of small-molecule aggregation is to use small amounts of detergent in cell culture (Owen, Doak, Wassam, Shoichet, & Shoichet, 2012). Specifically, Tween-80 is able to prevent small-molecule aggregation and has been shown by Owen and coworkers to have negligible toxicity in cell culture at low concentration (i.e., less than 0.1%). Recently, we have had success using this assay to block 1541 activity (O. Julien and J. A. Wells, data to be published).

3.3.7. Use of active-site titrants to rule out the involvement of mature caspases in proenzyme activation

Activation by 1541 requires a small amount of mature caspase, which can be tested for and blocked by addition of substoichiometric amounts of DEVD-chloromethyl ketone. We found mature caspase contaminants are unavoidable when using *E. coli* to express the procaspase. Such contaminants are even present if one uses the “noncleavable” D_3A mutant. It is possible that alternate cleavage sites by host proteases are the cause of this mature enzyme contamination. Indeed, proteolysis at D169 has been shown to occur when the normal cleavage site D175 is unavailable (MacKenzie et al., 2013). In our hands, such spurious activation in *E. coli* expression systems can be reduced by using shorter expression times, but it is impossible to eliminate completely. Thus, the safest technique is to inactivate trace levels of mature caspase molecules in proenzyme

preparations by adding as little as 0.01–0.05 equivalent of a covalent and irreversible caspase inhibitor (e.g., Ac-DEVD-chloromethyl ketone).

3.4. Conclusions

The most thoroughly characterized procaspase activators, PAC-1 and 1541, were shown to activate the proenzyme through unexpected mechanisms. PAC-1 is believed to remove zinc inhibition, and 1541 through nanofibril formation and activation by colocalization of mature and inactive caspase. These are still very useful tools and have provided important new insights about mechanisms of activation of caspases. Direct activation of executioner caspases remains a big challenge due to the high zymogenicity barrier of the proenzyme (Zorn et al., 2012). It may be easier to target procaspase-7 instead of procaspase-3 because of its lower zymogen activation barrier (Thomsen et al., 2013). It may even be more achievable to target the initiator caspases since they have even lower barriers and compounds that induce dimerization could potentially be found. Finding new drugs here would have a big impact, but many challenges remain.

ACKNOWLEDGMENTS

We are grateful to Dan Gray, Julie Zorn, and Dennis Wolan for their pioneering work on 1 and 3, and Cindy Yang and Dan Gray for their work on Section 2. We also thank Allison Doak, Jason Porter, Justin Rettenmaier, Cheryl Tajon, Nathan Thomsen, for their thoughtful discussions and careful reading of the chapter. C. W. M. is supported by a NSF Graduate Fellowship. O. J. is supported by a Banting Fellowship from the Government of Canada and the Canadian Institutes of Health Research. E. K. U. is supported by NIH grant F31NS078959. N. M. S. is supported by The Ellison Medical Foundation and the NIH (grants DP1MH099900, R01NS049488, and R01NS083872). J. A. W. is supported by NIH (grants R01 CA136779 and R01 GM081051).

REFERENCES

Amara, J. F., T. Clackson, et al. (1997). “A versatile synthetic dimerizer for the regulation of protein-protein interactions.” Proceedings of the National Academy of Sciences of the United States of America 94(20): 10618-10623.

Atasoy, D., Y. Aponte, et al. (2008). “A FLEX switch targets Channelrhodopsin-2 to multiple cell types for imaging and long-range circuit mapping.” The Journal of neuroscience : the official journal of the Society for Neuroscience 28(28): 7025-7030.

Belshaw, P. J., D. M. Spencer, et al. (1996). “Controlling programmed cell death with a cyclophilin-cyclosporin-based chemical inducer of dimerization.” Chemistry & biology 3(9): 731-738.

Brockschnieder, D., C. Lappe-Siefke, et al. (2004). “Cell depletion due to diphtheria toxin fragment A after Cre-mediated recombination.” Molecular and cellular biology 24(17): 7636-7642.

Chai, J., Q. Wu, et al. (2001). “Crystal structure of a procaspase-7 zymogen: mechanisms of activation and substrate binding.” Cell 107(3): 399-407.

Chang, D. W., Z. Xing, et al. (2003). “Interdimer processing mechanism of procaspase-8 activation.” The EMBO journal 22(16): 4132-4142.

Chelur, D. S. and M. Chalfie (2007). “Targeted cell killing by reconstituted caspases.” Proceedings of the National Academy of Sciences of the United States of America 104(7): 2283-2288.

Chen, M., A. Orozco, et al. (2002). “Activation of initiator caspases through a stable dimeric intermediate.” The Journal of biological chemistry 277(52): 50761-50767.

Coan, K. E. and B. K. Shoichet (2007). “Stability and equilibria of promiscuous aggregates in high protein milieus.” Molecular bioSystems 3(3): 208-213.

Coan, K. E. and B. K. Shoichet (2008). “Stoichiometry and physical chemistry of

promiscuous aggregate-based inhibitors." Journal of the American Chemical Society 130(29): 9606-9612.

Cooray, S., S. J. Howe, et al. (2012). "Retrovirus and lentivirus vector design and methods of cell conditioning." Methods in enzymology 507: 29-57.

Denault, J. B., M. Drag, et al. (2007). "Small molecules not direct activators of caspases." Nature chemical biology 3(9): 519; author reply 520.

Di Stasi, A., S. K. Tey, et al. (2011). "Inducible apoptosis as a safety switch for adoptive cell therapy." The New England journal of medicine 365(18): 1673-1683.

Edwards, S. R. and T. J. Wandless (2007). "The rapamycin-binding domain of the protein kinase mammalian target of rapamycin is a destabilizing domain." The Journal of biological chemistry 282(18): 13395-13401.

Farago, A. F., R. B. Awatramani, et al. (2006). "Assembly of the brainstem cochlear nuclear complex is revealed by intersectional and subtractive genetic fate maps." Neuron 50(2): 205-218.

Fegan, A., B. White, et al. (2010). "Chemically controlled protein assembly: techniques and applications." Chemical reviews 110(6): 3315-3336.

Feng, B. Y., A. Simeonov, et al. (2007). "A high-throughput screen for aggregation-based inhibition in a large compound library." Journal of medicinal chemistry 50(10): 2385-2390.

Galluzzi, L., S. A. Aaronson, et al. (2009). "Guidelines for the use and interpretation of assays for monitoring cell death in higher eukaryotes." Cell death and differentiation 16(8): 1093-1107.

Gao, J., S. S. Sidhu, et al. (2009). "Two-state selection of conformation-specific antibodies." Proceedings of the National Academy of Sciences of the United States of America 106(9): 3071-3076.

Gao, J. and J. A. Wells (2012). "Identification of specific tethered inhibitors for caspase-5." Chemical biology & drug design 79(2): 209-215.

Gossen, M. and H. Bujard (1992). “Tight control of gene expression in mammalian cells by tetracycline-responsive promoters.” Proceedings of the National Academy of Sciences of the United States of America 89(12): 5547-5551.

Gossen, M. and H. Bujard (2001). Tetracyclines in the control of gene expression in eukaryotes. Tetracyclines in Biology, Chemistry and Medicine M. Nelson, W. Hillen and R. Green: 139-157.

Gray, D. C., S. Mahrus, et al. (2010). “Activation of specific apoptotic caspases with an engineered small-molecule-activated protease.” Cell 142(4): 637-646.

Grieshammer, U., M. Lewandoski, et al. (1998). “Muscle-specific cell ablation conditional upon Cre-mediated DNA recombination in transgenic mice leads to massive spinal and cranial motoneuron loss.” Developmental biology 197(2): 234-247.

Gronostajski, R. M. and P. D. Sadowski (1985). “The FLP recombinase of the Saccharomyces cerevisiae 2 microns plasmid attaches covalently to DNA via a phosphotyrosyl linkage.” Molecular and cellular biology 5(11): 3274-3279.

Hardy, J. A., J. Lam, et al. (2004). “Discovery of an allosteric site in the caspases.” Proceedings of the National Academy of Sciences of the United States of America 101(34): 12461-12466.

Hughes, M. A., N. Harper, et al. (2009). “Reconstitution of the death-inducing signaling complex reveals a substrate switch that determines CD95-mediated death or survival.” Molecular cell 35(3): 265-279.

Ivanova, A., M. Signore, et al. (2005). “In vivo genetic ablation by Cre-mediated expression of diphtheria toxin fragment A.” Genesis 43(3): 129-135.

Kang, T. B., G. S. Oh, et al. (2008). “Mutation of a self-processing site in caspase-8 compromises its apoptotic but not its nonapoptotic functions in bacterial artificial chromosome-transgenic mice.” Journal of immunology 181(4): 2522-2532.

Lein, E. S., M. J. Hawrylycz, et al. (2007). “Genome-wide atlas of gene expression in the adult mouse brain.” Nature 445(7124): 168-176.

Lowe, S. W. and C. J. Sherr (2003). “Tumor suppression by Ink4a-Arf: progress and puzzles.” Current opinion in genetics & development 13(1): 77-83.

Mackenzie, S. H., J. L. Schipper, et al. (2013). “Lengthening the Intersubunit Linker of Procaspase 3 Leads to Constitutive Activation.” Biochemistry.

McGovern, S. L., E. Caselli, et al. (2002). “A common mechanism underlying promiscuous inhibitors from virtual and high-throughput screening.” Journal of medicinal chemistry 45(8): 1712-1722.

Murphy, B. M., E. M. Creagh, et al. (2004). “Interchain proteolysis, in the absence of a dimerization stimulus, can initiate apoptosis-associated caspase-8 activation.” The Journal of biological chemistry 279(35): 36916-36922.

Muzio, M., B. R. Stockwell, et al. (1998). “An induced proximity model for caspase-8 activation.” The Journal of biological chemistry 273(5): 2926-2930.

Oberst, A., C. Pop, et al. (2010). “Inducible dimerization and inducible cleavage reveal a requirement for both processes in caspase-8 activation.” The Journal of biological chemistry 285(22): 16632-16642.

Orban, P. C., D. Chui, et al. (1992). “Tissue- and site-specific DNA recombination in transgenic mice.” Proceedings of the National Academy of Sciences of the United States of America 89(15): 6861-6865.

Ory, D. S., B. A. Neugeboren, et al. (1996). “A stable human-derived packaging cell line for production of high titer retrovirus/vesicular stomatitis virus G pseudotypes.” Proceedings of the National Academy of Sciences of the United States of America 93(21): 11400-11406.

Owen, S. C., A. K. Doak, et al. (2012). “Colloidal aggregation affects the efficacy of anticancer drugs in cell culture.” ACS chemical biology 7(8): 1429-1435.

Pajvani, U. B., M. E. Trujillo, et al. (2005). “Fat apoptosis through targeted activation of caspase 8: a new mouse model of inducible and reversible lipoatrophy.” Nature medicine 11(7): 797-803.

Paxinos, G. and K. B. J. Franklin (2004). The Mouse Brain in Stereotaxic Coordinates, Elsevier Academic Press.

Perry, D. K., M. J. Smyth, et al. (1997). “Zinc is a potent inhibitor of the apoptotic protease, caspase-3. A novel target for zinc in the inhibition of apoptosis.” The Journal of biological chemistry 272(30): 18530-18533.

Peterson, Q. P., D. R. Goode, et al. (2009). “PAC-1 activates procaspase-3 in vitro through relief of zinc-mediated inhibition.” Journal of molecular biology 388(1): 144-158.

Pop, C., P. Fitzgerald, et al. (2007). “Role of proteolysis in caspase-8 activation and stabilization.” Biochemistry 46(14): 4398-4407.

Provost, E., J. Rhee, et al. (2007). “Viral 2A peptides allow expression of multiple proteins from a single ORF in transgenic zebrafish embryos.” Genesis 45(10): 625-629.

Putt, K. S., G. W. Chen, et al. (2006). “Small-molecule activation of procaspase-3 to caspase-3 as a personalized anticancer strategy.” Nature chemical biology 2(10): 543-550.

Remy, I. and S. W. Michnick (2007). “Application of protein-fragment complementation assays in cell biology.” BioTechniques 42(2): 137, 139, 141 passim.

Riedl, S. J., P. Fuentes-Prior, et al. (2001). “Structural basis for the activation of human procaspase-7.” Proceedings of the National Academy of Sciences of the United States of America 98(26): 14790-14795.

Saito, M., T. Iwawaki, et al. (2001). “Diphtheria toxin receptor-mediated conditional and targeted cell ablation in transgenic mice.” Nature biotechnology 19(8): 746-750.

Salvesen, G. S. and V. M. Dixit (1999). “Caspase activation: the induced-proximity model.” Proceedings of the National Academy of Sciences of the United States of America 96(20): 10964-10967.

Sauer, B. (1987). “Functional expression of the cre-lox site-specific recombination

system in the yeast Saccharomyces cerevisiae.” Molecular and cellular biology 7(6): 2087-2096.

Sauer, B. and N. Henderson (1988). “Site-specific DNA recombination in mammalian cells by the Cre recombinase of bacteriophage P1.” Proceedings of the National Academy of Sciences of the United States of America 85(14): 5166-5170.

Scheer, J. M., M. J. Romanowski, et al. (2006). “A common allosteric site and mechanism in caspases.” Proceedings of the National Academy of Sciences of the United States of America 103(20): 7595-7600.

Schipper, J. L., S. H. MacKenzie, et al. (2011). “A bifunctional allosteric site in the dimer interface of procaspase-3.” Biophysical chemistry 159(1): 100-109.

Schnutgen, F., N. Doerflinger, et al. (2003). “A directional strategy for monitoring Cre-mediated recombination at the cellular level in the mouse.” Nature biotechnology 21(5): 562-565.

Seidler, J., S. L. McGovern, et al. (2003). “Identification and prediction of promiscuous aggregating inhibitors among known drugs.” Journal of medicinal chemistry 46(21): 4477-4486.

Sohn, D., K. Schulze-Osthoff, et al. (2005). “Caspase-8 can be activated by interchain proteolysis without receptor-triggered dimerization during drug-induced apoptosis.” The Journal of biological chemistry 280(7): 5267-5273.

Spencer, D. M., P. J. Belshaw, et al. (1996). “Functional analysis of Fas signaling in vivo using synthetic inducers of dimerization.” Current biology : CB 6(7): 839-847.

Spencer, D. M., T. J. Wandless, et al. (1993). “Controlling signal transduction with synthetic ligands.” Science 262(5136): 1019-1024.

Steller, H. (1998). “Artificial death switches: induction of apoptosis by chemically induced caspase multimerization.” Proceedings of the National Academy of Sciences of the United States of America 95(10): 5421-5422.

Stennicke, H. R. and G. S. Salvesen (2000). “Caspases - controlling intracellular signals

by protease zymogen activation." Biochimica et biophysica acta 1477(1-2): 299-306.

Straathof, K. C., M. A. Pule, et al. (2005). "An inducible caspase 9 safety switch for T-cell therapy." Blood 105(11): 4247-4254.

Tang, W., I. Ehrlich, et al. (2009). "Faithful expression of multiple proteins via 2A-peptide self-processing: a versatile and reliable method for manipulating brain circuits." The Journal of neuroscience : the official journal of the Society for Neuroscience 29(27): 8621-8629.

Thomsen, N. D., J. T. Koerber, et al. (2013). "Structural snapshots reveal distinct mechanisms of procaspase-3 and -7 activation." Proceedings of the National Academy of Sciences of the United States of America 110(21): 8477-8482.

Tonikian, R., Y. Zhang, et al. (2007). "Identifying specificity profiles for peptide recognition modules from phage-displayed peptide libraries." Nature protocols 2(6): 1368-1386.

Vaughn, A. E. and M. Deshmukh (2008). "Glucose metabolism inhibits apoptosis in neurons and cancer cells by redox inactivation of cytochrome c." Nature cell biology 10(12): 1477-1483.

Vickers, C. J., G. E. Gonzalez-Paez, et al. (2013). "Small-molecule procaspase activators identified using fluorescence polarization." Chembiochem : a European journal of chemical biology 14(12): 1419-1422.

Wang, K., X. M. Yin, et al. (1996). "BID: a novel BH3 domain-only death agonist." Genes & development 10(22): 2859-2869.

Wehr, M. C., R. Laage, et al. (2006). "Monitoring regulated protein-protein interactions using split TEV." Nature methods 3(12): 985-993.

Wei, Y., T. Fox, et al. (2000). "The structures of caspases-1, -3, -7 and -8 reveal the basis for substrate and inhibitor selectivity." Chemistry & biology 7(6): 423-432.

West, D. C., Y. Qin, et al. (2012). "Differential effects of procaspase-3 activating

compounds in the induction of cancer cell death." Molecular pharmaceutics 9(5): 1425-1434.

Williams, D. J., H. L. Puhl, 3rd, et al. (2009). "Rapid modification of proteins using a rapamycin-inducible tobacco etch virus protease system." PloS one 4(10): e7474.

Wolan, D. W., J. A. Zorn, et al. (2009). "Small-molecule activators of a proenzyme." Science 326(5954): 853-858.

Yamaizumi, M., E. Mekada, et al. (1978). "One molecule of diphtheria toxin fragment A introduced into a cell can kill the cell." Cell 15(1): 245-250.

Yang, C. F., M. C. Chiang, et al. (2013). "Sexually dimorphic neurons in the ventromedial hypothalamus govern mating in both sexes and aggression in males." Cell 153(4): 896-909.

Yang, X., H. Y. Chang, et al. (1998). "Autoproteolytic activation of pro-caspases by oligomerization." Molecular cell 1(2): 319-325.

Zorn, J. A. and J. A. Wells (2010). "Turning enzymes ON with small molecules." Nature chemical biology 6(3): 179-188.

Zorn, J. A., H. Wille, et al. (2011). "Self-assembling small molecules form nanofibrils that bind procaspase-3 to promote activation." Journal of the American Chemical Society 133(49): 19630-19633.

Zorn, J. A., D. W. Wolan, et al. (2012). "Fibrils colocalize caspase-3 with procaspase-3 to foster maturation." The Journal of biological chemistry 287(40): 33781-33795.

Chapter 5

Medial Amygdalar Aromatase Neurons Regulate Aggression in Both Sexes

Elizabeth K. Unger,[1] Kenneth J. Burke, Jr.,[2] Cindy F. Yang,[2,6] Kevin J. Bender,[3] Patrick M. Fuller,[5] and Nirao M. Shah[4,*]

[1] Program in Biomedical Sciences, University of California, San Francisco, San Francisco, CA 94158, USA

[2] Program in Neuroscience, University of California, San Francisco, San Francisco, CA 94158, USA

[3] Department of Neurology, University of California, San Francisco, San Francisco, CA 94158, USA

[4] Department of Anatomy, University of California, San Francisco, San Francisco, CA 94158, USA

[5] Department of Neurology, Beth Israel Deaconess Medical Center, Harvard Medical School, Boston, MA 02215, USA

[6] Present address: David Geffen School of Medicine, University of California, Los Angeles, Los Angeles, CA 90095, USA

*Correspondence: nms@ucsf.edu

The text of this chapter is a reprint of material that appeared in Cell Reports.

Cell Reports DOI: http://dx.doi.org/10.1016/j.celrep.2014.12.040

IN BRIEF

Aromatase controls sexually dimorphic social behaviors in both sexes. Unger et al. show that the small population of aromatase-expressing neurons in the medial amygdala is required for intermale and maternal aggression, but not other sexually dimorphic behaviors. Thus, aromatase-expressing medial amygdalar neurons control complex social behaviors in a modular manner

HIGHLIGHTS

- MeApd aromatase neurons regulate male aggression, but not marking, singing, or mating
- MeApd aromatase neurons regulate maternal aggression, but not female sexual behavior
- MeApd aromatase neurons regulate specific components of aggression in both sexes
- MeApd aromatase neurons control aggression in a modular manner

SUMMARY

Aromatase-expressing neuroendocrine neurons in the vertebrate male brain synthesize estradiol from circulating testosterone. This locally produced estradiol controls neural circuits underlying courtship vocalization, mating, aggression, and territory marking in male mice. How aromatase-expressing neuronal populations control these diverse estrogen-dependent male behaviors is poorly understood, and the function, if any, of aromatase-expressing neurons in females is unclear. Using targeted genetic approaches, we show that aromatase-expressing neurons within the male posterodorsal medial amygdala (MeApd) regulate components of aggression, but not other estrogen-dependent male-typical behaviors. Remarkably, aromatase-expressing MeApd neurons in females are specifically required for components of maternal aggression, which we show is distinct

from intermale aggression in pattern and execution. Thus, aromatase-expressing MeApd neurons control distinct forms of aggression in the two sexes. Moreover, our findings indicate that complex social behaviors are separable in a modular manner at the level of genetically identified neuronal populations.

INTRODUCTION

Sexually reproducing species exhibit sex differences in social interactions such as courtship and aggression that are critical for reproductive success. Accordingly, such behaviors are developmentally programmed and can be elicited in naive animals without prior training. Within a species, each of these behaviors consists of many stereotyped components, thereby enabling sensitive detection of alterations in behavioral displays subsequent to functional manipulations. Although many brain regions are implicated in the control of sexually dimorphic behaviors in mammals, how these complex behaviors are encoded by such brain regions is poorly understood (reviewed in Yang and Shah, 2014).

Sex hormones essentially act as master regulators of the entire repertoire of sex-typical social interactions in most vertebrates (Arnold, 2009, Morris et al., 2004, Yang and Shah, 2014). Sex hormone signaling pathways therefore offer a functional entry point into neural circuits underlying these behaviors. As has been known for several decades (Ball, 1937), estrogen signaling controls sex-typical behaviors in both sexes in rodents and many other vertebrates (reviewed in McCarthy, 2008, Yang and Shah, 2014). In particular, it is critical for male-typical ultrasonic courtship vocalizations, sexual displays, aggression, and territory marking (Finney and Erpino, 1976, Kimura and Hagiwara, 1985, Matsumoto et al., 2003, Nunez et al., 1978, Ogawa et al., 2000, Wallis and Luttge, 1975, Wersinger et al., 1997). A role of estradiol in controlling male behaviors seems counterintuitive because it is essentially undetectable in the male mouse circulation. Estrogenic steroids in vivo are derived from testosterone or related androgens in a reaction catalyzed by aromatase,

and aromatase+ cells in the male brain convert circulating androgens into estrogenic derivatives (Naftolin et al., 1971). It is this locally synthesized estradiol that is thought to control male-typical behaviors (Figure 5.1A) (MacLusky and Naftolin, 1981).

Aromatase+ cells represent <0.05% of neurons in the adult mouse brain, and they are sparsely distributed within a few brain regions thought to be important for sexually dimorphic behaviors (Wu et al., 2009). Given the role of estradiol in diverse male-typical behaviors, aromatase+ neuronal populations exert a profound effect on such behaviors. However, the behavioral function of individual aromatase+ neuronal pools is unclear. In one scenario, each aromatase+ population globally controls social interactions in males. Alternatively, individual aromatase+ populations regulate one or a subset of male-typical behaviors. Although there is little circulating testosterone in female mice and the female brain is exposed to circulating estradiol secreted by ovaries, there is aromatase expression in the female rodent brain, albeit at lower levels than in males (Roselli, 1991, Roselli et al., 1985, Wu et al., 2009). The function, if any, of aromatase+ neurons in female mice is unknown (Figure 5.5.1A).

We utilized genetic strategies to test the function of aromatase+ posterodorsal medial amygdala (MeApd) neurons in sexually dimorphic behaviors. Aromatase+ neurons comprise ~40% of neurons within the MeApd, a region important for reproductive behaviors and responsive to pheromone sources such as urine (Baum and Bakker, 2013, Bergan et al., 2014, Choi et al., 2005, DiBenedictis et al., 2012, Sokolowski and Corbin, 2012, Swanson, 2000, Wu et al., 2009). We find that aromatase+ MeApd neurons in males regulate the display of specific features of aggression, but not mating, courtship vocalization, or territory marking. In females, these neurons regulate specific features of maternal aggression, but not other aspects of maternal care or fertility and sexual behavior. Taken together, our findings reveal a role for aromatase+ MeApd neurons in aggression in both sexes, and furthermore, they demonstrate a surprising modularity in

the neural control of sexually dimorphic behaviors.

RESULTS

A Genetic Strategy to Target Aromatase+ Neurons in Adult Mice

The medial amygdala (MeA) is a large structure that extends >1 mm rostrocaudally (Paxinos and Franklin, 2003) and influences diverse behaviors in rodents, including sexually dimorphic behaviors (Petrovich et al., 2001, Swanson, 2000, Swanson and Petrovich, 1998). In keeping with its size and functional diversity, the mouse MeA is molecularly heterogeneous (Carney et al., 2010, Choi et al., 2005, Keshavarzi et al., 2014, Xu et al., 2012, Yang et al., 2013). These considerations make it difficult to selectively target the small pool of aromatase+ MeApd neurons (Wu et al., 2009). In order to target these neurons, we knocked in an IRES-Cre transgene into the 3' UTR of the aromatase locus (Figures 5.1B and 5.1C). As described before, this strategy does not disrupt function or expression of the modified locus (Yang et al., 2013), and it permits expression of Cre recombinase in aromatase+ cells. Indeed, in contrast to *aromatase*$^{-/-}$ mice (Matsumoto et al., 2003), mice bearing the aromataseCre (aroCre) allele are fertile and have wild-type (WT) levels of circulating sex hormones (Figure 5.1D). In situ hybridization for Cre shows this enzyme to be expressed in a pattern mirroring that of aromatase (Figure 5.1E). To validate functional Cre expression in aromatase+ MeApd neurons, we injected an adeno-associated virus (AAV) harboring a Cre-dependent reporter in mice doubly heterozygous for aroCre and the previously described knockin *aromatase*^{IPIN} (*aro*^{IPIN}) allele that drives nuclear β-galactosidase in aromatase+ cells (Wu et al., 2009). In these animals, we observed colocalization of β-galactosidase and mCherry, confirming functional expression of Cre in aroCre mice (Figure 5.1F and see below). In addition, these studies confirmed the highly restricted nature of aromatase expression within the MeA (Figure 5.1F) (Wu et al., 2009).

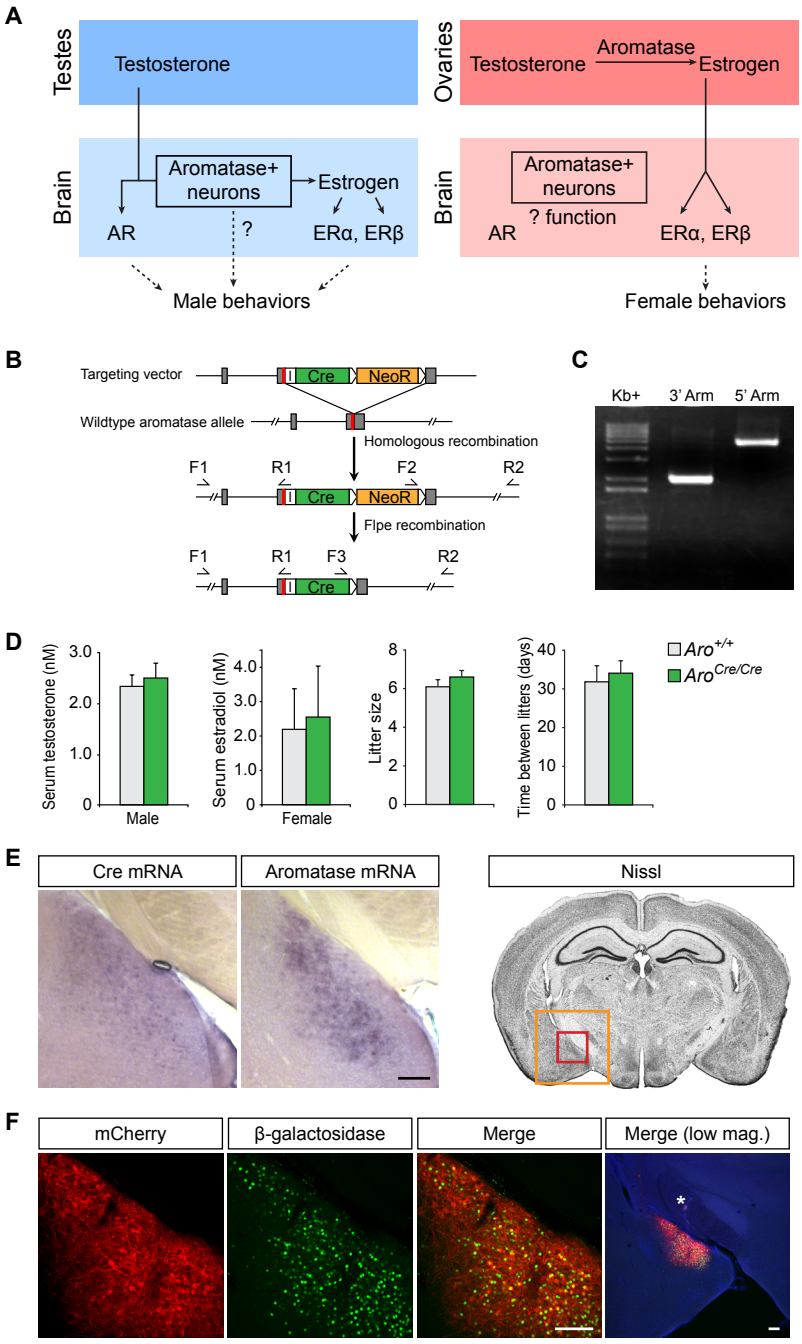

Figure 5.1: Generation and Characterization of Mice Expressing Cre Recombinase in Aromatase+ Cells

(A) Role of aromatase in sexually dimorphic behaviors. Aromatase+ neurons in the male brain produce estradiol that controls many male-typical behaviors, but the function of individual aromatase+ neuronal populations in these behaviors is unknown. Given that the female brain is exposed to circulating estradiol, the function, if any, of aromatase+ neurons is unclear in females. (B) Generating the aroCre allele. Gray boxes represent last two exons of aromatase, and the red line in 3' exon denotes stop codon. Primers (F1–F3 and R1 and R2) used for PCR-based genotyping are shown. Schematic not drawn to scale. (C) PCR verification of homologous recombination at the aromatase locus from tail DNA of an $aro^{Cre/Cre}$ mouse. (D) No difference in serum hormone titers, litter size, or time between litters between WT and $aro^{Cre/Cre}$ mice (mean ± SEM; n = 10 WT and 6 $aro^{Cre/Cre}$ of each sex). (E) Cre mRNA expression mirrors that of aromatase mRNA in an adjacent section through the MeA. Boxed area in red in Nissl-stained coronal section highlights the MeApd (Paxinos and Franklin, 2003). (F) Injection of AAV encoding a Cre-dependent mCherry into the MeA activates mCherry expression in aromatase+ neurons expressing β-galactosidase in $aro^{Cre/IPIN}$ mice. The low-magnification (mag.) merge panel is counterstained with DAPI (blue) to show that aromatase expression (and Cre-dependent reporter) is restricted to the MeApd and not to be found in neighboring regions; asterisk in the low-magnification panel denotes needle track. Boxed areas in red and orange in Nissl-stained coronal section (E) highlight the areas shown at high and low magnification, respectively. Scale bars represent 200 μm.

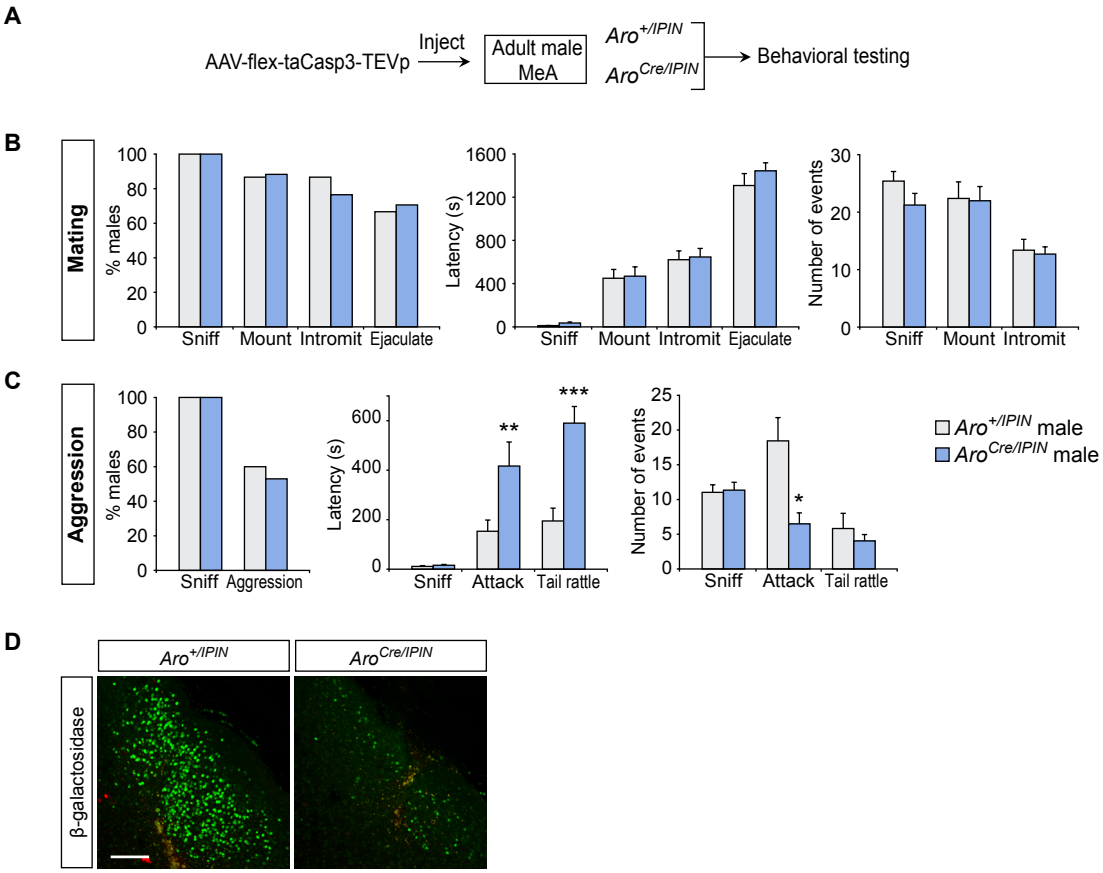

Figure 5.2: Ablation of Aromatase+ MeApd Neurons Reduces Specific Components of Male Aggression

(A) Experimental strategy to ablate Cre-expressing aromatase+ MeApd neurons and test for behavioral deficits. AAV encoding Cre-dependent caspase-3 was injected into the MeA of *aro*$^{Cre/IPIN}$ and *aro*$^{+/IPIN}$ males that were subsequently tested for mating and aggression.

(B) No difference between *aro*$^{Cre/IPIN}$ and control *aro*$^{+/IPIN}$ males in mating with a WT estrus female.

(C) Comparable percent of *aro*$^{Cre/IPIN}$ and *aro*$^{+/IPIN}$ males sniff and attack a WT intruder male. *Aro*$^{Cre/IPIN}$ males take significantly longer to attack and tail rattle, and they attack the intruder less.

(D) Histological verification of ablation of aromatase+ neurons in MeApd of *aro*$^{Cre/IPIN}$ males. Some autofluorescence is visible in the red channel.

Mean ± SEM; n = 14 *aro*$^{+/IPIN}$, n = 15 *aro*$^{Cre/IPIN}$; *p < 0.05, **p < 0.01, ***p < 0.005. Scale bar represents 200 μm. See also Figure 5.S1.

Aromatase+ MeApd Neurons Specifically Regulate Male Aggression

We tested the requirement of aromatase+ MeApd neurons in sexually dimorphic behaviors. We first ablated these neurons in adult mice via bilateral targeted delivery to the MeA of an AAV encoding a genetically modified caspase-3 whose activation requires Cre recombinase (Figure 5.2A) (Yang et al., 2013). Activation of this caspase-3 triggers

apoptosis exclusively in Cre+ cells without bystander toxicity to neighboring cells not expressing Cre (Morgan et al., 2014, Nelson et al., 2014, Yang et al., 2013). Only those aroCre males with a substantive loss (>50% loss bilaterally) of aromatase+ MeApd neurons were included for analysis of behavioral performance (Figures 5.2B–2D and 5.S1A–S1F). AAV-injected *aro*$^{Cre/IPIN}$ (experimental) and *aro*$^{+/IPIN}$ (control) males were allowed to recover for 4 weeks to ensure maximal cell loss, singly housed thereafter, and tested for behavioral performance (Figure 5.2A). Male mice exhibit a stereotyped routine of mating displays toward females, consisting of bouts of anogenital sniffing, mounting, and intromission (penetration) that can culminate in ejaculation (McGill, 1962). We observed no difference in these mating components between *aro*$^{Cre/IPIN}$ and control males when they were presented with a sexually receptive intruder female (Figure 5.2B). Male mice vocalize to females, and there was no difference between *aro*$^{Cre/IPIN}$ and control males in such courtship vocalization (Figure 5.S1A). *Aro*$^{Cre/IPIN}$ males also directed their courtship vocalizations preferentially to females (Figure 5.S1A), indicative of unaltered sex discrimination (Stowers et al., 2002). Taken together, our findings show that despite the importance of the MeApd in reproductive behavior (Baum and Bakker, 2013, Bergan et al., 2014, Choi et al., 2005, DiBenedictis et al., 2012, Sokolowski and Corbin, 2012, Swanson, 2000), most aromatase+ MeApd neurons are not essential for WT levels of male sexual behavior and courtship vocalizations in mice.

We next tested these resident males for aggression toward an unfamiliar adult WT intruder male. Both *aro*$^{Cre/IPIN}$ and *aro*$^{+/IPIN}$ residents chemoinvestigated, groomed, and attacked intruders, but *aro*$^{Cre/IPIN}$ males took significantly longer time to initiate aggression (Figures 2C and S1A). There was a corresponding decrease in the number of attacks directed toward the intruder by *aro*$^{Cre/IPIN}$ males (Figure 5.2C). The deficits in attacks correlated strongly with the extent of loss of aromatase+ MeApd neurons (Figure 5.S1G). Resident males often tail rattle as a threat to intruder males, and we observed a significant increase

in the latency to tail rattle in *aro*$^{Cre/IPIN}$ males (Figure 5.2C). In addition to attacking intruder males, male mice also mark their home territory with numerous urine spots. Despite the reduced aggression toward intruders, *aro*$^{Cre/IPIN}$ males marked their territory similar to controls (Figure 5.S1C). We tested *aro*$^{Cre/IPIN}$ males to determine if they exhibited pervasive deficits that could contribute to the deficits in aggression. However, these males did not exhibit deficits in finding hidden food, anxiety-type behavior on an elevated plus maze, and locomotor activity, and they maintained body weight and circulating testosterone (Figures 5.S1D–S1F). The anatomically restricted nature of aromatase expression (Wu et al., 2009) allows specific ablation of aromatase+ MeApd neurons (Figure 5.2D). It also ensures that other non-MeApd aromatase+ populations such as those in the bed nucleus of the stria terminalis (BNST) are distant from the injection site and are not infected by the stereotactically delivered virus. Indeed, the number of aromatase+ BNST neurons was unchanged (*aro*$^{Cre/IPIN}$, 660 ± 198; *aro*$^{+/IPIN}$, 565 ± 132; n = 5, $p > 0.1$) following viral delivery to the MeA. Ablation of progesterone receptor-expressing neurons in the ventromedial hypothalamus reduces all aspects of aggression, including the pattern of attacks as measured by interattack interval and mean duration of an attack bout (Yang et al., 2013). Although we cannot exclude a subtle role of aromatase+ MeApd neurons in all components of aggression, our findings reveal that ablation of a majority of these neurons reduces aggression without altering the pattern of attack (Figure 5.S1B). It is possible that aromatase+ MeApd neurons relay pheromonal information relating to aggression rather than regulating different aspects of this behavior. If so, this would represent the identification of a class of molecularly specified MeA neurons that respond to pheromonal cues relating to aggression but not other social behaviors. Regardless of the underlying mechanism, our findings show that aromatase+ MeApd neurons are required for the display of WT levels of specific components of aggression.

Aromatase+ MeApd Neurons Acutely Regulate Male Aggression

We used a chemogenetic approach to acutely silence aromatase+ MeApd neurons (Sternson and Roth, 2014). Most aromatase+ neuroendocrine cells in the MeApd express glutamate decarboxylase 1 (GAD1), suggesting that they are GABAergic neurons (Figure 5.S2A). Silencing these neurons allows us to test directly whether their neural activity is essential for social behaviors. Moreover, this approach permits testing whether the chronic loss of neurons following caspase-mediated ablation activates compensatory mechanisms that mask a role of these neurons in marking, mating, or courtship vocalization. We delivered AAVs encoding a Cre-dependent fusion protein consisting of a Gi-coupled DREADD (designer receptor exclusively activated by designer drug) and mCherry bilaterally to the MeA (Figure 5.3A). This DREADD-Gi is activated exclusively by the biologically inert small-molecule clozapine-N-oxide (CNO) such that CNO-bound DREADD-Gi hyperpolarizes neurons and silences them (Armbruster et al., 2007, Sternson and Roth, 2014). Only *aro*$^{Cre/IPIN}$ males where a majority of aromatase+ MeApd neurons coexpressed mCherry were included for behavioral analysis (Figures 5.3B–3D and 5.S2B–S2G). We singly housed males 1 week after viral injection and began behavior testing 1 week later. They were tested in behavioral assays following CNO administration (Ray et al., 2011, Sasaki et al., 2011). There was no difference between *aro*$^{Cre/IPIN}$ males administered saline or CNO in assays of mating, courtship vocalization, urine marking, anxiety-type behavior, food finding, and locomotor activity (Figures 5.3B, 5.S2B, 5.S2D, and 5.S2E); these males also maintained body weight and circulating testosterone (Figures 5.S2F and 5.S2G). Thus, control levels of neural activity of most aromatase+ MeApd neurons are not required for these aspects of male physiology or behaviors, including male sexual behaviors.

Comparable proportions of *aro*$^{Cre/IPIN}$ males administered saline or CNO sniffed and attacked a WT male intruder (Figure 5.3C). *Aro*$^{Cre/IPIN}$ males administered CNO had a

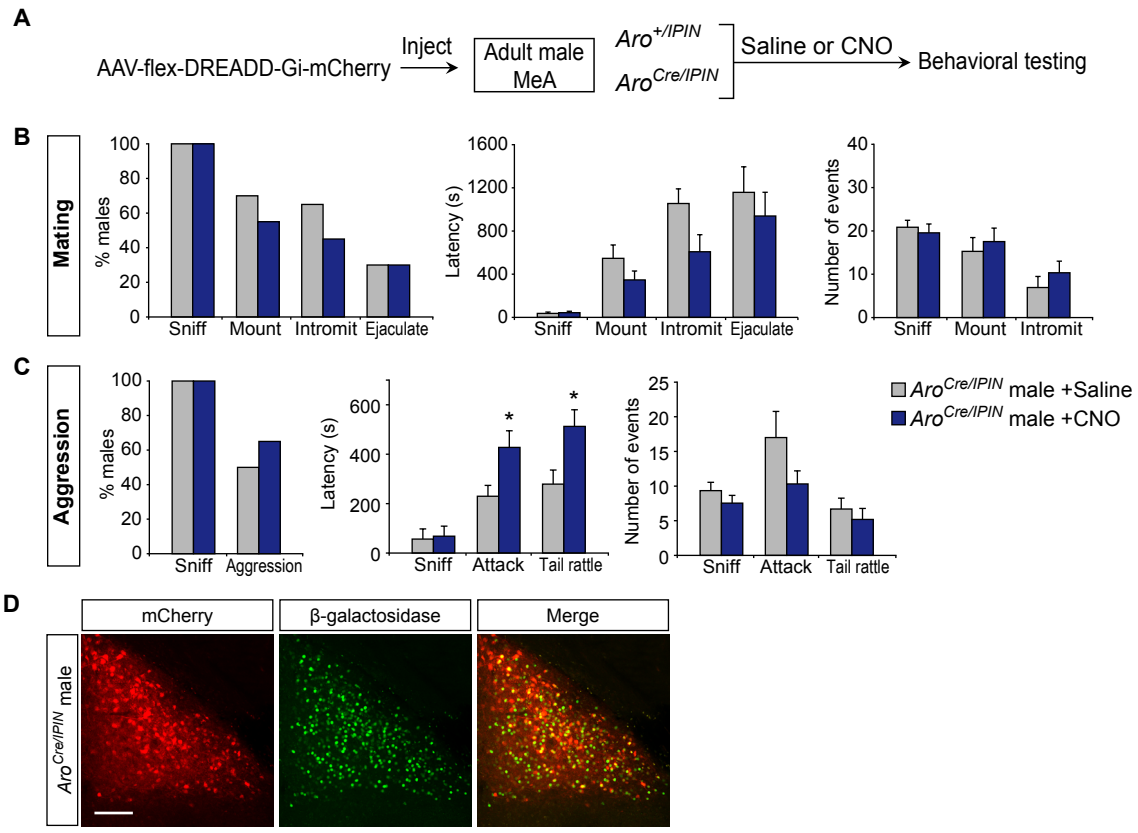

Figure 5.3: Inhibiting Aromatase+ MeApd Neurons with DREADD-Gi Reduces Specific Components of Male Aggression

(A) Experimental strategy to inhibit Cre-expressing aromatase+ MeApd neurons and test for behavioral deficits in males. AAV encoding Cre-dependent DREADD-Gi was injected into the MeA of aroCre/IPIN males that were subsequently tested for behaviors following intraperitoneal CNO or saline administration.

(B) No difference between aroCre/IPIN males administered saline or CNO in mating with a WT estrus female.

(C) No difference between percent aroCre/IPIN males given saline and CNO that sniffed or attacked a WT intruder male. AroCre/IPIN males administered CNO took significantly longer to initiate attacks or tail rattle.

(D) Histological verification of DREADD-Gi (mCherry) expression in aromatase+ neurons in MeApd of aroCre/IPIN males.

Mean ± SEM; n = 20 aroCre/IPIN; for parallel studies with aro+/IPIN, please see Figure 5.S2; *p < 0.05. Scale bars represent 200 μm. See also Figures S2 and S3.

significantly longer latency to initiate attacks and tail rattle toward intruder males (Figure 5.3C) without a change in the pattern of attack as measured by attack duration and interattack interval (Figure 5.S2C). There was a strong correlation between the increased latency to attack in the presence of CNO and DREADD-Gi expression (Figure 5.S2H). Importantly, *aro*$^{+/IPIN}$ control males injected with this AAV showed unaltered mating and

aggressive behaviors even in the presence of CNO (Figures S2I and S2J), demonstrating that CNO itself does not modulate social behaviors. Our histological studies confirmed that DREADD-Gi expression was limited to the MeApd and did not spread to other aromatase-expressing locations such as the BNST (Figure 5.S2K). Thus, acute silencing of aromatase+ MeApd neurons parallels the specific deficits in aggression observed with targeted ablation of these neurons. Importantly, activating these neurons with a Gq-coupled DREADD that increases neuronal activity (Sternson and Roth, 2014) did not alter sexual or aggressive displays at CNO doses previously shown by us and others to activate neurons and modulate behavior (Figure 5.S3) (Anaclet et al., 2014, Sasaki et al., 2011). Indeed, CNO elicited a large increase in c-Fos+ neurons in the MeApd in vivo and depolarized and increased spike rate in aromatase+ MeApd neurons in acute brain slices (Figures S3A and S3B). The lack of behavioral modulation with activation of aromatase+ MeApd neurons may reflect that a larger subset of MeApd neurons needs to be activated to alter aggression. Alternatively, these neurons may relay chemosensory information to neurons that receive additional inputs required to drive mating or aggression. Indeed, fly sensory neurons that relay the presence of pheromones are required, but not sufficient, for WT levels of aggression (Wang et al., 2011). Regardless, our findings demonstrate that neural activity of a majority of aromatase+ MeApd neuroendocrine neurons is required for appropriate display of male aggression, but not other sexually dimorphic behaviors.

Aromatase+ MeApd Neurons Specifically Regulate Maternal Aggression

We tested the function of aromatase+ MeApd neurons in female-typical displays of receptivity and parental care by ablating them via targeted delivery of AAV encoding Cre-dependent caspase-3 (Figure 5.4A). As with males, we only analyzed females with a substantive loss (>50%) of aromatase+ MeApd neurons (Figures 4B–4D and S4A–S4F). To test for sexual behavior, female $aro^{Cre/IPIN}$ and $aro^{+/IPIN}$ mice were injected bilaterally into the MeA with virus, and their ovaries were removed to permit estrus induction on the

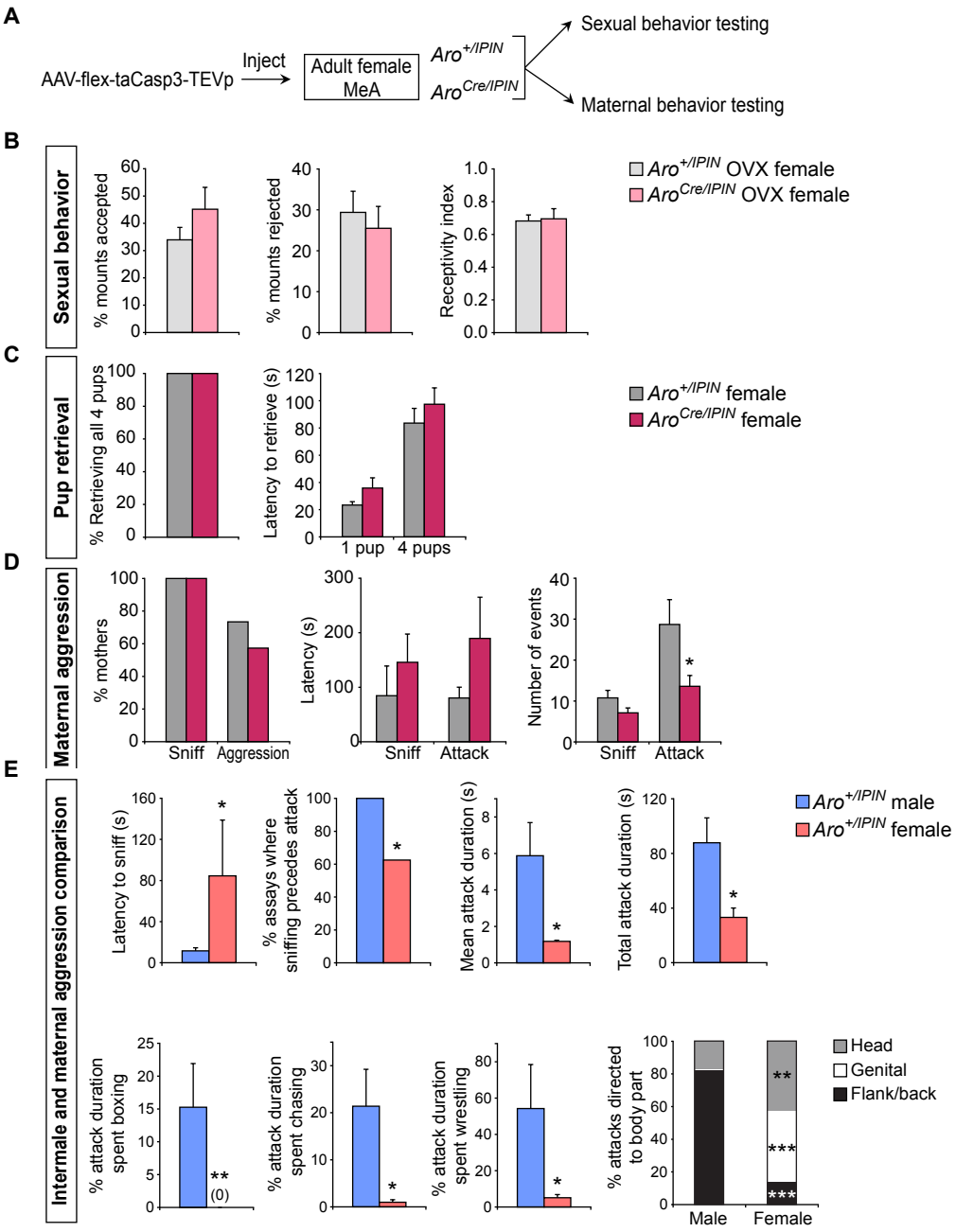

Figure 5.4: Ablation of Aromatase+ MeApd Neurons Reduces Specific Components of Maternal Aggression

(A) Experimental strategy to ablate Cre-expressing aromatase+ MeApd neurons and test for behavioral deficits. AAV encoding Cre-dependent caspase-3 was injected into the MeA of separate cohorts of aroCre/IPIN and aro+/IPIN females for testing performance in mating and maternal behaviors.

(B) No difference in fraction of mounts that were accepted or rejected and no difference in receptivity index (# intromissions/# mounts) between aroCre/IPIN and aro+/IPIN females.

(C) Vast majority of aroCre/IPIN and aro+/IPIN females retrieved all pups to the nest, and they did so with similar latencies.

day of testing. These mice were allowed to recover from surgery for 4 weeks, hormonally primed to be in estrus, and inserted into the home cage of sexually experienced WT males. We observed that sexual behavior of both groups of females was comparable, such that they stayed still rather than running away when the male approached and mounted them (Figure 5.4B). This receptive behavior permitted mounts to proceed to intromission (receptivity index) equivalently between these two sets of females (Figure 5.4B). WT males also appeared equally interested in *aro*$^{Cre/IPIN}$ and *aro*$^{+/IPIN}$ females as they investigated, mounted, and intromitted them with comparable latency and number (Figure 5.S4A). These females did not exhibit deficits in finding food, anxiety-type behavior, and locomotor activity, and they maintained their body weight (Figures S4B and S4C). In summary, despite the importance of the MeA in female sexual behavior (DiBenedictis et al., 2012), a majority of aromatase+ MeApd neurons are not essential for this behavior.

To test whether aromatase+ MeApd neurons regulate maternal behaviors, we ablated them in a separate cohort of females that were subsequently mated with WT males to generate litters (Figure 5.4A). *Aro*$^{Cre/IPIN}$ and *aro*$^{+/IPIN}$ females were inseminated (as determined by the presence of a vaginal plug) and generated litters at equivalent rates (Figure 5.S4D), indicating that ablation of aromatase+ MeApd neurons does not render females infertile.

(D) Comparable percent of aroCre/IPIN and aro+/IPIN females sniff and attack a WT intruder male. Significant decrease in number of attacks directed to intruder male by aroCre/IPIN females.

(E) A WT male intruder was inserted into the cage of a resident male or lactating female for 15 min. Mothers have a longer latency to sniff the intruder and, unlike resident males, can attack the intruder prior to chemoinvestigation. The duration of individual attacks as well as total duration of attacks initiated by mothers is significantly shorter. Mothers spend significantly less time chasing or wrestling with the intruder male. No boxing was observed in attacks initiated by mothers. Mothers bite the intruder significantly more on the head or anogenital region compared to resident males. Resident males bite the intruder significantly more on the back and flank compared to mothers. Data for these behavioral comparisons are taken from animals used to generate data for panels in Figures 2C, 4D, S1B, and S4D.

Mean ± SEM; n > 14 aro+/IPIN and n > 7 aroCre/IPIN for tests of sexual and maternal behaviors each (A–D); n = 7 aro+/IPIN males and 6 aro+/IPIN mothers (E); *p < 0.05,**p < 0.01,***p < 0.005; OVX, ovaries surgically removed. See also Figure 5.S4.

Upon parturition, *aro*$^{Cre/IPIN}$ as well as *aro*$^{+/IPIN}$ females ate their afterbirths, cleaned pups, and nursed them in their nest. Pups can crawl away from the nest, and dams efficiently retrieve them to the nest. Experimental removal of pups from their nest elicited pup retrieval with comparable efficiency between the two groups of females (Figure 5.4C). In addition, *aro*$^{Cre/IPIN}$ females did not exhibit deficits in finding hidden food, anxiety-type behavior on an elevated plus maze, and locomotor activity, and they maintained their body weight (Figures S4E and S4F). Thus, most aromatase+ MeApd neurons are not essential for these behaviors, including many components of maternal care.

Nursing mice attack unfamiliar intruder mice because such intruders can be infanticidal toward pups (Gandelman, 1972, Wu et al., 2014). We tested whether aromatase+ MeApd neurons were required for such maternal aggression by inserting a WT male into the cage of experimental and control nursing females. Both groups of females investigated and attacked intruders with equivalent probability (Figure 5.4D). There was a significant 2.4-fold decrease in the number of attacks by *aro*$^{Cre/IPIN}$ females that strongly correlated with the degree of cell loss within the MeApd (Figures 4D and S4G). Similar to males (Figure 5.S1B), once aggression was initiated, there was no difference in the attack pattern between control and *aro*$^{Cre/IPIN}$ females (Figure 5.S4D). Thus, ablation of aromatase+ MeApd neurons leads to a specific deficit in maternal aggression. We wished to test whether these neurons also acutely regulate maternal aggression by using DREADD-Gi mediated chemogenetic control of neural activity. However, we consistently observed only a few weakly expressing mCherry+ neurons within the MeApd of *aro*$^{Cre/IPIN}$ females (data not shown), presumably reflecting the lower levels of aromatase in the female brain. Given that caspase-3 is extremely cytotoxic (Morgan et al., 2014), it is not surprising that despite the lower efficiency of Cre recombination in females, we succeeded in ablating aromatase+ MeApd neurons. In any event, our findings demonstrate that aromatase+ MeApd neurons are required for WT levels of maternal aggression. Moreover, our studies

reveal that aromatase+ neurons are, in fact, functional in females.

Different forms of fighting such as intermale and maternal aggression are thought to be controlled by different neural pathways (Moyer, 1968). Indeed, there are distinct sensory, hormonal, and molecular requirements for intermale and maternal aggression (Demas et al., 1999, Finney and Erpino, 1976, Gammie and Nelson, 1999, Gammie et al., 2000, McDermott and Gandelman, 1979, Nelson et al., 1995, Svare and Gandelman, 1975, Svare and Gandelman, 1976a, Svare and Gandelman, 1976b). Previous work suggested that these two forms of aggression may be executed differently (Gandelman, 1972, Scott, 1966). Given our finding that aromatase+ MeApd neurons regulate both intermale and maternal aggression, we sought to determine the nature of the differences in these two forms of fighting. We identified many quantitative differences between intermale and maternal aggression (Figure 5.4E). Moreover, there were striking qualitative differences between these two forms of aggression. Males typically attack the back and flank of the intruder, whereas dams attack the head and genital regions of the intruder and they rarely box, chase, or wrestle (Figure 5.4E; Movies S1 and S2). In summary, these findings show that aromatase+ MeApd neurons regulate distinct forms of aggression in the two sexes.

DISCUSSION

A Shared Neural Pathway for Distinct Forms of Aggression

It can be argued that intermale and maternal aggression are different forms of a common behavioral display, fighting. However, we observe dramatic differences between intermale and maternal aggression. Nevertheless, we find that aromatase+ MeApd neurons regulate both maternal and intermale aggression, demonstrating a hitherto unknown neural circuit link between different forms of aggression. More broadly, our findings suggest the possibility that a primordial neural pathway underlying aggression predates the divergent needs of the two sexes to fight in different contexts. Such a neural circuit could be modified

during evolution and sexual selection such that it is activated by different stimuli and drives different motor programs in the two sexes.

Aromatase+ MeApd Neurons Subserve Distinct Behaviors in the Two Sexes

Most sexual dimorphisms in the vertebrate brain represent quantitative rather than qualitative differences in gene expression or neurocytological features. Indeed, there are significantly more aromatase+ MeApd neurons in males compared to females (Wu et al., 2009). It is possible that a sexually dimorphic neuronal pool is nonfunctional in one sex, drives distinct behaviors in both sexes, or functions to suppress a behavior of the opposite sex (De Vries and Boyle, 1998). We show here that aromatase+ MeApd neurons control distinct forms of aggression in males and females. The cell number difference in aromatase+ MeApd neurons could drive distinct behaviors (such as tail rattling or boxing) in the two sexes. The MeApd also expresses many other sex hormone-dependent genes in sex-specific patterns (Xu et al., 2012), and these may also permit aromatase+ MeApd neurons to regulate distinct behaviors in the two sexes. We have previously shown that sexually dimorphic progesterone receptor-expressing neurons in the ventromedial hypothalamus control distinct behaviors in males and females (Yang et al., 2013). Such functional bivalence may therefore be a general property of sexually dimorphic neuronal populations.

Global versus Modular Control of Complex Social Behaviors

Sex hormones exert global control over the display of sexually dimorphic social behaviors. For example, estrogen signaling in males governs vocalization, sexual displays, aggression, and territory marking. By contrast, we find that aromatase+ MeApd neurons are only required for WT levels of aggression. At least some components of the global control of vertebrate male behavior by estradiol likely result from paracrine signaling and masculinizing neural circuits during development (Balthazart and Ball, 1998, Forlano et

al., 2006, McCarthy, 2008, Wu et al., 2009). In addition, specificity in behavioral control may be a general feature of molecularly defined neuronal populations such as those in the MeApd that are close to sensory input. In this case, aromatase+ neuronal populations more distant from sensory input, such as those in the hypothalamus, are predicted to control multiple features of different male-typical behaviors.

Our data show that it is possible to dissociate specific components of a complex social behavior such as aggression without altering other features of the behavior. In fact, the MeA itself is critical for aggressive as well as courtship displays in both sexes, whereas we find that the aromatase+ MeApd neurons regulate aggression, but not territory marking or sexual behaviors (Baum and Bakker, 2013, Bergan et al., 2014, Choi et al., 2005, DiBenedictis et al., 2012, Sokolowski and Corbin, 2012, Swanson, 2000, Wu et al., 2009). Aromatase+ MeApd neurons comprise ~40% of neurons within the MeApd and, we estimate, ~10%–20% of neurons within the MeA. Given the molecular heterogeneity within the MeA, we anticipate that other molecularly specified MeA neuronal subsets regulate other aspects of social interactions. Such exquisite modularity in behavioral control may be a general property of many similarly discrete neuronal populations in other brain regions. It will be interesting to understand how such neural modules underlying particular behavioral components are coordinated to generate apparently seamless behavioral displays. Presumably, neurons close to motor output pathways encode multiple features of a behavioral program. Indeed, neurons expressing progesterone receptor (and estrogen receptor α) in the ventromedial hypothalamus that are distant from sensory input are necessary and sufficient for multiple components of mating and aggression (Lee et al., 2014, Yang et al., 2013). Such modularity in the neuronal control of social behavior is likely to be a general mechanism whereby other complex behaviors such as feeding are regulated (Sternson, 2013). As discussed recently (Yang et al., 2013), such modular control of behavior resembles the modularity in signaling proteins and networks and may

enable rapid evolution of behaviors.

Hong et al. (2014)) recently published a study describing the contribution of MeA neurons to male mating, aggression, and grooming. Our study genetically identifies the aromatase+ subset of MeA neurons as specifically underlying male aggression and further shows that these neurons also regulate maternal aggression.

AUTHOR CONTRIBUTIONS

E.K.U. and N.M.S. designed the experiments. E.K.U. and K.J. Burke performed the experiments. P.M.F. and C.F.Y. provided viral reagents. E.K.U., K.J. Burke, K.J. Bender, and N.M.S. analyzed the data. E.K.U. and N.M.S. wrote the paper.

ACKNOWLEDGMENTS

We thank members of the N.M.S. laboratory, T. Clandinin, Z. Knight, and L. Stowers for comments on the manuscript; D. Anderson for communication of unpublished findings; and M. Tran and A. Basbaum for *aro*$^{+/IPIN}$; *GAD1*$^{+/EGFP}$ mice. This work was supported by funds from the Ellison Medical Foundation (N.M.S.) and the NIH F31NS078959 (E.K.U.), R01DA035913 and R00DC011080 (K.J. Bender), R01NS073613 (P.M.F.), and R01NS049488 and R01NS083872 (N.M.S.).

SUPPLEMENTAL INFORMATION

SUPPLEMENTAL FIGURES

Figure 5.S1

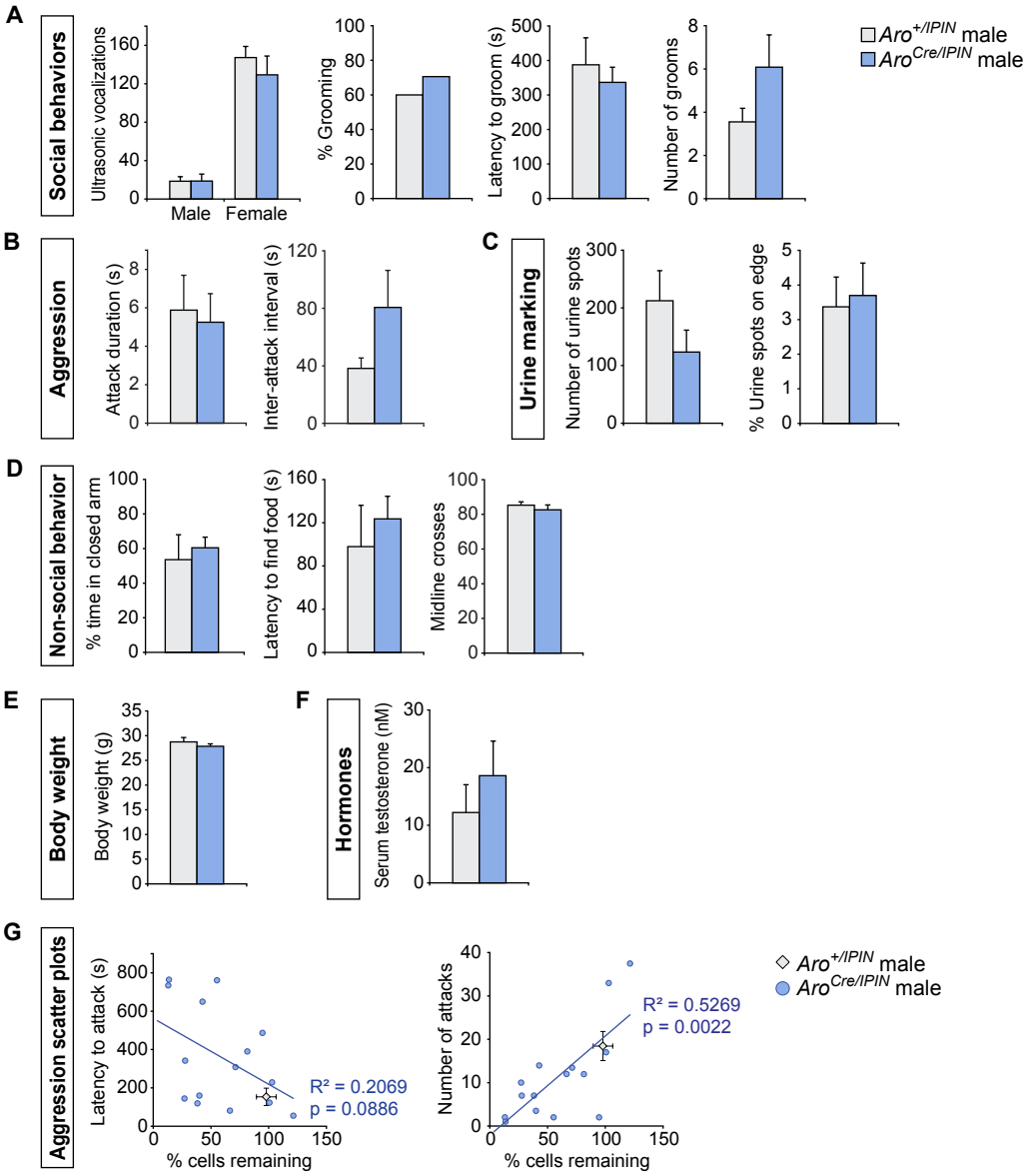
A
Social behaviors
Ultrasonic vocalizations
Male
Female
% Grooming
Latency to groom (s)
Number of grooms
Aro+/IPIN male
AroCre/IPIN male
B
Aggression
Attack duration (s)
Inter-attack interval (s)
C
Urine marking
Number of urine spots
% Urine spots on edge
D
Non-social behavior
% time in closed arm
Latency to find food (s)
Midline crosses
E
Body weight
Body weight (g)
F
Hormones
Serum testosterone (nM)
G
Aggression scatter plots
Latency to attack (s)
% cells remaining
R² = 0.2069
p = 0.0886
Number of attacks
R² = 0.5269
p = 0.0022
Aro+/IPIN male
AroCre/IPIN male

Figure 5.S1. Ablation of male aromatase+ MeApd neurons reduces specific components of aggression, Related to Figure 5.2.

(A) No difference between *aro*$^{Cre/IPIN}$ and *aro*$^{+/IPIN}$ males in emitting ultrasonic vocalizations toward WT male and female intruders or in grooming WT intruder males.

(B) No difference between *aro*$^{Cre/IPIN}$ and *aro*$^{+/IPIN}$ males in pattern of attacks (mean attack bout duration and inter-attack interval) toward a WT intruder male.

(C) No difference between *aro*$^{Cre/IPIN}$ and *aro*$^{+/IPIN}$ males in marking territory with urine.

(D) No difference between *aro*$^{Cre/IPIN}$ and *aro*$^{+/IPIN}$ males in anxiety-type behavior (elevated-plus maze), finding food when starved, or locomotor activity as measured by number of midline crosses.

(E, F) No difference between *aro*$^{Cre/IPIN}$ and *aro*$^{+/IPIN}$ males in body weight or serum testosterone.

(G) Significant correlation between loss of aromatase+ MeApd neurons and number of attacks toward a WT intruder male. Scatter plots include data from all *aro*$^{Cre/IPIN}$ males who displayed any attacks (15/27); gray diamond in the plots depicts number of attacks by *aro*$^{+/IPIN}$ males toward WT intruder males.

Mean ± SEM; n = 14 *aro*$^{+/IPIN}$ (A-G), n = 15 *aro*$^{Cre/IPIN}$ (A-F), n = 27 *aro*$^{Cre/IPIN}$ (G).

Figure 5.S2

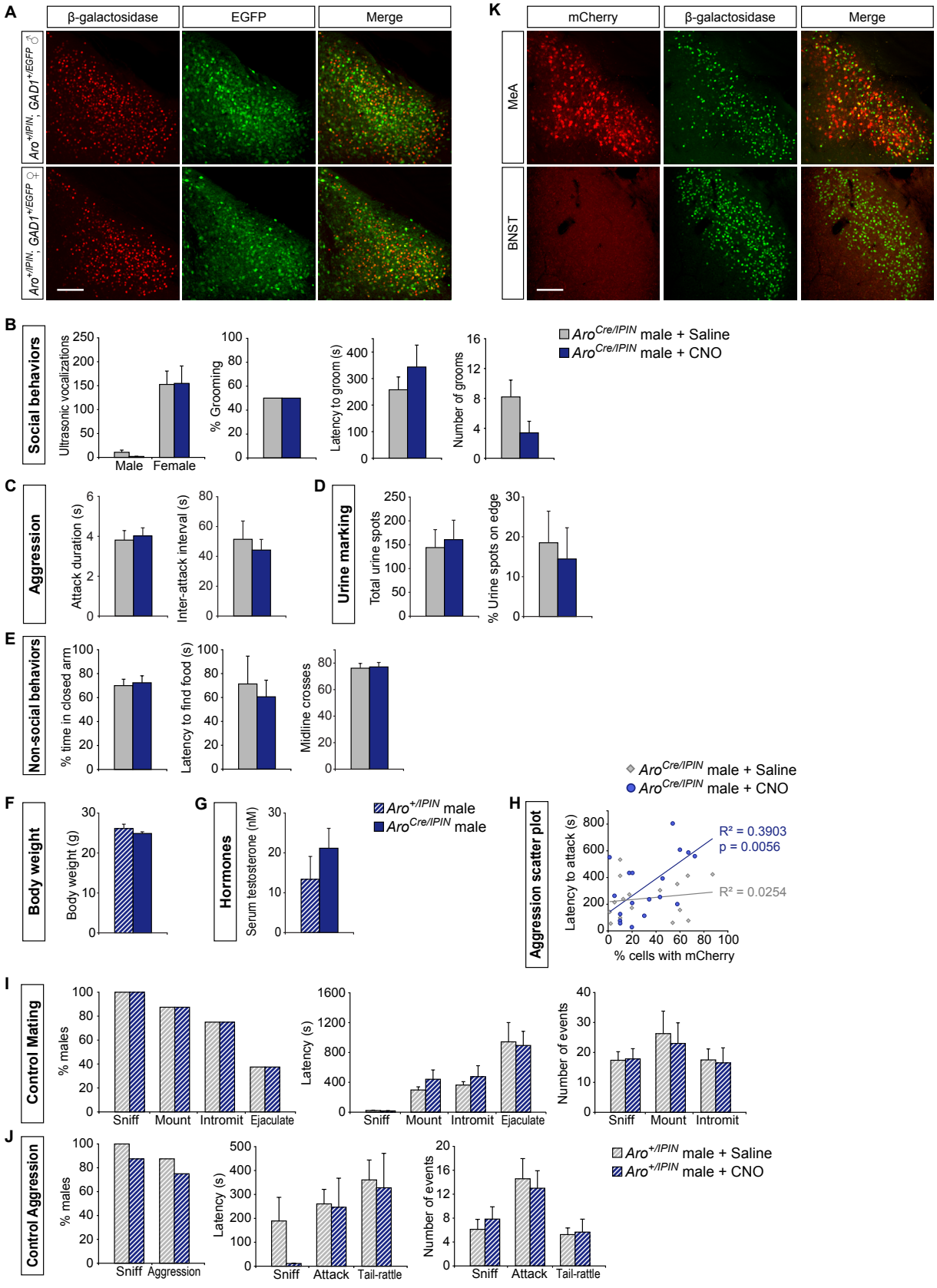
A
β-galactosidase
EGFP
Merge
Aro+/IPIN; GAD1+/EGFP ♂
Aro+/IPIN; GAD1+/EGFP ♀
K
mCherry
β-galactosidase
Merge
MeA
BNST
B
Social behaviors
Ultrasonic vocalizations
Male
Female
% Grooming
Latency to groom (s)
Number of grooms
AroCre/IPIN male + Saline
AroCre/IPIN male + CNO
C
Aggression
Attack duration (s)
Inter-attack interval (s)
D
Urine marking
Total urine spots
% Urine spots on edge
E
Non-social behaviors
% time in closed arm
Latency to find food (s)
Midline crosses
F
Body weight
Body weight (g)
G
Hormones
Serum testosterone (nM)
Aro+/IPIN male
AroCre/IPIN male
H
Aggression scatter plot
AroCre/IPIN male + Saline
AroCre/IPIN male + CNO
Latency to attack (s)
% cells with mCherry
R² = 0.3903
p = 0.0056
R² = 0.0254
I
Control Mating
% males
Latency (s)
Number of events
Sniff
Mount
Intromit
Ejaculate
J
Control Aggression
% males
Sniff
Aggression
Latency (s)
Attack
Tail-rattle
Number of events
Aro+/IPIN male + Saline
Aro+/IPIN male + CNO

Figure 5.S2. Inhibiting male aromatase+ MeApd neurons reduces specific components of aggression, Related to Figure 5.3.

(A) Most aromatase+ MeApd neurons co-express GAD1, a biosynthetic enzyme for the neurotransmitter GABA. (% aromatase+ MeApd neurons that are GAD1+: Male, 83.7% ± 3.4; Female, 90.6% ±4.8; n = 2 for each sex).

(B) No difference between *aro*$^{Cre/IPIN}$ males given CNO or saline in emitting ultrasonic vocalizations toward WT male and female intruders or in grooming WT intruder males.

(C) No difference between *aro*$^{Cre/IPIN}$ males given CNO or saline in pattern of attacks (mean attack bout duration and inter-attack interval) toward a WT intruder male.

(D) No difference between *aro*$^{Cre/IPIN}$ males given CNO or saline in marking territory with urine.

(E) No difference between *aro*$^{Cre/IPIN}$ males given CNO or saline in anxiety-type behavior (elevated-plus maze), finding food when starved, or locomotor activity as measured by number of midline crosses.

(F, G) No difference between *aro*$^{Cre/IPIN}$ and *aro*$^{+/IPIN}$ males in body weight or serum testosterone.

(H) Significant correlation between more aromatase+ MeApd neurons expressing DREADD-G_i and increased latency to attack WT intruder male following CNO administration. Scatter plot includes data from all *aro*$^{Cre/IPIN}$ males who displayed any attacks (18/28, CNO; 16/28, saline).

(I, J) No difference between *aro*$^{+/IPIN}$ males given CNO or saline in mating or aggression with WT female and male intruders, respectively.

(K) Injection of AAV encoding the Cre-dependent fusion protein DREADD-G_i:mCherry into the MeA results in expression of mCherry in this region but not in other aromatase+ (Cre+) regions such as the BNST.

Mean ± SEM; n = 8 *aro*$^{+/IPIN}$ (F, G, I, J), n = 20 *aro*$^{Cre/IPIN}$ (B-G), n = 28 *aro*$^{Cre/IPIN}$ (H).

Scale bars = 200 μm.

Figure 5.S3

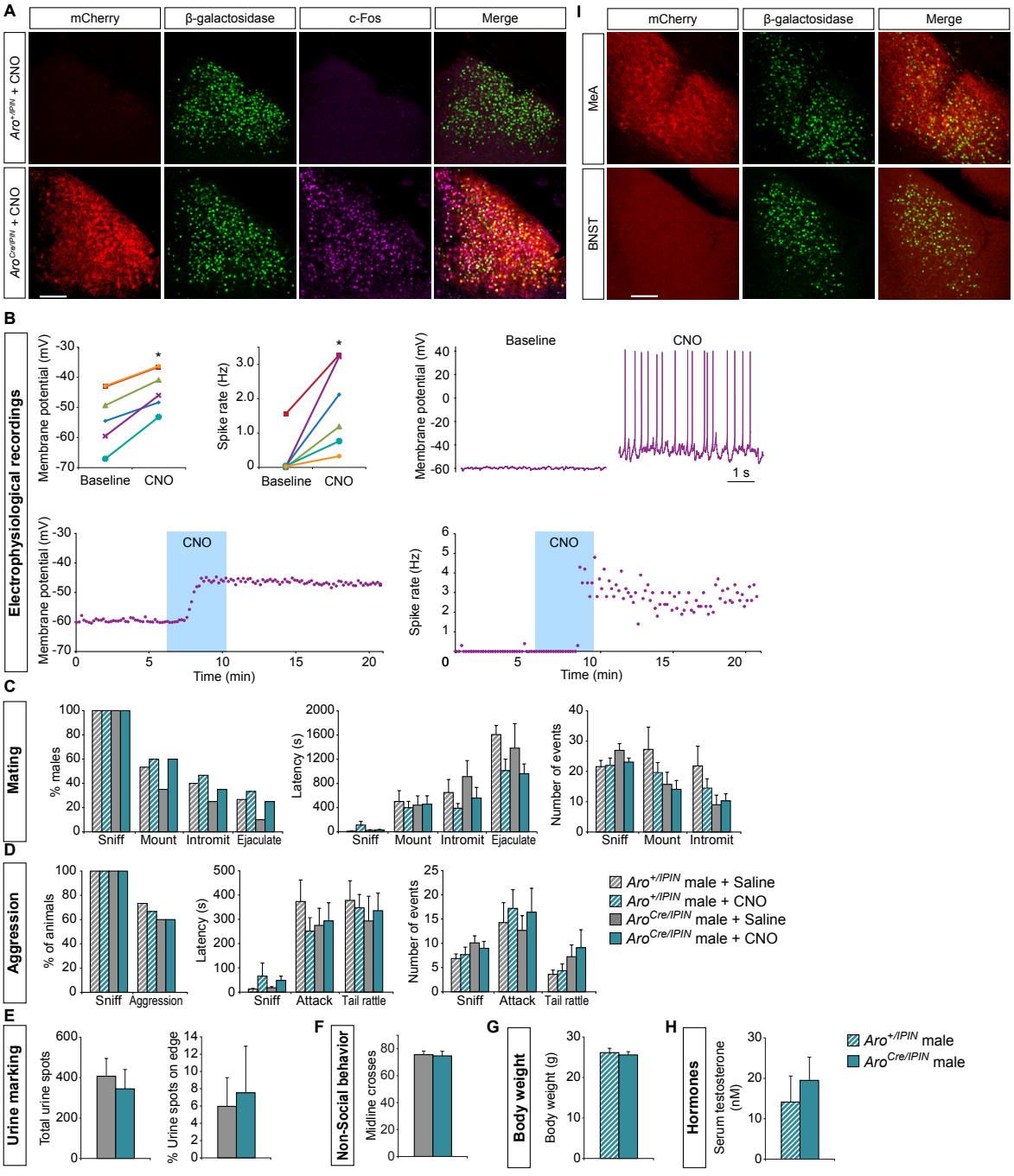
A
mCherry
β-galactosidase
c-Fos
Merge
Aro+/IPIN + CNO
AroCre/IPIN + CNO
I
mCherry
β-galactosidase
Merge
MeA
BNST
B
Electrophysiological recordings
Membrane potential (mV)
Baseline
CNO
Spike rate (Hz)
Baseline
CNO
Membrane potential (mV)
Baseline
CNO
1 s
Membrane potential (mV)
CNO
Time (min)
Spike rate (Hz)
CNO
Time (min)
C
Mating
% males
Sniff
Mount
Intromit
Ejaculate
Latency (s)
Sniff
Mount
Intromit
Ejaculate
Number of events
Sniff
Mount
Intromit
D
Aggression
% of animals
Sniff
Aggression
Latency (s)
Sniff
Attack
Tail rattle
Number of events
Sniff
Attack
Tail rattle
Aro+/IPIN male + Saline
Aro+/IPIN male + CNO
AroCre/IPIN male + Saline
AroCre/IPIN male + CNO
E
Urine marking
Total urine spots
% Urine spots on edge
F
Non-Social behavior
Midline crosses
G
Body weight
Body weight (g)
H
Hormones
Serum testosterone (nM)
Aro+/IPIN male
AroCre/IPIN male

Figure 5.S3. Activating male aromatase+ MeApd neurons does not modulate behavior, Related to Figure 5.3.

AAV encoding Cre-dependent DREADD-G_q:mCherry was injected bilaterally into the MeA of *aro*$^{Cre/IPIN}$ and *aro*$^{+/IPIN}$ males, and animals were allowed to recover for >10 days.

(A) CNO administration leads to c-Fos activation in MeApd of *aro*$^{Cre/IPIN}$ but not *aro*$^{+/IPIN}$ males.

(B) Electrophysiological recordings were performed on coronal brain slices (225-230 μm thick) containing the MeA. Aromatase+ neurons expressing DREADD-G_q were selected for patch-clamp recording based on mCherry expression. Both membrane potential and spike rate increased after the application of 1 μM CNO in aCSF for 4 min. Panels at top left show increases in membrane potential and spike rate in the presence of CNO for each of the 6 neurons (each cell represented in a different color). Other panels show changes in membrane potential and spike rate in an example neuron; the blue box denotes time of CNO application. n = 6 cells from 4 animals. *$p < 0.05$ (sign-rank test).

(C-F) No difference between *aro*$^{Cre/IPIN}$ and *aro*$^{+/IPIN}$ males given saline or CNO in displays of mating, aggression, urine marking, or locomotor behavior.

(G, H) No difference between *aro*$^{Cre/IPIN}$ and *aro*$^{+/IPIN}$ males in body weight or serum testosterone.

(I) Injection of AAV encoding the Cre-dependent fusion protein DREADD-G_q:mCherry into the MeA results in expression of mCherry in this region but not in other aromatase+ (Cre+) regions such as the BNST.

Mean ± SEM; n ≥ 5 for both genotypes (A), n = 5 *aro*$^{+/IPIN}$ (B-G), n = 24 *aro*$^{Cre/IPIN}$ (B-G).

Scale bars = 200 μm.

Figure 5.S4

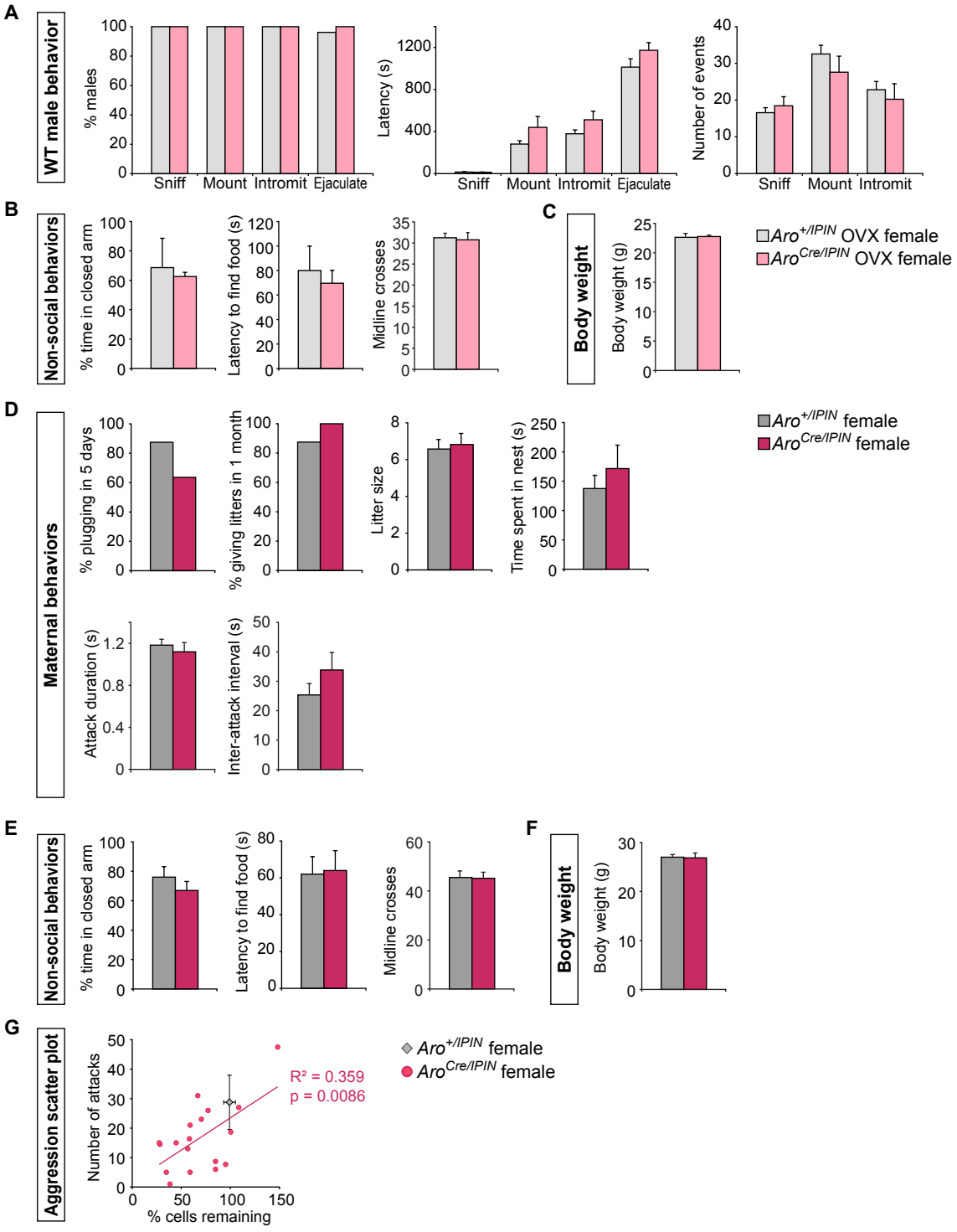
A
WT male behavior
% males
Latency (s)
Number of events
Sniff
Mount
Intromit
Ejaculate
B
Non-social behaviors
% time in closed arm
Latency to find food (s)
Midline crosses
C
Body weight
Body weight (g)
Aro+/IPIN OVX female
AroCre/IPIN OVX female
D
Maternal behaviors
% plugging in 5 days
% giving litters in 1 month
Litter size
Time spent in nest (s)
Attack duration (s)
Inter-attack interval (s)
Aro+/IPIN female
AroCre/IPIN female
E
Non-social behaviors
% time in closed arm
Latency to find food (s)
Midline crosses
F
Body weight
Body weight (g)
G
Aggression scatter plot
Number of attacks
% cells remaining
R² = 0.359
p = 0.0086
Aro+/IPIN female
AroCre/IPIN female

Figure 5.S4. Ablation of aromatase+ MeApd neurons reduces specific components of maternal aggression, Related to Figure 5.4.

For tests of sexual behavior (A-C), *aro*$^{Cre/IPIN}$ and *aro*$^{+/IPIN}$ females were ovariectomized (OVX) and estrus was hormonally induced prior to testing. For tests of maternal behavior (D-G), *aro*$^{Cre/IPIN}$ and *aro*$^{+/IPIN}$ females were gonadally intact, mated with a WT male, and allowed to deliver a litter.

(A) WT males mate equivalently with *aro*$^{Cre/IPIN}$ and *aro*$^{+/IPIN}$ females.

(B) No difference between *aro*$^{Cre/IPIN}$ and *aro*$^{+/IPIN}$ females in anxiety-type behavior (elevated-plus maze), finding food when starved, or locomotor activity as measured by number of midline crosses.

(C) No difference between *aro*$^{Cre/IPIN}$ and *aro*$^{+/IPIN}$ females in body weight.

(D) No difference between *aro*$^{Cre/IPIN}$ and *aro*$^{+/IPIN}$ females in percent plugged by WT male, percent producing litters, litter size, and time spent in the nest in 15 min during pup retrieval. No difference between *aro*$^{Cre/IPIN}$ and *aro*$^{+/IPIN}$ mothers in pattern of attacks (mean attack bout duration and inter-attack interval) toward a WT intruder male.

(E) No difference between *aro*$^{Cre/IPIN}$ and *aro*$^{+/IPIN}$ females in anxiety-type behavior (elevated-plus maze), finding food when starved, or locomotor activity as measured by number of midline crosses.

(F) No difference between *aro*$^{Cre/IPIN}$ and *aro*$^{+/IPIN}$ females in body weight.

(G) Significant correlation between extent of loss of aromatase+ MeApd neurons and reduced number of attacks toward WT intruder male. Scatter plot includes data from all *aro*$^{Cre/IPIN}$ mothers who displayed any attacks; gray diamond in the plot depicts number of attacks by *aro*$^{+/IPIN}$ mothers toward WT intruder males (18/28).

Mean ± SEM; n ≥ 14 *aro*$^{+/IPIN}$ (A-G), n = 7 *aro*$^{Cre/IPIN}$ (A-C), n = 8 *aro*$^{Cre/IPIN}$ (D-F), n = 28 *aro*$^{Cre/IPIN}$ (G)

SUPPLEMENTAL MOVIE LEGENDS

Movie S1: Resident male attacks intruder male, Related to Figure 5.4.

A WT resident male is shown attacking a WT intruder male with attacks to the flank, wrestling, and boxing.

Movie S2: Maternal aggression toward an intruder male, Related to Figure 5.4.

A WT mother (pups have been removed for safety) shows aggression toward a WT intruder male by directing attack toward the genital area.

SUPPLEMENTAL EXPERIMENTAL PROCEDURES

Animals

Adult mice 10–24 weeks of age were used in all studies. Mice were housed in a UCSF barrier facility with a 12:12 hr light:dark cycle, and food and water were available *ad libitum*. *Aro*$^{Cre/IPIN}$ mice and their control *aro*$^{+/IPIN}$ same-sex siblings were used for behavioral studies. In order to examine GABA co-localization with aromatase, we mated *aro*$^{+/IPIN}$ mice with mice bearing an EGFP knocked-in to the *GAD1* locus such that it faithfully colabels GABA neurons within the MeA and examined progeny doubly heterozygous for *LacZ* and *egfp* (Bian, 2013; Tamamaki et al., 2003). Animals were group-housed by sex after weaning at 3 weeks of age. All studies with animals were done in accordance with UCSF IACUC protocols.

Generation of aromatase^{Cre} *mice*

We used previously described homology DNA arms to generate a targeting construct for the *aromatase* locus (Wu et al., 2009). A transgene encoding IRES-Cre recombinase followed immediately by a previously described FRT-flanked neomycin selection (FNF) cassette was inserted as an *AscI* fragment 3 bp 3' of the stop codon in the last exon of

the *aromatase* locus in mouse 129/SvEv ES cells (Yang et al., 2013). We screened G418-resistant ES clones for homologous recombination of the 3' arm with PCR, using a primer (5'-CATCGCCTTCTATCGCCTTCTTGAC, F2) that was complementary to the neomycin selection cassette and an external primer (5'-CTTGATCATTGGAGCCAAATCTGGATG, R2) that was complementary to genomic sequence located 3' of the 3' homology arm of the targeting vector. A subset of positive clones was tested by PCR for homologous targeting of the 5' arm using an external primer (5'-CCAGCTGGATTTCTTGGGATCAAATTCAGG, F1) and a primer unique to the modified allele (5'-GAATTCGGCGCGCCTCTTCACTGTTG, R1). ES clones harboring the homologously recombined modified aromatase allele were injected into blastocysts to obtain chimeric mice that were crossed to C57Bl/6J females to obtain germline transmission. Chimeric mice that transmitted the *aro*^{Cre} allele were obtained from one positive clone. F1 progeny of these chimeric mice were mated with mice expressing Flpe recombinase ubiquitously to delete the FNF cassette (Rodríguez et al., 2000). This deletion event was verified with PCR, using a primer complementary to Cre recombinase (5'-AGGATGACTCTGGTCAGAGATACCTG, F3) and the external primer R2. Progeny with a successful deletion of this selection cassette were backcrossed >5 generations in C57Bl/6J and used for experimental analysis.

Stereotaxic surgery and viruses

Stereotaxic surgery was performed as described previously (Morgan et al., 2014; Yang et al., 2013). Briefly, a mouse was placed in a stereotaxic frame (Kopf Instruments) under anesthesia (0.5-2% isofluorane), the skull was exposed with a midline scalp incision, and the stereotaxic frame was aligned at bregma using visual landmarks. The drill (drill bit #85; ~279 µm diameter) on the stereotaxic frame was placed over the skull at coordinates corresponding to the MeA (rostrocaudal, −1.6 mm; mediolateral, ± 2.2 mm), and a hole was drilled through the skull bone to expose the brain. A 33 gauge steel needle connected via PE20 tubing to a Hamilton syringe was loaded with virus, aligned at bregma (including

in the z-axis) and slowly lowered to a depth of 5.15 mm. Virus was delivered bilaterally (1 µl of the previously described AAV-flex-taCasp3-TEVp (Yang et al., 2013), or 0.7 µl of AAV-flex-DREADD-G_i:mCherry, or 0.7 µL of AAV-flex-DREADD-G_q:mCherry) at 100 nL/min with a Hamilton syringe using a micropump (Harvard Apparatus). We used AAV serotypes 1 or 10 for delivering caspase-3 and AAV serotype 10 for all DREADD studies. AAV serotype 1 virus (3 x 10^{12} IU/mL) was generated at the University of North Carolina Vector core, and AAV serotype 10 viruses (1 x 10^{13} genomes copies/mL) were packaged by PMF and colleagues. The needle was left in place for an additional 5 min to allow diffusion of the virus and then was slowly withdrawn. Mice used for receptivity assays were ovariectomized during stereotaxic surgery while the virus was being delivered. Mice were weighed and allowed to recover on a heating pad before being returned to their home cage.

Behavior

Behavioral testing was performed ≥ 1 hr after onset of the dark cycle and recorded and analyzed as described previously, except for testing in the elevated-plus maze which was performed 2-3 hours before the onset of the dark cycle (Wu et al., 2009; Yang et al., 2013). There were ≥ 2 days between behavioral tests, and residents were always exposed to a novel intruder. For sexual receptivity assays, sequential tests were 7 days apart to allow hormone levels to subside prior to estrus induction for the next assay.

Male residents were singly housed 7-10 days prior to behavior testing. Briefly, they were tested twice for mating (30 min with an estrus female), once for territory marking (1 hr in a fresh cage lined with Whatman filter paper), twice for aggression (15 min with a group housed intruder male), and once for ultrasonic vocalization (3 min with a male intruder, then 3 min with female intruder). For studies with DREADDs, CNO and saline were administered randomly such that 50% of the mice received CNO (or saline) on the

first trial, and the treatment was reversed on the second trial; in these studies, males were tested once each with CNO and saline in tests of mating, territory marking, aggression, ultrasonic vocalization, and performance on an elevated-plus maze (as described below). Animals were tested 30 min subsequent to intraperitoneal injection of CNO or saline.

For tests of sexual receptivity, a group-housed ovariectomized female was hormonally primed to be in estrus (see below) and inserted for 30 min into the cage of a sexually experienced WT resident male. The female was returned to group-housing following such an assay. All females were tested three times for sexual receptivity. For tests of maternal behavior, females were allowed one week to recover from stereotaxic surgery and then co-housed with a sexually experienced male. These females were checked daily for the presence of vaginal plugs for the first 5 days. They were singly housed 3-5 days prior to parturition and checked daily for the presence of a litter. Upon parturition the cage was examined for the presence of placentae and to determine whether pups had been licked clean and gathered into nest. Nursing females were tested for pup retrieval twice for 15 min each with 2-6 day old pups. Four pups from the nest were scattered across the cage, and various parameters of pup retrieval were scored. Females were tested twice for maternal aggression 6-10 days after parturition. The pups were removed and a group-housed WT intruder male was inserted into the nursing female's cage for 15 min. The pups were returned to the dam at the end of the assay.

Once all tests of social behavior were completed, males and females were tested once on an elevated-plus maze for 5 min after being placed in the center, open compartment. They were subsequently tested for 5 min for their ability to find a cracker (Cheez-It or Goldfish) after being deprived of food for 6 hr. Following behavior testing, mice were weighed, blood was collected for hormone titers, and they were perfused for histological analysis. All tests were scored by an experimenter blind to the genotype and drug treatment of the mice, using a software package we developed in MATLAB (Wu et al., 2009).

Histology

Animals were perfused with 4% paraformaldehyde as described previously (Yang et al., 2013), and sections were collected at a thickness of 65 μm for immunolabeling or 100 μm for *in situ* hybridization using a vibrating microtome (Leica). Immunolabeling was performed using previously published protocols (Wu et al., 2009). *In situ* hybridization was performed as described previously, using published probes for aromatase and Cre recombinase (Wu et al., 2009; Yang et al., 2013). The primary antisera used are: chicken anti-β-gal (Abcam, 1:6,000), rabbit anti-GFP (Invitrogen, 1:2,000), rabbit anti-c-Fos (Millipore, 1:10,000), rat anti-dsRed (Clontech, 1:2,000), and alkaline phosphatase-conjugated sheep anti-digoxygenin (Roche, 1:5,000). The fluorophore conjugated secondary antisera are: Cy3 donkey anti-rabbit, Cy3 donkey anti-rat, Cy3 donkey anti-chicken (Jackson ImmunoResearch, 1:800), AlexaFluor 647 donkey anti-chicken (Jackson ImmunoResearch, 1:500), and AlexaFluor 488 donkey anti-rabbit, AlexaFluor 488 donkey anti-chicken (Invitrogen, 1:300).

Sections were imaged using a confocal microscope (Zeiss). To estimate cell loss following caspase-3 mediated ablation, images were obtained from every section spanning the MeApd, using a 20X objective to collect z-stacks with a 2 μm step. These images were processed in Fiji software prior to enumeration. We improved signal:noise by subtracting any auto-fluorescence from the imaging channel as necessary and applying a Gaussian blur protocol. We subsequently used the plug-in Image-based Tool for Counting Nuclei (Byun et al., 2006). In initial studies, these automated count estimates were validated with manual counts of cell number in randomly chosen sections through the MeApd; we also routinely performed manual enumeration in randomly chosen sections to validate automated estimates of cell counts for every experiment. All experimental and control animals for a given experiment were analyzed using the same set of parameters in Fiji to minimize any bias. Only animals where both the left and right MeApd showed cell

loss of >50% compared to the number of aromatase neurons in the control group were included in the analysis shown in bar graph plots. The scatterplot data were plotted using cell numbers from the side of the MeApd (left or right) with the most cells surviving (least efficient cell death). A Pearson correlation coefficient was used to determine the relation between the behavioral deficit and cell loss. In studies that sought to determine overlap of markers (GAD1, mCherry) with nuclear β-galactosidase (*aro*^{IPIN}), histological sections were obtained, imaged, and initially processed in Fiji as described above. β-galactosidase+ nuclei were identified, and the average pixel intensity signal reflecting labeling for GAD1 or mCherry was measured in the appropriate channel. β-galactosidase+ nuclei co-labeled with a minimum average pixel intensity exceeding noise in the relevant channel were deemed to co-express GAD1 or mCherry as appropriate.

Hormones and Drugs

Hormone titers were determined from blood drawn via cardiac puncture prior to perfusion or submandibular vein puncture, using kits and protocols from DRG International. Estrus was induced in ovariectomized females as described previously (Yang et al., 2013). Briefly, 17 β-estradiol was injected subcutaneously on days -2 and -1 (10 µg in 100 µL sesame oil and 5 µg in 50 µL sesame oil, respectively), and progesterone was injected subcutaneously on day 0 (50 µg in 50 µL sesame oil) 4-6 hours prior to behavioral testing.

CNO dissolved in saline (0.5 mg/mL) was injected intraperitoneally to achieve a dose (5 mg/kg) consistent with previous studies (Ray et al., 2011; Sasaki et al., 2011), and control animals received an equivalent volume of saline.

Electrophysiology

As described above, AAV-flex-DREADD-G_q:mCherry was injected bilaterally into the MeA of *aro*$^{IPIN/Cre}$ males 8 weeks of age. The mice were allowed to recover >10 days from

surgery and then sacrificed brain slice preparation. Slices were cut in ice-cold HEPES buffer solution, incubated for 15 min at 33 ºC in NMDG recovery solution, and finally maintained for 1-5 hrs before recording at room temperature in HEPES buffer solution. HEPES solution composition (in mM): 92 NaCl, 2.5 KCl, 1.2 NaH_2PO_4, 30 $NaHCO_3$, 20 HEPES, 25 Glucose, 5 Na^+ Ascorbate, 2 Thiourea, 3 Na^+ Pyruvate, 10 $MgSO_4$, 0.5 $CaCl_2$, 305 mOsm, 7.3-7.4 pH. NMDG solution was identical to HEPES, except for an equimolar replacement of NaCl for NMDG.

Neurons were visualized under differential interference contrast optics and epifluorescence and selected for recording based on mCherry expression. Whole cell current-clamp recordings were made using the following recording solutions (in mM): *Internal*: 9 HEPES, 113 K-Gluconate, 4.5 $MgCl_2$, 0.1 EGTA, 14 Tris-phosphocreatine, 4 Na_2ATP, 0.3 Tris-GTP, 10 Sucrose, 290 mOsm, 7.2-7.25 pH ; *External*: 125 NaCl, 2.5 KCl, 1 $MgCl_2$, 1.25 NaH_2PO_4, 25 $NaHCO_3$, 25 Glucose, 2 $CaCl_2$, 305 mOsm, 7.25-7.30 pH. Synaptic transmission was maintained to allow for any potential DREADD effects on synaptic input. Spontaneously spiking cells (n = 4 of 6 cells) were held with constant negative holding current (“bias current”, -18.9 ± 7.2 pA) to prevent cells from entering depolarization block with CNO application. Bias current was determined before the baseline period and was held constant throughout individual recordings. V_m were not corrected for junction potential (12 mV). All statistics were performed in MATLAB and exclusion criteria were as follows: if cells did not appear to have a stable baseline during the experiment, CNO was not applied. Linear regression was also performed on the baseline period V_m for each cell; if a statistically significant ($p < 0.05$) slope of greater than ± 0.5 mV/min was observed during this period, the cell was excluded from analysis (n = 0 cells).

Data Analysis

Behavioral and histological studies were performed and analyzed by an experimenter

blinded to the genotype and to other experimental manipulations (such as CNO versus saline treatment in DREADD studies). For analysis of non-categorical parameters of mating, aggression, receptivity and maternal care, we only included data from the animals that performed the behavior. In instances where an animal was tested more than once in the same assay (male and female mating, intermale and maternal aggression, and pup retrieval subsequent to caspase-3 mediated ablation) the behavioral performance for each animal was averaged prior to further analysis across animals. Linear regression analysis was performed using MATLAB and R. We used Fisher's exact test to analyze categorical data. For all other comparisons, we first analyzed the data distribution with the Lilliefors' goodness-of-fit test of normality. Data sets not violating this test of normality were analyzed with Student's *t* test; otherwise we used the nonparametric Wilcoxon rank sum test.

REFERENCES

Alexander, G.M., Rogan, S.C., Abbas, A.I., Armbruster, B.N., Pei, Y., Allen, J.A., Nonneman, R.J., Hartmann, J., Moy, S.S., Nicolelis, M.A., et al. (2009). Remote control of neuronal activity in transgenic mice expressing evolved G protein-coupled receptors. Neuron 63, 27–39.

Anaclet, C., Ferrari, L., Arrigoni, E., Bass, C.E., Saper, C.B., Lu, J., and Fuller, P.M. (2014). The GABAergic parafacial zone is a medullary slow wave sleep-promoting center. Nat. Neurosci. 17, 1217–1224.

Armbruster, B.N., Li, X., Pausch, M.H., Herlitze, S., and Roth, B.L. (2007). Evolving the lock to fit the key to create a family of Gprotein-coupled receptors potently activated by an inert ligand. Proc. Natl. Acad. Sci. USA 104, 5163–5168.

Arnold, A.P. (2009). The organizational-activational hypothesis as the foundation for a unified theory of sexual differentiation of all mammalian tissues. Horm. Behav. 55, 570–578.

Ball, J. (1937). Sex activity of castrated male rats increased by estrin administration. J. Comp. Psychol. 24, 135–144.

Balthazart, J., and Ball, G.F. (1998). New insights into the regulation and function of brain estrogen synthase (aromatase). Trends Neurosci. 21, 243–249.

Baum, M.J., and Bakker, J. (2013). Roles of sex and gonadal steroids in mammalian pheromonal communication. Front. Neuroendocrinol. 34, 268–284.

Bergan, J.F., Ben-Shaul, Y., and Dulac, C. (2014). Sex-specific processing of social cues in the medial amygdala. eLife 3, e02743.

Carney, R.S.E., Mangin, J.-M., Hayes, L., Mansfield, K., Sousa, V.H., Fishell, G., Machold, R.P., Ahn, S., Gallo, V., and Corbin, J.G. (2010). Sonic hedgehog expressing and responding cells generate neuronal diversity in the medial amygdala. Neural Dev. 5, 14.

Choi, G.B., Dong, H.-W., Murphy, A.J., Valenzuela, D.M., Yancopoulos, G.D., Swanson,

L.W., and Anderson, D.J. (2005). Lhx6 delineates a pathway mediating innate reproductive behaviors from the amygdala to the hypothalamus. Neuron 46, 647–660.

De Vries, G.J., and Boyle, P.A. (1998). Double duty for sex differences in the brain. Behav. Brain Res. 92, 205–213.

Demas, G.E., Kriegsfeld, L.J., Blackshaw, S., Huang, P., Gammie, S.C., Nelson, R.J., and Snyder, S.H. (1999). Elimination of aggressive behavior in male mice lacking endothelial nitric oxide synthase. J. Neurosci. 19, RC30.

DiBenedictis, B.T., Ingraham, K.L., Baum, M.J., and Cherry, J.A. (2012). Disruption of urinary odor preference and lordosis behavior in female mice given lesions of the medial amygdala. Physiol. Behav. 105, 554–559.

Finney, H.C., and Erpino, M.J. (1976). Synergistic effect of estradiol benzoate and dihydrotestosterone on aggression in mice. Horm. Behav. 7, 391–400.

Forlano, P.M., Schlinger, B.A., and Bass, A.H. (2006). Brain aromatase: new lessons from non-mammalian model systems. Front. Neuroendocrinol. 27, 247–274.

Gammie, S.C., and Nelson, R.J. (1999). Maternal aggression is reduced in neuronal nitric oxide synthase-deficient mice. J. Neurosci. 19, 8027–8035.

Gammie, S.C., Huang, P.L., and Nelson, R.J. (2000). Maternal aggression in endothelial nitric oxide synthase-deficient mice. Horm. Behav. 38, 13–20.

Gandelman, R. (1972). Mice: postpartum aggression elicited by the presence of an intruder. Horm. Behav. 3, 23–28.

Hong, W., Kim, D.-W., and Anderson, D.J. (2014). Antagonistic control of social versus repetitive self-grooming behaviors by separable amygdala neuronal subsets. Cell 158, 1348–1361.

Juntti, S.A., Tollkuhn, J., Wu, M.V., Fraser, E.J., Soderborg, T., Tan, S., Honda, S., Harada, N., and Shah, N.M. (2010). The androgen receptor governs the execution, but not programming, of male sexual and territorial behaviors. Neuron

66, 260–272.

Keshavarzi, S., Sullivan, R.K.P., Ianno, D.J., and Sah, P. (2014). Functional properties and projections of neurons in the medial amygdala. J. Neurosci. 34, 8699–8715.

Kimura, T., and Hagiwara, Y. (1985). Regulation of urine marking in male and female mice: effects of sex steroids. Horm. Behav. 19, 64–70.

Lee, H., Kim, D.-W., Remedios, R., Anthony, T.E., Chang, A., Madisen, L., Zeng, H., and Anderson, D.J. (2014). Scalable control of mounting and attack by Esr1+ neurons in the ventromedial hypothalamus. Nature 509, 627–632.

MacLusky, N.J., and Naftolin, F. (1981). Sexual differentiation of the central nervous system. Science 211, 1294–1302.

Matsumoto,T.,Honda, S.,andHarada,N. (2003). Alteration in sex-specific behaviors in male mice lacking the aromatase gene. Neuroendocrinology 77, 416–424.

McCarthy, M.M. (2008). Estradiol and the developing brain. Physiol. Rev. 88, 91–124.

McDermott, N.J., and Gandelman, R. (1979). Exposure to young induces post-partum-like fighting in virgin female mice. Physiol. Behav. 23, 445–448.

McGill, T.E. (1962). Sexual behavior in three inbred strains of mice. Behavior 19, 341–350.

Morgan, C.W., Julien, O., Unger, E.K., Shah, N.M., and Wells, J.A. (2014). Turning on caspases with genetics and small molecules. Methods Enzymol. 544, 179–213.

Morris, J.A., Jordan, C.L., and Breedlove, S.M. (2004). Sexual differentiation of the vertebrate nervous system. Nat. Neurosci. 7, 1034–1039.

Moyer, K. (1968). Kinds of aggression and their physiological basis. Commun. Behav. Biol. 2, 65–87.

Naftolin, F., Ryan, K.J., and Petro, Z. (1971). Aromatization of androstenedione by the diencephalon. J. Clin. Endocrinol. Metab. 33, 368–370.

Nelson, R.J., Demas, G.E., Huang, P.L., Fishman, M.C., Dawson, V.L., Dawson, T.M., and Snyder, S.H. (1995). Behavioural abnormalities in male mice lacking

neuronal nitric oxide synthase. Nature 378, 383–386.

Nelson, A.B., Hammack, N., Yang, C.F., Shah, N.M., Seal, R.P., and Kreitzer, A.C. (2014). Striatal cholinergic interneurons Drive GABA release from dopamine terminals. Neuron 82, 63–70.

Nunez, A.A., Nyby, J., and Whitney, G. (1978). The effects of testosterone, estradiol, and dihydrotestosterone on male mouse (Mus musculus) ultrasonic vocalizations. Horm. Behav. 11, 264–272.

Ogawa, S., Chester, A.E., Hewitt, S.C., Walker, V.R., Gustafsson, J.A., Smithies, O., Korach, K.S., and Pfaff, D.W.(2000). Abolition of male sexual behaviors in mice lacking estrogen receptors alpha and beta (alpha beta ERKO). Proc. Natl. Acad. Sci. USA 97, 14737–14741.

Paxinos, G., and Franklin, K.B.J. (2003). The Mouse Brain in Stereotaxic Coordinates: Compact, Second Edition (New York: Academic Press).

Petrovich, G.D., Canteras, N.S., and Swanson, L.W. (2001). Combinatorial amygdalar inputs to hippocampal domains and hypothalamic behavior systems. Brain Res. Brain Res. Rev. 38, 247–289.

Ray, R.S., Corcoran, A.E., Brust, R.D., Kim, J.C., Richerson, G.B., Nattie, E., and Dymecki, S.M. (2011). Impaired respiratory and body temperature control upon acute serotonergic neuron inhibition. Science 333, 637–642.

Roselli, C.E. (1991). Sex differences in androgen receptors and aromatase activity in microdissected regions of the rat brain. Endocrinology 128, 1310–1316.

Roselli, C.E., Horton, L.E., and Resko, J.A. (1985). Distribution and regulation of aromatase activity in the rat hypothalamus and limbic system. Endocrinology 117, 2471–2477.

Sasaki, K., Suzuki, M., Mieda, M., Tsujino, N., Roth, B., and Sakurai, T. (2011). Pharmacogenetic modulation of orexin neurons alters sleep/wakefulness states in mice. PLoS ONE 6, e20360.

Scott, J.P. (1966). Agonistic behavior of mice and rats: a review. Am. Zool. 6, 683–701.

Sokolowski, K., and Corbin, J.G. (2012). Wired for behaviors: from development to function of innate limbic system circuitry. Front. Mol. Neurosci. 5, 55.

Sternson, S.M. (2013). Hypothalamic survival circuits: blueprints for purposive behaviors. Neuron 77, 810–824.

Sternson, S.M., and Roth, B.L. (2014). Chemogenetic tools to interrogate brain functions. Annu. Rev. Neurosci. 37, 387–407.

Stowers,L.,Holy,T.E.,Meister, M.,Dulac,C.,andKoentges,G.(2002). Loss of sex discrimination and male-male aggression in mice deficient for TRP2. Science 295, 1493–1500.

Svare, B., and Gandelman, R. (1975). Postpartum aggression in mice: inhibitory effect of estrogen. Physiol. Behav. 14, 31–35.

Svare, B., and Gandelman, R. (1976a). Postpartum aggression in mice: the influence of suckling stimulation. Horm. Behav. 7, 407–416.

Svare, B., and Gandelman, R. (1976b). Suckling stimulation induces aggression in virgin female mice. Nature 260, 606–608.

Swanson, L.W. (2000). Cerebral hemisphere regulation of motivated behavior. Brain Res. 886, 113–164.

Swanson, L.W., and Petrovich, G.D. (1998). What is the amygdala? Trends Neurosci. 21, 323–331.

Wallis, C.J., and Luttge, W.G. (1975). Maintenance of male sexual behavior by combined treatment with oestrogen and dihydrotestosterone in CD-1 mice. J. Endocrinol. 66, 257–262.

Wang, L., Han, X., Mehren, J., Hiroi, M., Billeter, J.-C., Miyamoto, T., Amrein, H., Levine, J.D., and Anderson, D.J. (2011). Hierarchical chemosensory regu- lation of male-male social interactions in Drosophila. Nat. Neurosci. 14, 757–762.

Wersinger, S.R., Sannen, K., Villalba, C., Lubahn, D.B., Rissman, E.F., and DeVries,

G.J. (1997). Masculine sexual behavior is disrupted in male and femalemice lacking a functional estrogen receptor alpha gene. Horm. Behav. 32, 176–183.

Wu, M.V., Manoli, D.S., Fraser, E.J., Coats, J.K., Tollkuhn, J., Honda, S., Harada, N., and Shah, N.M. (2009). Estrogen masculinizes neural pathways and sex-specific behaviors. Cell 139, 61–72.

Wu, Z., Autry, A.E., Bergan, J.F., Watabe-Uchida, M., and Dulac, C.G. (2014). Galanin neurons in the medial preoptic area govern parental behaviour. Nature 509, 325–330.

Xu,X.,Coats,J.K., Yang,C.F., Wang,A.,Ahmed,O.M., Alvarado, M.,Izumi,T., and Shah, N.M. (2012). Modular genetic control of sexually dimorphic behaviors. Cell 148, 596–607.

Yang, C.F., and Shah, N.M. (2014). Representing sex in the brain, one module at a time. Neuron 82, 261–278.

Yang, C.F., Chiang, M.C., Gray, D.C., Prabhakaran, M., Alvarado, M., Juntti, S.A., Unger, E.K., Wells, J.A., and Shah, N.M. (2013). Sexually dimorphic neurons in the ventromedial hypothalamus govern mating in both sexes and aggression in males. Cell 153, 896–909.

SUPPLEMENTAL REFERENCES

Bian, X. (2013). Physiological and morphological characterization of GABAergic neurons in the medial amygdala. Brain Res. *1509*, 8–19.

Byun, J., Verardo, M.R., Sumengen, B., Lewis, G.P., Manjunath, B.S., and Fisher, S.K. (2006). Automated tool for the detection of cell nuclei in digital microscopic images: application to retinal images. Mol. Vis. *12*, 949–960.

Rodríguez, C.I., Buchholz, F., Galloway, J., Sequerra, R., Kasper, J., Ayala, R., Stewart, A.F., and Dymecki, S.M. (2000). High-efficiency deleter mice show that FLPe is an alternative to Cre-loxP. Nat. Genet. *25*, 139–140.

Tamamaki, N., Yanagawa, Y., Tomioka, R., Miyazaki, J.-I., Obata, K., and Kaneko, T. (2003). Green fluorescent protein expression and colocalization with calretinin, parvalbumin, and somatostatin in the GAD67-GFP knock-in mouse. J. Comp. Neurol. *467*, 60–79.

Chapter 6

Two subregions of the posterior dorsal medial amygdala

Elizabeth K. Unger, Jessica Tollkuhn, Taehong Yang, Nirao M. Shah

INTRODUCTION

In chapter 5 I showed that ablation and inhibition of the medial amygdala (MeA) lead to decreases in aggression in both males and females (Unger et al., 2015). I also showed that their olfactory discrimination was not affected. However this does not mean there is some deficit in identification of males based on pheromonal profile, as we pointed out. In fact it is likely, due to the position of the MeA as a direct recipient of accessory olfactory bulb (AOB) projections (Canteras et al., 1992), and based on electrophysiological recordings within the MeA from the Dulac lab (Bergan et al., 2014), that the purpose of the MeA is to process olfactory information and identify the sex of the conspecific being investigated. However, it is also highly likely that there is redundancy in the system which would explain why the deficit is small and manifests merely as a delay in initiating aggression, rather than a larger behavioral phenotype. In addition, there may be local inhibitory circuits within the MeA and serve an important function, but when both output and inhibitory control are eliminated together, the result is only a mild phenotype. In order to further understand these possibilities it is necessary to identify the circuit in which *aromatase+* (*aro+*) MeA neurons act.

In this chapter I explore this circuit. While these experiments remain incomplete and a subject for future investigation, my findings suggest more complex circuitry than previously thought. I show that there are two major outputs from the MeA which are defined by somewhat intermixed, but anatomically distinct populations of neurons within the MeA, and that these populations are also functionally and molecularly different. While I was unable to finely parse their function, due to technical difficulties, I provide several possible approaches and offer speculation as to their possible role in social behaviors.

RESULTS

Upstream projections of aro+ MeA neurons

The MeA is one of the few regions in the brain to receive direct input from the AOB (Canteras et al., 1992). However, the AOB is not the only source of input onto the MeA (Canteras et al., 1995, Swanson 2003), and it is not clear that this input is onto *aro*+ neurons. In order to identify other upstream projection partners of aro+ neurons in the MeA, I used a replication incompetent form of a pseudorabies virus (PRV), where the replication gene and a tGFP have been placed behind a floxed stop cassette (Card and Enquist, 2001). I injected this virus into the MeA of $aro^{Cre/LacZ}$ mice. In this way, *aro*+ neurons will return replication competence to the virus and it will travel retrogradely to the upstream targets of aro+ MeA neurons. This process takes about two days. However, once replication competence has been rescued, the virus will continue to travel to more distant upstream targets, thus obfuscating primary targets. Therefore, histology must be performed within the first few days. In addition, pseudorabies is toxic to infected cells, so in order to avoid widespread cell death, histology must be performed quickly. Thus it is not possible to use these animals for any sort of behavioral analysis. Newer forms of retrograde tracing have emerged recently, involving a rabies virus and 2 helper viruses (Luo et al., 2008, Osakada et al., 2011). I tried this technique with no success, likely do to the low probability of infecting my small number of cells with all three viruses (data not shown). Similarly, the PRV approach is also prone to a low success rate. Of the 31 animals I injected, only two showed any GFP at all and only one showed GFP in upstream regions (Figure 6.1). Nonetheless, the upstream regions include the AOB, accessory olfactry nucleus (AON), lateral septum (Lat. Sep.), preoptic area (POA), bed nucleus of the stria terminalis (BNST), posteromedial cotrical amygdala (PMCo), and piriform cortex, all regions that are known to be involved in olfaction and social behaviors. Thus *aro*+ MeA neurons are part of the circuit that transforms olfactory pheromonal cues into social behaviors.

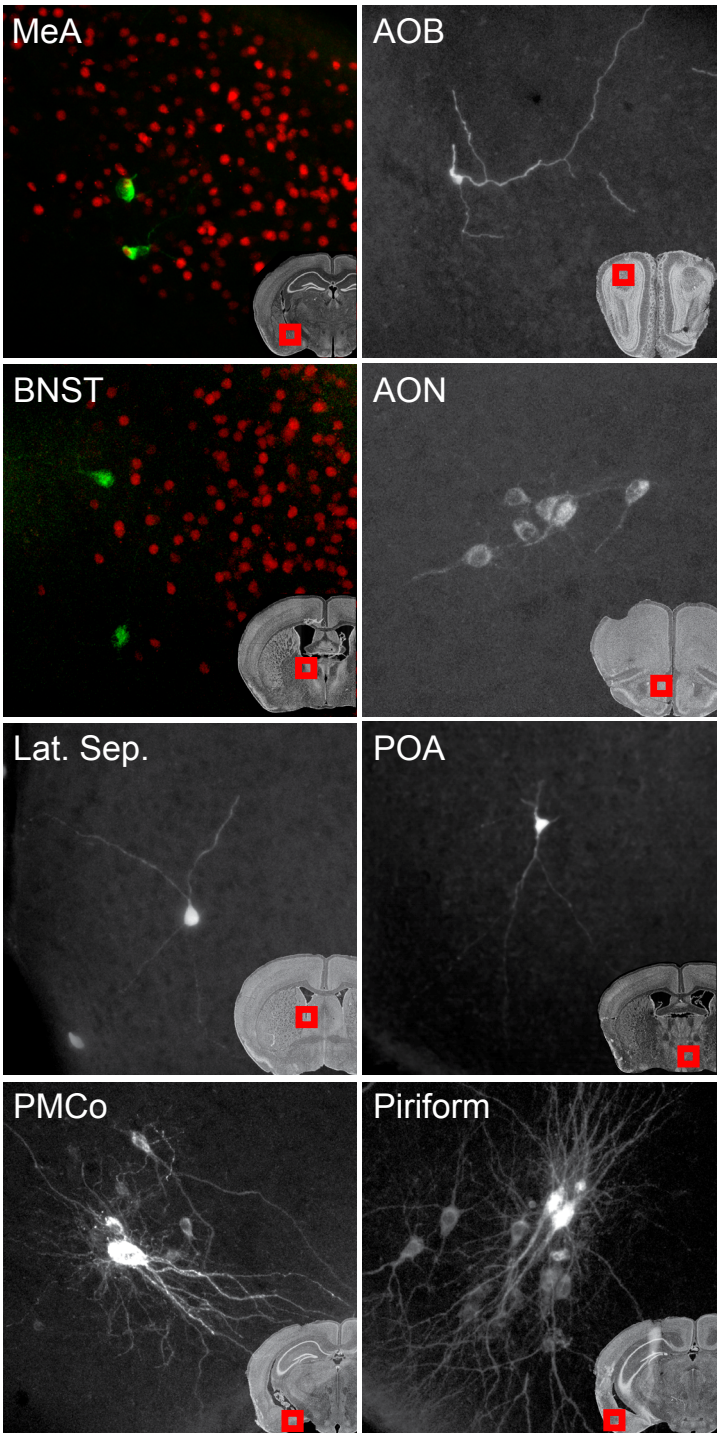

Figure 6.1: Upstream projections of aro+ MeA neurons

A replication incompetent form of a pseudorabies virus was injected into the MeA of *aro*$^{Cre/LacZ}$ males. In the presence of Cre, the virus becomes replication competent and expresses a τGFP, allowing it to travel retrogradely to upstream areas. Red box in inset represents the area of the brain pictured.

Downstream projections of aro+ MeA neurons

Because I see essentially the same phenotype in both sexes despite the execution of the behaviors being substantially different (Unger et al., 2015), that implies that the the circuit upstream of the MeA is similar between the two sexes. It must diverge downstream of the MeA in order to produce these different behaviors. Previous work has shown that the MeA projects to the BNST, the POA, the anteroventral periventricular nucleus (AVPV), the Lat. Sep., the ventromedial hypothalamus (VMH), and the ventral premammillary nucleus (PMV) (Canteras et al., 1995). However, I wanted to identify the downstream projection partners of *aro*+ neurons in the MeA, so I injected a cre-dependent neural tracer (AAV-DIO-ChR2-EYFP, Sohal et al., 2009) into the MeA of *aro*$^{Cre/LacZ}$ mice (Figure 6.2A). I also injected a much more sensitive Cre-

dependent colormetric tracer, AAV-flex-PLAP (placental alkaline phosphatase, Yang et al., 2013), in order to visualize even fainter projections (Figure 6.2B). However this strategy does not allow the colocalization of *aro*+ cells because the reporter allele contains the same alkaline phosphatase (Wu et al., 2009) and thus cannot be included in the experiment. I see fibers coming from *aro*+ MeA neurons that innervate many of the previously identified areas, and in addition I discovered a previously unidentified projection from the MeA to the accessory olfactory bulb (AOB). However I was only able to see this projection in the

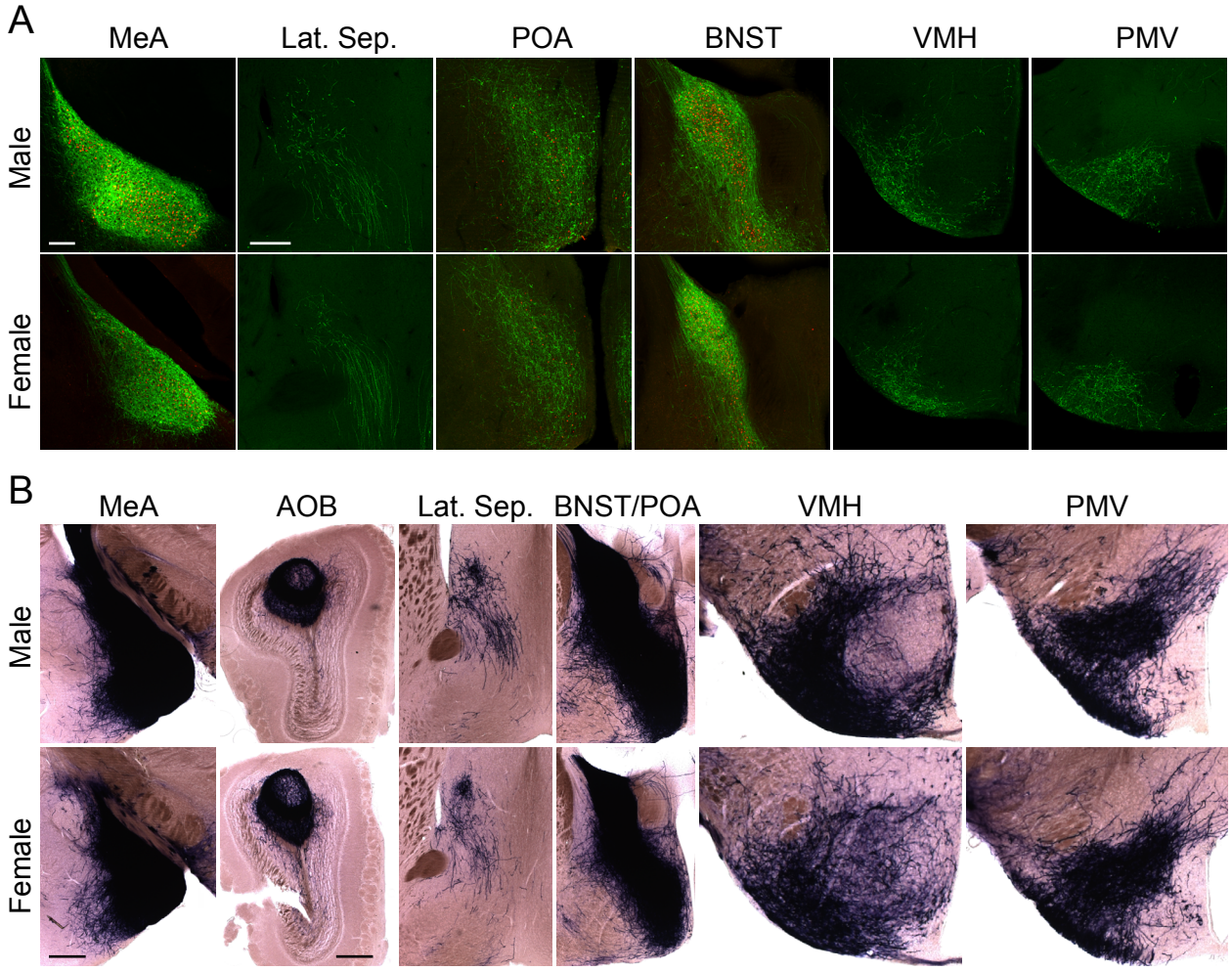

Figure 6.2: Anterograde tracing of aro+ MeA neurons

A) AAV-flex-ChR2-EYFP was injected into the MeA of $aro^{LacZ/Cre}$ males and females. After 3 mice were perfused and processed for histology. (B) AAV-flex-PLAP was injected unilaterally into the MeA of $aro^{Cre/Cre}$ males and females. After 1-3 weeks, mice were perfused and processed for histology. n = 6 males, 3 females (ChR2) and 19 males, 21 females (PLAP). Scale bar = 200 µm.

PLAP-injected animals and not the ChR-injected animals (Figure 6.2). Also the dense nature of the staining in the target region does not allow for the assessment of local projections. Nonetheless, we can conclude that these *aro*+ MeA cells are, at least in part, inhibitory projection neurons (Unger et al., 2015).

Projection-specific subregions of the MeA

While imaging these sections, I noticed a trend: there seemed to be two major fiber tracts leaving the MeA, one that travels up, along the base of the lateral ventricles to the Lat. Sep., BNST, POA, and AVPV, and one that travels laterally around the optic tract and innervates the VMH and PMV. In fact there appears also to be a third set of fibers that

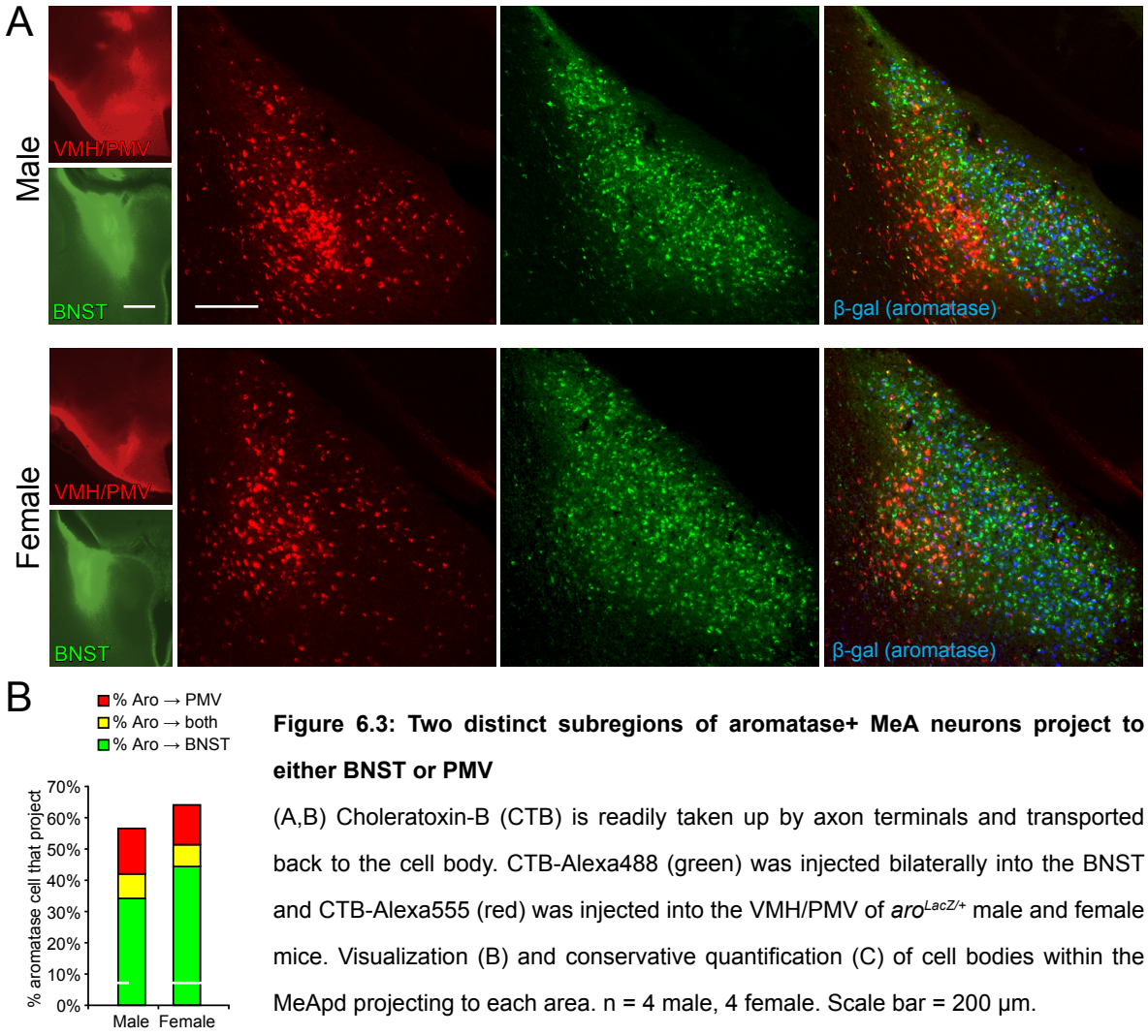

Figure 6.3: Two distinct subregions of aromatase+ MeA neurons project to either BNST or PMV

(A,B) Choleratoxin-B (CTB) is readily taken up by axon terminals and transported back to the cell body. CTB-Alexa488 (green) was injected bilaterally into the BNST and CTB-Alexa555 (red) was injected into the VMH/PMV of *aro*$^{LacZ/+}$ male and female mice. Visualization (B) and conservative quantification (C) of cell bodies within the MeApd projecting to each area. n = 4 male, 4 female. Scale bar = 200 μm.

travels forward along the exterior of the hypothalamus and forebrain to innervate the AOB. However this projection pathway could not be replicated in ChR injected animals and thus was not analyzed further.

In order to determine if these different projection pathways originate from neurons whose axons branch or different populations of neurons that each project to one location, I injected two differently colored retrograde tracers (choleratoxin subunit B (CTB) - alexa488 and alexa555) simultaneously into both downstream regions (Ericson and Blomqvist, 1988). I find that in fact there are two anatomically distinct populations of neurons: a larger, more medial population that projects to the BNST and nearby areas, and smaller lateral population that projects to the VMH and PMV (Figure 6.3).

Molecular and functional differences between the projection-specific subregions

Previous studies in rats have identified a cluster of neurons in the lateral MeA that strongly express c-Fos, an immediate early gene (Dragunow and Faull, 1989), and a marker of neuronal activation, following mating behavior (Veening and Coolen, 1998). In order to determine if these neurons also express aromatase, I exposed male mice to a number of different stimuli, a sexually receptive female, and co-stained for aromatase and c-Fos or Arc, another immediate early gene (Guzowski et al., 1999). Indeed *aro*+ neurons (and non-*aro*+ neurons) in the lateral (VMH-projecting) population in the MeA colocalize with both c-Fos and Arc (Figure 6.4A,B). Surprisingly, this c-Fos and Arc expression was specific to ejaculation as it was not seen in the condition where the male was allowed to intromit several times with the female, but not allowed to ejaculate (Figure 6.4A,B). A similar population exists within the aro+ population within the BNST, which is also comprised of inhibitory projection neurons (data not shown). This suggests that ejaculation induces an inhibitory response from the MeA and BNST to the VMH.

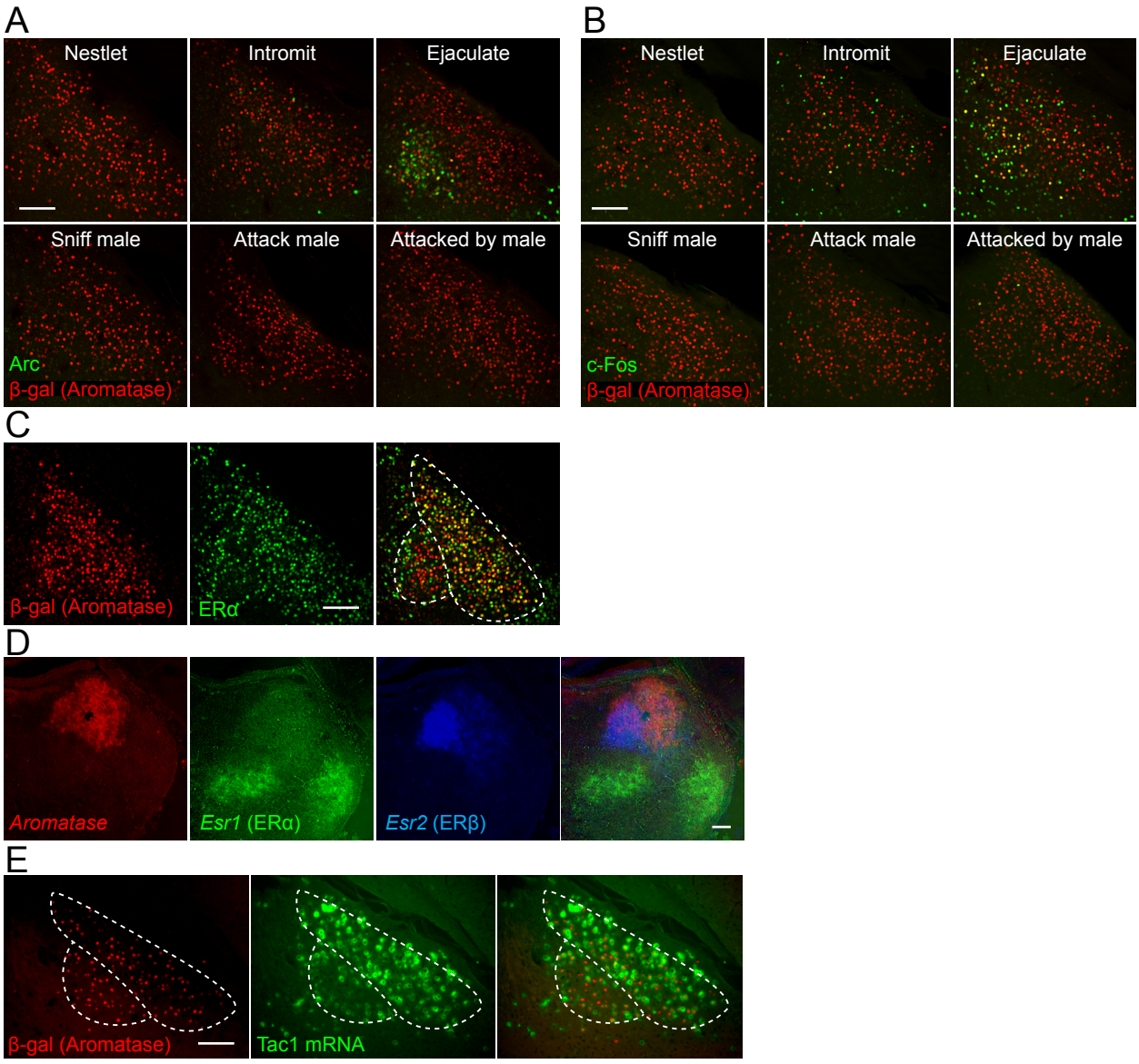

Figure 6.4: Functional and molecular differences between the two MeApd subregions

(A,B) Male *aro*$^{LacZ/+}$ mice were presented with the indicated stimuli for 30 min. Immediate early gene (Arc (A) and c-Fos (B)) expression was evaluated 1 hour later, by staining floating 65 µm sections. After ejaculation, the lateral subregion appears to be activated. (C) Floating 65 µm sections from a female *aro*$^{LacZ/+}$ mouse were stained for colocalization of ERα and β-gal (aromatase). Colocalization appears to be restricted to the lateral subregion, though both are present throughout. (D) Serial 12 µm frozen sections from a neonatal (P0) male mouse were stained individually by *in situ* hybridization with probes for *aromatase*, *Esr1* (ERα) and *Esr2* (ERβ), then imaged using a brightfield microscope and recombined and pseudocolored in Photoshop. *Esr2* expression appears to be concentrated in the lateral subregion. It should be noted that gene expression patterns differ between developping and adult brains. Image courtesy of Jessica Tollkuhn. (E) Dual *in situ* hybridization and immunofluorescence was performed for *Tac1* and β-gal (aromatase) respectively on 12 µm frozen sections from adult male *aro*$^{LacZ/+}$ mice. Brightfield images of Tac1 were pseudocolored in Photoshop. *Tac1* expression appears to be more prominent in the medial subregion. Scale bar = 200 µm

Several studies have shown that the MeA is activated after different social behaviors, however, close examination of these studies indicates that there are regional differences in the patterns of activation between mating and aggression. Three studies show activation of the MeA after aggressive behaviors (Hong et al., 2014, Lee et al., 2014, Veening et al., 2005), however these c-fos+ neurons tend to be located in the anterior region of the MeA and the aro+ population is primarily in the posterior dorsal section. In addition one of the studies identified a population whose expression pattern matches that of the glutametergic population (Lien et al., 2007). Hong et al., (2014) stimulated a glutamatergic population that likely included these cells and found that mice engaged in self grooming. Clearly there are many different subregions within the MeA with diverse functions, that cannot be parsed using a single molecular marker.

In addition to differences in activation following ejaculation, I also found several differences in gene expression between the two MeApd subregions. The function of aromatase is to synthesize estrogen; therefore *aro*+ neurons need to be able to sense estrogen. The primary receptor for estrogen is estrogen receptor alpha (ERα, *Esr1*). In females, expression of ERα in the MeApd is quite strong, while in males it is much weaker (see chapter 2). Interestingly, when I stain for ERα and aromatase together in females I find that while ERα is fairly widespread throughout the MeApd, it is only colocalized with *aro*+ neurons in the medial subregion (Figure 6.4B). The lateral region contains both ERα and aromatase, but they are not colocalized. Even more interesting, in an experiment done by Jessica Tollkuhn in , the lateral region appears to contain more estrogen receptor beta (ERβ, *Esr2*) than surrounding areas (Figure 6.4D). ERβ is considered the secondary receptor for estrogen, and the knockout has a much milder phenotype (Dupont et al., 2000). This suggests that within the BNST-projecting population of *aro*+ MeApd neurons, the primary means of sensing estrogen is through ERα, while in the VMH-projecting population, its primary means of sensing estrogen is through ERβ. This could potentially

lead to differential regulation of aromatase itself, as well as many other genes.

Another intriguing difference I discovered was the expression of substance P (*Tac1*) and its receptor (*TacR1*). The medial population appears to have high *Tac1* expression, while the lateral population shows much lower expression. Conversely, expression of *TacR1* is much higher in the lateral portion and lower in the medial portion (Lein et al., 2007). The functional consequence of these differences has yet to be determined, however, it is possible that this gives a hint as to the circuitry. Because the medial portion expresses the ligand and the lateral portion expressed the receptor, it is possible that local circuitry exists wherein the medial subregion serves as inhibitory input onto the lateral subregion. As mentioned before, it was not possible to determine local circuitry from the tracing experiments (Figure 6.2), but newer more sparsely labeling tracing techniques will provide these answers in the future (Wall et al., 2010).

Targeting the MeApd in a projection-specific manner

It is clear that these two projection-specific subregions of the MeApd are different in several ways, but it is important to know their precise function. In order to do that I need a way of manipulating the two sets of neurons separately. However, both populations expression aromatase and all other molecular markers are much more widespread than aromatase, so it is not possible to use a simple Cre-lox strategy; I need a strategy that incorporates both cell-type specificity and projection specificity. While aromatase is only expressed in a small number of MeApd neurons, its expression is limited to the MeApd, thus restricting targeting to within that area, and reducing the risk of off-target effects.

DREADDs + local application of clozapine-N-oxide (CNO)

The most straightforward method for targeting these neurons in a projection-specific manner is to inject a Cre-activatable AAV-DREADD (Sternson and Roth, 2014) into the

MeA of *aro*^{Cre} mice and apply CNO directly to the target site, minimizing activation of surrounding areas. This technique was successfully used by the Sternson lab to parse the different projections of the arcuate nucleus (Stachniak et al., 2014). In order to see if this strategy could work for me, I injected the DREADD-Gq virus described in chapter 5, into the MeA of *aro*$^{Cre/LacZ}$ mice, and simultaneously implanted a guide cannula just above the VMH/PMV. I used a DREADD-Gq such that I would be able to use c-Fos as a readout, as the MeA is silent under normal conditions (Bergan et al., 2014, Unger et al., 2015). I also chose to start with the VMH-projecting subset because it is smaller and easier to recognise in histological sections I injected the DREADD bilaterally, but only placed the cannula on one side, to test the spread of the CNO and to have an internal control for each

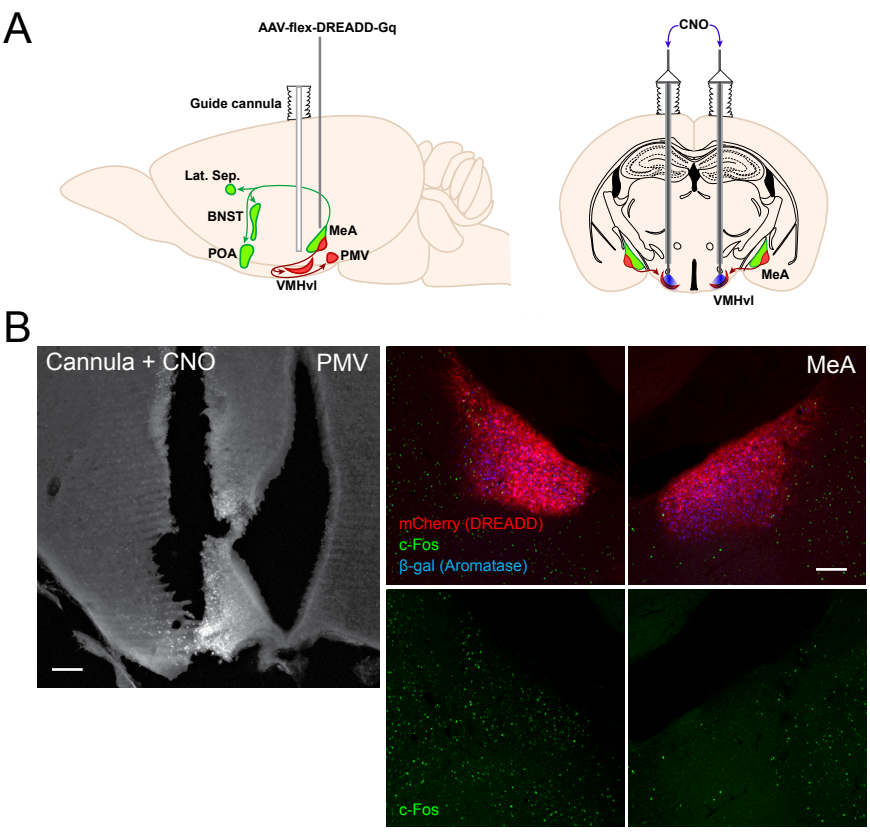

Figure 6.5: Selective projection-specific activation of aro+ MeA neurons using locally delivered CNO

A) Strategy to activate only VMH/PMV-projecting aro+ MeA neurons, by injecting an AAV-flex-DREADD-Gq into the MeA and placing a cannula above the VMH/PMV. After the recovery period, CNO is injected through the cannula. B) Aro$^{LacZ/Cre}$ mice were injected bilaterally with AAV-DREADD-Gq into the MeA and at the same time a cannula was placed above the VMH/PMV on one side only. After 2 weeks, CNO (1.5µg/100nl + 200nl fluorogold) was injected through the cannula and delivered to the left side only. c-Fos expression was assessed 1 hr later. There is minimal activation of the contralateral side (right), but significant activation (likely not limited to the VMH/PMV-projecting population) on the ipsilateral side (left). n = 4. Scale bar = 200 µm

mouse. However, I did not inject CTB into the cannula to determine the cells projecting to each downstream region (primarily for technical reasons: our confocal microscope only supports 4 colors and all 4 channels had been accounted for – blue-DAPI (the channel is too faint for other stains), green-Fos, red-mCherry (DREADD), far red-aromatase (β-gal)).

When I performed the experiment I found that unfortunately activation of the MeApd was not restricted to neurons projecting to either target specifically (Figure 6.4). Although I could not confirm this because I did not inject CTB, based on anatomical markers it appeared that c-Fos activation was widespread throughout the MeApd. Therefore this is not a viable option for targeting the separately projecting populations of neurons. I also cannot rule out the possibility that activation of certain neurons lead to indirect activation of other neurons, however, if this is the case, then this strategy will not produce the desired result in any case. According to Sternson, the techniqe only works for brain regions that are substantially far apart, and that leak of CNO into the source region from the target region will occur over shorter distances (Stachniak et al., 2014). Consistent with this, I see no activation of neurons in the contralateral MeApd. In addition, this technique works well for the DREADD-Gq, but the DREADD-Gi does not typically localize to axon terminals (which can be seen in the staining patterns in chapter 5). In chpater 5 I show that inhibition, but not activation of the entire population leads to a behavioral deficit. Therefore, the logical course of action would be to inhibit the populations separately. However, this

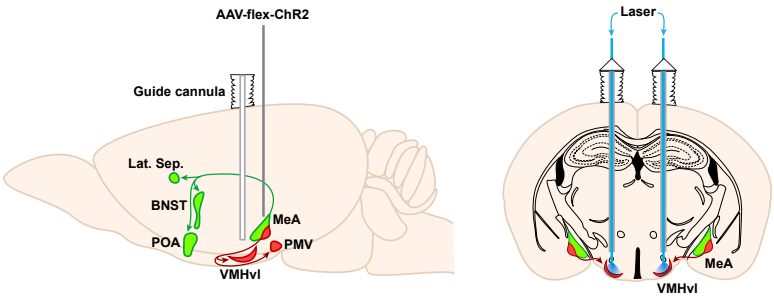

Figure 6.6: Selective projection-specific activation of aro+ MeA neurons using optogenetics

Strategy to activate only VMH/PMV-projecting aro+ MeA neurons, by injecting an AAV-flex-ChR2 into the MeA and placing a cannula above the VMH/PMV. After the recovery period, a fiber optic coupled to a blue laser (473nm) is inserted through the cannula, stimulating the axon terminals of aro+ MeA neurons projecting to the VMH/PMV.

would not be possible with the current viruses available. To solve this problem Sternson's group generated a new DREADD-Gi that is targeted to axon terminals (Stachniak et al., 2014). However, while the construct is available from addgene, the virus is not currently available, and given that I was not successful in specifically activating each region using the DREADD-Gq, I chose not to pursue these experiments further.

ChR + projection-specific light delivery

An alternative and fairly similar method for stimulating or inhibiting downstream projections is to instead inject channelrhodopsin (ChR, Nagel et al., 2003) or halorhodopsin (eNpHR3, Zhang et al., 2007) into the MeA and place the fiber optic cable above either the BNST or the VMH. However, eNpHR3 has proven to be problematic despite initial reports and very poor when it comes to inhibiting axon terminals (Gradinaru et al., 2008). Alternative methods for silencing neurons, such as proton pumps like Arch (Chow et al., 2010, Han et al., 2011) and modified channelrhodopsins (Berndt et al., 2014, Wietek et al., 2014) have proven to have their own problems and none seems to work consistently to inhibit action potentials at the axon terminal. As my goal is inhibition of these neurons, this particular line of experiments seems less worthwhile. Nonetheless, activating one subregion or the other may elicit a behavioral response that is otherwise masked when the entire population is activated. Therefore I injected a Cre-activatable AAV-ChR2-EYFP (Sohal et al., 2009) bilaterally into the MeA and simultaneously implanted a cannula above the VMH/PMV. I chose to specifically target the VMH/PMV for these pilot experiments because the PMV-projecting population in the MeApd is smaller and thus easier to distinguish during histological analysis.

On the day of testing I inserted a fiber optic coupled to a blue laser (473 nm) and stimulated at a series of different frequencies and laser powers in the hopes of inducing c-Fos expression in the MeA during one or more of these conditions. I then perfused and

analyzed the brains for c-Fos expression after one hour. Unfortunately, I was not able to see any activation of neurons within the MeApd. I did note that the area near the cannula tip was heavily damaged. It is possible that even though the cannula was placed 0.5 mm above the target site, that the damage it caused resulted in improper function of the target site. It is also possible that the stimulation parameters I chose were not sufficient to cause those neurons to fire. Because no one has successfully recorded the firing patterns of the MeApd in an awake behaving animal (although I did take steps down this path), the natural firing pattern of the region is not known. Again, because of these technical

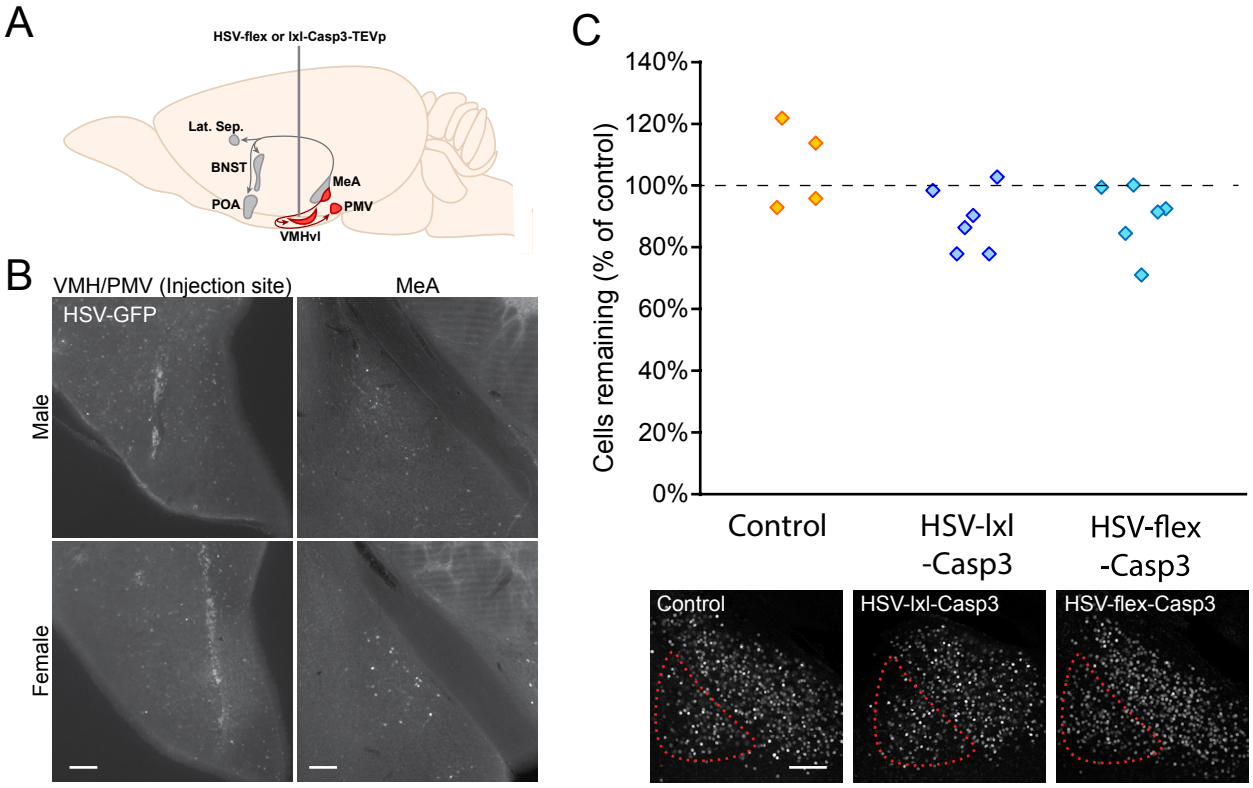

Figure 6.7: Projection specific ablation of aro+ MeA neurons using an HSV-Casp3

A) Strategy to target specifically VMH/PMV-projecting aro+ MeA neurons by injecting a Cre-dependent HSV-Casp3-TEVp. B) HSV-GFP was injected into the PMV of male and female mice in order to retrogradely label VMH/PMV-projecting neurons in the MeA, and to assess infection efficiency. Infection efficiency was low, and ventricles were enlarged indicative of an inflammatory response. C) HSV-lox-stop-lox (lxl)-Casp3-TEVp or HSV-flex-Casp3-TEVp were injected into the PMV of Aro$^{LacZ/Cre}$ male mice. After 4 weeks, cell counts were assessed specifically in the red outlined areas (as determined by anatomical landmarks), and compared to control. Again, ventricles were enlarged. n = 2, 3, 3. Scale bar = 200 µm.

challenges and the caveats listed previously, I chose not to pursue this line of inquiry.

HSV-Casp3

Another fairly straightforward means of targeting the MeA in a projection specific manner is to use a retrograde virus. HSVs (herpes simplex virus) are known to enter the cell through the axon terminal and travel back to the cell body (Antinone and Smith, 2010; Diefenbach et al., 2008; Frampton et al., 2005). In this way HSVs are not strictly speaking retrograde viruses, however they accomplish the same goal and have the added benefit over true retrograde viruses such as rabies and pseudorabies in that they do not jump multiple synapses. Indeed much time and effort has been expended to restrict those viruses to a single synapse (Callaway, 2008; Osakada and Callaway, 2013; Wickersham et al., 2007). Thus in order to ablate or inhibit aro+ MeApd neurons in a projection-specific manner, we used the same Casp3 and DREADD constructs described in chapter 5, and inserted them into an HSV backbone.

However, this virus has one major caveat which is that it can be activated by cre no matter the location within the brain. That means that I cannot inject this virus into the BNST, which expresses aromatase, and expect it to travel only to the MeA. Cells within the BNST that express aromatase will also express the virus. Similarly, other regions upstream of the target region that express cre will be affected as well. Therefore simply in order to test the virus, to see if it would be an option worth pursuing

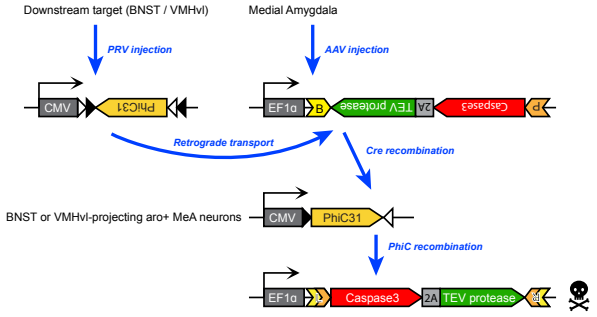

Figure 6.8: Projection-specific ablation of aro+ MeA neurons using a Cre-Frt combination

Strategy to selectively ablate only BNST or VMH/PMV-projecting aro+ MeA neurons. A PRV containing a Cre-dependent PhiC is injected into the downstream target, and is then transported retrogradely to the MeA. Cre-expressing neurons within the MeA recombine the virus to induce PhiC expression. Another PhiC-dependent AAV is injected into the MeA, which, when recombined, expresses the auto-activating caspase3 and thus leads to ablation of neurons that both express cre and project to the target region.

and refining, I only injected this virus into the VMH/PMV of *aro*^{Cre} mice. I used the Casp3 virus because it was available at the time, and injected it bilaterally into the VMH/PMV. I also injected an HSV-GFP for comparison.

When I performed the histology to see how many cells had been ablated, I found essentially no difference between the Casp3-injected animals and the GFP-injected animals. What is more, I noticed that every single animal had greatly enlarged ventricles, an indicator of inflammation. HSVs are known to cause inflammation in the brain (anecdotal evidence from multiple labs). Some studies claim that diluting the virus will reduce this inflammation, however, the virus was not effective at ablating the neurons within the MeA at the concentration I used and is unlikely to be effective at lower concentrations. For this reason and the caveat listed above, further experiments on this were not pursued.

Cre-activatiable PhiC/PRV

Because the strategy described above utilizes a virus whose expression, while limited to cre-expressing cells, is not limited to the source region, and can also be activated within the target region and other upstream regions as well, we decided to employ a more specific strategy and use a dual virus approach. For this the idea was to create a caspase virus, similar to the one described in chapters 4 and 5, but instead of being cre-activatable, it would be PhiC-activatable. PhiC and ATTP/B is similar to Cre-lox, wherein an integrase (PhiC) recognises and recombines two specific genetic sequence (ATTP/B). This strategy has been used to great effect in fish and flies previously (Gao et al., 2008; Lister, 2011; Lu et al., 2011; Ou and Lei, 2013). I replaced the loxP sites in our AAV-flex-Casp3-T2A-TEVp virus with ATTB and ATTP sites (flATTed) using standard cloning techniques. The other virus was to be provided by our collaborator, who would make a Cre-activatable PhiC with a PRV backbone. This virus would be injected into the downstream targets of the MeA (BNST or VMH/PMV) and travel retrogradely (Figure 6.8). Plasmids of this virus

were sent to us for testing, which I did using HEK293T cells. I transiently transfected both the plasmids, as well as a Cre-GFP into these cells. However, unlike the original Caspase virus which yielded markedly decreased cell numbers within days of transfection, I saw no significant decrease in cell number. As a positive control, I also transfected another well with the Cre-GFP, the Cre-activatable PhiC and a flATTed mCherry plasmid. I did see a few mCherry positive cells, but not sufficient number to continue with those experiments (data not shown). One possible explanation for the low expression rate of mCherry and caspase is that PhiC functions best at room temperature, and thus its popularity in flies, while Cre functions most efficiently at 37C, thus its popularity in mammalian systems. In addition this strategy uses a PRV which is toxic to cells, as previously mentioned, and not as efficient. For these reasons, this strategy was not pursued further.

Split-Casp3

Yet another refinement of the dual virus approach is to split the caspase virus itself. There are two parts to it: the modified caspase and the cleavage enzyme (TEVp). My next attempt to target the MeApd in a projection-specific manner was to keep the caspase in a Cre-activatable AAV, and place the TEVp into a retrograde virus (HSV). In this way, the cre-dependent caspase could be injected into the MeA and the protease could be injected into the downstream target. In addition, we (Taehong Yang) added an mCherry to the caspase virus and a GFP to the TEVp such that I would be able to visualize the extent of the viral infection. It was not possible to add a fluorophore to the original caspase virus because AAVs are quite small and only able to accept 4-5kb of additional genetic material, and there was no space for a GFP or mCherry.

Taehong tested these plasmids successfully in cell culture and I agreed to the viruses in vivo. Despite earlier experiments in which HSV-GFP and HSV-Casp3 showed poor expression in the MeApd when injected into the VMH/PMV (Figure 6.6), this HSV was

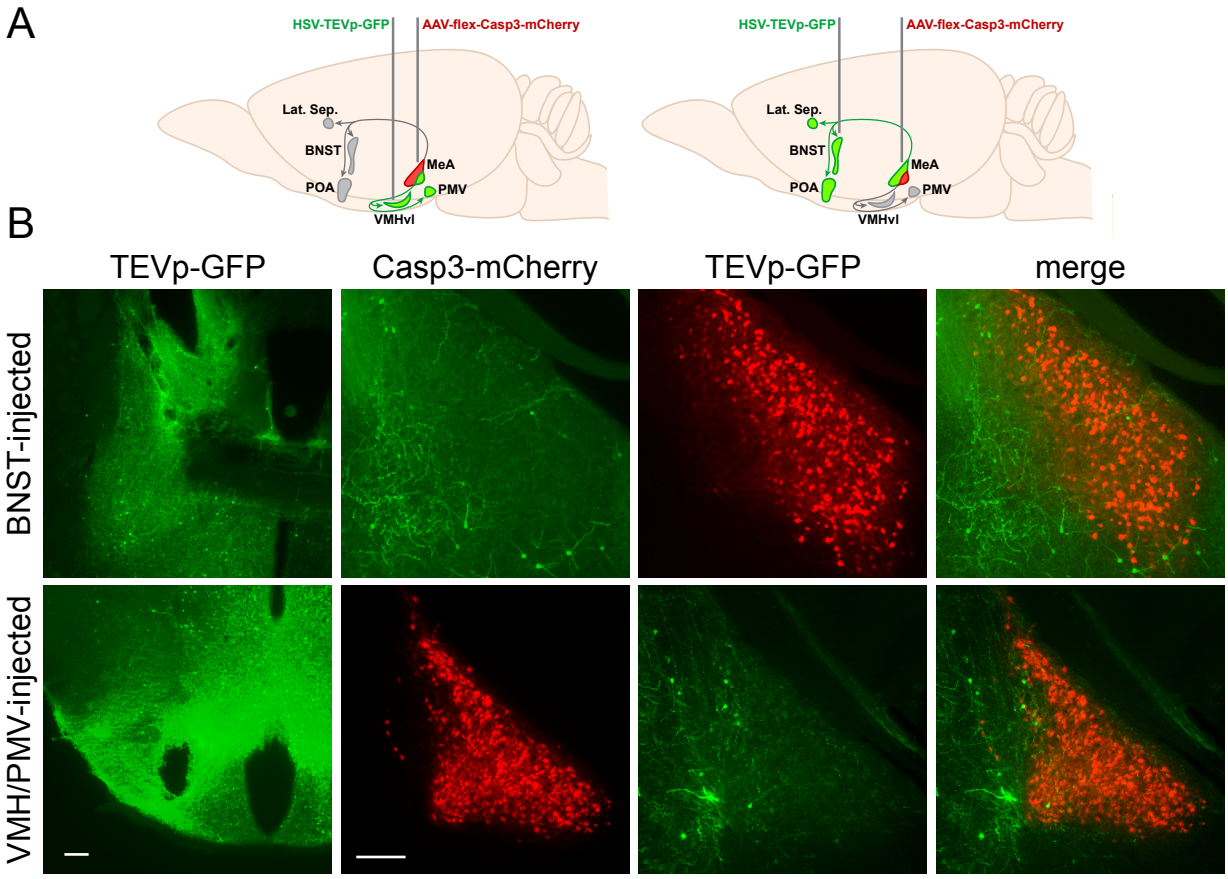

Figure 6.9: Projection-specific ablation of aro+ MeA neurons using a split caspase3

A) Strategy to selectively ablate only BNST or VMH/PMV-projecting aro+ MeA neurons. An HSV containing a TEV protease is injected into the downstream target region, while an AAV containing a Cre-dependent modified caspase3 is injected into the MeA. The HSV will travel retrogradely to the MeA to activate the modified caspase3 that is expressed in aro+ MeA neurons projecting to the target region. B) HSV-TEVp-GFP was injected into either the BNST or the VMH/PMV of adult male mice, and at the same time a Cre-dependent AAV-flex-Casp3-mCherry was injected into the MeA per the strategy in A. n = 5, 4. Scale bar = 200 μm.

of higher titer and more likely to be successful. I injected the AAV-flex-Casp3-mCherry bilaterally into the MeA of 9 males and at the same time the HSV-TEVp-GFP into the BNST of 5 and into the VMH/PMV of 4 of them. All were allowed to recover for 3 weeks, then singly housed and tested for in behavior assays of mating and aggression before histological analysis. One mouse died during behavior testing, and all mice displayed greatly enlarged ventricles, typical of HSV infection and indicative of an inflammatory response. Thus HSV is unlikely to be a feasible choice for further behavioral studies.

Nonetheless, I analyzed the brains for GFP and mCherry expression as well as loss of *aro+* MeA neurons. While there was substantial mCherry and substaintial GFP expression, the GFP expression was not localized to the MeA. Either retrograde transport to the MeA is poor, or the projection themselves are less robust than the CTB experiment would suggest. In addition, because the two regions are anatomically distinct, but still somewhat overlapping, it will be difficult to obtain truly accurate counts. However, a large proportion of laterally localized MeApd neurons project to the BNST and I did not see substantial cell loss in BNST-injected animals, and I see a strong lateral portion in VMH/PMV-injected animals. Given the low success rate and the number of caveats associated with HSVs I chose not to pursue this strategy further, although it may be refined and utilized by other lab members.

Despite several attempts to target these *aro+* MeApd neurons in a projection-specific manner I was not able to do so. Other labs have successfully performed similar studies (Stackniak et al., 2014), and so as these techniques and new ones become more prevalent and refined it may be possible to revisit these important questions. Nearly all brain regions currently being studied are proving to be much more complex than previously thought. Understanding differences in projection targets will undoubtedly prove to be essential to understanding the function of different circuits within the brain. Presumably each connection exists to serve a purpose that is unique, and deciphering how each contributes to the final output will allow us to create a unified picture of the brain and all of its diverse functions. Hopefully future advances in technology and insight will provide the opportunity to address these questions.

DISCUSSION

A possible function for the two different MeA subregions

Despite my inability to complete this study, the successful experiments nonetheless

provide insight into the circuitry. Clearly there are two different processes happening in the MeApd. There are at least two somewhat anatomically distinct subregions, one of which projects to the BNST/POA/Lat. Sep., and the other of which projects to the VMHvl/PMV. Based on our data and the data from other labs, it is possible to speculate as to the function of these two subregions. An obvious assumption is that they are both involved in social behaviors. This is highly likely given that the region as a whole is necessary for social behaviors, particularly aggression, and potentially even the olfactory discrimination of males and females. Because of the limited nature of the PRV tracing, I cannot say which of the two subregions, (or both) receives direct input from the olfactory bulb. However, I would guess that if it is only one, it would be the medial, BNST-projecting population. The BNST also receives direct olfactory input (observed in CTB injected animals - data not shown). Massive fiber tracts form reciprocal connections between the BNST and the MeA, thus it is possible that these brain regions and connections are calculating the likelihood that a conspecific is male or female. If this is true and the MeA is responsible for deciding if a conspecific is male or not, while the BNST is responsible for deciding if a

Choi et al showed that varying levels of stimulation using channelrhodopsin in ERα neurons in the VMH causes either mating (low) or aggression (high). Data acquired by Taehong shows that low doses of CNO in animals where DREADD-Gq is expressed in PR neurons in the VMH also show mating towards females, whereas higher doses cause indiscriminate aggression. However, at middle doses, males will mate with females and then immediately after ejaculation, they will begin attacking the female. These results point to a very specific possible function for the VMH-projecting population of the MeA.

Because the MeA is primarily inhibitory (see chapter 5), and it is the lateral VMH-projecting region that is activated immediately upon ejaculation, it is possible that the role of these neurons is to inhibit the VMH after ejaculation. The Lin lab showed that the VMH is activated during both mating and aggression, although the anatomy and extent

of the activation was different between the two (Falkner et al., 2014; Lin et al., 2011). It is possible that mating behavior causes activation of the VMH, which must then be shut down after ejaculation to prevent attack behavior towards the female who may now be carrying the male's offspring. This, however, is not consistent with my complete lack of a mating phenotype in chapter 5. An explanation that is congruent with these results is that there is a redundant circuit originating in the BNST which serves the same purpose. Indeed, the BNST is also primarily inhibitory and also shows a similar patch of neurons that are strongly activated immediately upon ejaculation (data not shown). The BNST also projects to the VMHvl (Scott Juntti data not shown). It is possible that preventing the attack of females is so important as to warrant such strong redundancy and that merely eliminating the MeA is not sufficient to uncover the behavior. To test this, one would need to eliminate both the MeA and the BNST simultaneously and subject the animal to a mating assay, or simply eliminate or silence the connections between the VMHvl and the MeA and BNST. If this is true, this should produce the same abberrant attack behavior seen in mice where PR neurons in the VMHvl are somewhat activated, which would indicate that after ejaculation inhibition from both the MeA and BNST act to silence neurons in that would otherwise cause aggression. It would further suggest that these neurons must not be acting during aggression. This raises further questions regarding how they themselves are regulated.

The MeA to AOB projection

During my tracing experiments, I noticed one very striking projection: that from the MeA to the AOB. The projection from the AOB to the MeA has been known, but here I show that there is top-down control of olfactory input onto the MeA. It is possible that this connection is merely to acknowledge the reciept of olfactory input, or it could be playing a more active role. Based on previous speculations that the MeA is responsible for identifying males from non-males, it is possible that this connection is causing AOB neurons to be

acutely sensitive to male or female pheromones, the same way that a bird that eats red berries would be extra sensitive to red objects when it is hungry. For example, in females, the onset of estrus could result in females seeking out males and needing to be more sensitive to their scent. Or conversely dominant males may need to find female pheromones particularly salient, while submissive males less so. Or it may be what causes males to ignore their own scent and that of their colony mates, with whom they have already established dominance hierarchies, and be extra sensitive to newcomers (Kual et al., 2014). The actual function of this connection is particularly interesting and I hope it will be the subject of study once the tools become available.

Male-female differences

The behaviors may be different, the sexes may be different, the cell numbers and expression levels and projection patterns may be different, but the effect on behavior is the same. This suggests that MeApd neurons act to relay the same relevant information to different downstream regions or pathways. This makes sense because it is considered to be fairly upstream and receives direct olfactory input. I would conjecture that the MeApd is processing pheromonal information to inform downstream regions as to the sex of the conspecific being investigated.

However, a few of the projections did appear to be sexually dimorphic, particularly that of the AVPV, which is located near the POA, and forms a thin stripe along the walls of the third ventricle. Not much is known abou the AVPV, except that it expresses kisspeptin, and is linked to ovulation in females (Clarkson et al., 2010; Dungan et al., 2006; Williams et al., 2010). However males, who obviously do not ovulate and thus require no brain regions to support this event, continue to develop this brain region, thus it must be serving a different purpose. Yang et al. (2013) showed that this region is strongly innervated by PR neurons in the VMHvl, but only in females. Males showed only a scattering of

fibers from the VMHvl. In contrast, strong innervation of the region by *aro*+ MeA neurons can be seen in males, while only a scattering of fibers can be seen in females (Figure 6.2). The function of this connection is currently a mystery, including whether it regulates reproductive behaviors, aggressive behaviors, or something else entirely, but it will be fascinating to find out.

METHODS

Animals

Adult mice 10–24 weeks of age were used in all studies, except for the neonatal *in situ* hybridization. Mice were housed in a UCSF barrier facility with a 12:12 hr light:dark cycle, and food and water were available *ad libitum*. $Aro^{Cre/IPIN}$ mice and their control $aro^{+/IPIN}$ same-sex siblings were used for behavioral studies. Animals were group-housed by sex after weaning at 3 weeks of age. All studies with animals were done in accordance with UCSF IACUC protocols.

Stereotaxic surgery

Stereotaxic surgery was performed as described previously (Morgan et al., 2014). Briefly, a mouse was placed in a stereotaxic frame (Kopf Instruments) under anesthesia (0.5-2% isofluorane), the skull was exposed with a midline scalp incision, and the stereotaxic frame was aligned at bregma using visual landmarks. The drill (drill bit #85; ~279 μm diameter) on the stereotaxic frame was placed over the skull at coordinates corresponding to the MeA (rostrocaudal, −1.6 mm; mediolateral, ± 2.2 mm), and a hole was drilled through the skull bone to expose the brain. A 33 gauge steel needle connected via PE20 tubing to a Hamilton syringe was loaded with virus, aligned at bregma (including in the z-axis) and slowly lowered to a depth of 5.15 mm. Virus was delivered bilaterally at 100 nL/min with a Hamilton syringe using a micropump (Harvard Apparatus). The needle was left in place for an additional 5 min to allow diffusion of the virus and then was slowly withdrawn. If a

cannula was to be implanted it was done so at this time. A larger hole was drilled in the skull for a custom 5.7 mm guide cannula (26G, PlasticsOne). The cannula was lowered into place slowly and secured using dental cement (Stoelting). The wound was then closed using vetbond (3M). Mice were weighed and allowed to recover on a heating pad before being returned to their home cage.

Histology

Animals were perfused with 4% paraformaldehyde as described previously (Yang et al., 2013), and sections were collected at a thickness of 65 μm for immunolabeling or 100 μm for *in situ* hybridization using a vibrating microtome (Leica). Immunolabeling was performed using previously published protocols (Wu et al., 2009). The primary antisera used are: chicken anti-β-gal (Abcam, 1:6,000), sheep anti-GFP (Invitrogen, 1:2,000), rabbit anti-c-Fos (Millipore, 1:10,000), rabbit anti-Arc (gift from Arnold Kriegstein), rat anti-dsRed (Clontech, 1:2,000), and alkaline phosphatase-conjugated sheep anti-digoxygenin (Roche, 1:5,000). The fluorophore conjugated secondary antisera are: Cy3 donkey anti-rabbit, Cy3 donkey anti-rat, Cy3 donkey anti-chicken (Jackson ImmunoResearch, 1:800), AlexaFluor 647 donkey anti-chicken (Jackson ImmunoResearch, 1:500), and AlexaFluor 488 donkey anti-rabbit, AlexaFluor 488 donkey anti-chicken (Invitrogen, 1:300).

Sections were imaged using a confocal microscope (Zeiss). To estimate cell loss following caspase-3 mediated ablation, images were obtained from every section spanning the MeApd, using a 20X objective to collect z-stacks with a 2 μm step. These images were processed in Fiji software prior to enumeration. I improved signal:noise by subtracting any auto-fluorescence from the imaging channel as necessary and applying a Gaussian blur protocol. I subsequently used the plug-in Image-based Tool for Counting Nuclei (Byun et al., 2006). In initial studies, these automated count estimates were validated with manual counts of cell number in randomly chosen sections through the MeApd; I

also routinely performed manual enumeration in randomly chosen sections to validate automated estimates of cell counts for every experiment. All experimental and control animals for a given experiment were analyzed using the same set of parameters in Fiji to minimize any bias.

For dual colorimetric *in situ* hybridization and fluorescent immunolabeling, perfused wtih 4% PFA and fixed overnight, then soaked in 20% sucrose/PBS overnight before being frozen in embedding medium (M1 Embedding Matrix, Thermo Scientific) and cryosectioned at 12 µm on to glass slides (Superfrost, Fisher). Sections were fixed in 4% PFA and then acetylated as described previously (Juntti et al., 2010). After permeabilization with 1% TritonX-100, sections were incubated with prehybridization solution in a humidifying chamber for 2-4 hours at room temperature. Sections were hybridized with digoxigenin-UTP-labeled Tac1 riboprobe (0.3 µg /ml) overnight at 65°C. After washes, brain sections were incubated with sheep anti-digoxigenin conjugated to alkaline phosphatase (Roche, 1:5000) and chicken anti-β-gal (Abcam, 1:3000) in 5% heat inactivated serum from sheep and donkey overnight at 4°C. The sections were washed and stained using a colorimetric reaction with NBT/BCIP (Roche) at 37°C overnight. The reaction was stopped with PBS containing 1 mM EDTA, and the sections were washed and incubated with a secondary antibody, donkey anti-chicken Cy3 antibody (Jackson ImmunoResearch, 1:800), and DAPI for 2 hours at room temperature. After washes and a 10 min post-fix in 4% PFA, slides were coverslipped with Aquamount mounting medium (Polysciences). I imaged these sections on an upright microscope (Zeiss) using a 20X objective, switching between brightfield illumination (*Tac1*) and epifluorescence (β-gal). These images were overlaid in Adobe Photoshop and black and white brightfield images were inverted and pseudocolored. *In situ* hybridization of neonatal brains was performed in the same way, except without the additional immunolabeling steps.

Drugs

CNO dissolved in aCSF (3 μM in 100 μl aCSF + 200 μl fluorogold) was injected using a custom 5.9 mm internal cannula (PlasticsOne), according to published protocols (Stachniak et al., 2014). This mixture was infused at a rate of 100 μl/min using the setup described above, and then the needle was left in place for 5 min to allow for diffusion away from the injection site. Mice were allowed to move freely within a limited area during this time.

Data Analysis

Behavioral and histological studies were performed and analyzed by an experimenter blinded to the genotype and to other experimental manipulations (such as CNO versus saline treatment in DREADD studies). For analysis of non-categorical parameters of mating and aggression I only included data from the animals that performed the behavior. In instances where an animal was tested more than once in the same assay (male and female mating, intermale and maternal aggression, and pup retrieval subsequent to caspase-3 mediated ablation) the behavioral performance for each animal was averaged prior to further analysis across animals.

REFERENCES

Antinone, S.E., and Smith, G.A. (2010). Retrograde axon transport of herpes simplex virus and pseudorabies virus: a live-cell comparative analysis. J. Virol. 84, 1504–1512.

Bergan, J.F., Ben-Shaul, Y., and Dulac, C. (2014). Sex-specific processing of social cues in the medial amygdala. eLife 3.

Berndt, A., Lee, S.Y., Ramakrishnan, C., and Deisseroth, K. (2014). Structure-Guided Transformation of Channelrhodopsin into a Light-Activated Chloride Channel. Science 344, 420–424.

Byun, J., Verardo, M.R., Sumengen, B., Lewis, G.P., Manjunath, B.S., and Fisher, S.K. (2006). Automated tool for the detection of cell nuclei in digital microscopic images: application to retinal images. Mol. Vis. 12, 949–960.

Callaway, E.M. (2008). Transneuronal circuit tracing with neurotropic viruses. Curr. Opin. Neurobiol. 18, 617–623.

Canteras, N.S., Simerly, R.B., and Swanson, L.W. (1992). Connections of the posterior nucleus of the amygdala. J Comp Neurol 324, 143–179.

Canteras, N.S., Simerly, R.B., and Swanson, L.W. (1995). Organization of projections from the medial nucleus of the amygdala: a PHAL study in the rat. J Comp Neurol 360, 213–245.

Card, J.P., and Enquist, L.W. (2001). Transneuronal circuit analysis with pseudorabies viruses. Curr Protoc Neurosci Chapter 1, Unit1 5.

Chow, B.Y., Han, X., Dobry, A.S., Qian, X., Chuong, A.S., Li, M., Henninger, M.A., Belfort, G.M., Lin, Y., Monahan, P.E., et al. (2010). High-performance genetically targetable optical neural silencing by light-driven proton pumps. Nature 463, 98–102.

Clarkson, J., Han, S.-K., Liu, X., Lee, K., and Herbison, A.E. (2010). Neurobiological mechanisms underlying kisspeptin activation of gonadotropin-releasing hormone

(GnRH) neurons at puberty. Molecular and Cellular Endocrinology 324, 45–50.

Diefenbach, R.J., Miranda-Saksena, M., Douglas, M.W., and Cunningham, A.L. (2008). Transport and egress of herpes simplex virus in neurons. Rev. Med. Virol. 18, 35–51.

Dragunow, M., and Faull, R. (1989). The use of c-fos as a metabolic marker in neuronal pathway tracing. Journal of Neuroscience Methods 29, 261–265.

Dungan, H.M., Clifton, D.K., and Steiner, R.A. (2006). Minireview: Kisspeptin Neurons as Central Processors in the Regulation of Gonadotropin-Releasing Hormone Secretion. Endocrinology 147, 1154–1158.

Dupont, S., Krust, A., Gansmuller, A., Dierich, A., Chambon, P., and Mark, M. (2000). Effect of single and compound knockouts of estrogen receptors alpha (ERalpha) and beta (ERbeta) on mouse reproductive phenotypes. Development 127, 4277–4291.

Ericson, H., and Blomqvist, A. (1988). Tracing of neuronal connections with cholera toxin subunit B: light and electron microscopic immunohistochemistry using monoclonal antibodies. Journal of Neuroscience Methods 24, 225–235.

Falkner, A.L., Dollar, P., Perona, P., Anderson, D.J., and Lin, D. (2014). Decoding Ventromedial Hypothalamic Neural Activity during Male Mouse Aggression. J. Neurosci. 34, 5971–5984.

Frampton, A.R., Goins, W.F., Nakano, K., Burton, E.A., and Glorioso, J.C. (2005). HSV trafficking and development of gene therapy vectors with applications in the nervous system. Gene Ther. 12, 891–901.

Gao, G., McMahon, C., Chen, J., and Rong, Y.S. (2008). A powerful method combining homologous recombination and site-specific recombination for targeted mutagenesis in Drosophila. Proc. Natl. Acad. Sci. U.S.A. 105, 13999–14004.

Gradinaru, V., Thompson, K.R., and Deisseroth, K. (2008). eNpHR: a Natronomonas halorhodopsin enhanced for optogenetic applications. Brain Cell Biol 36, 129–

139.

Guzowski, J.F., McNaughton, B.L., Barnes, C.A., and Worley, P.F. (1999). Environment-specific expression of the immediate-early gene Arc in hippocampal neuronal ensembles. Nat Neurosci 2, 1120–1124.

Han, X., Chow, B.Y., Zhou, H., Klapoetke, N.C., Chuong, A., Rajimehr, R., Yang, A., Baratta, M.V., Winkle, J., Desimone, R., et al. (2011). A high-light sensitivity optical neural silencer: development and application to optogenetic control of non-human primate cortex. Front. Syst. Neurosci. 5, 18.

Hong, W., Kim, D.-W., and Anderson, D.J. (2014). Antagonistic control of social versus repetitive self-grooming behaviors by separable amygdala neuronal subsets. Cell 158, 1348–1361.

Kaur, A.W., Ackels, T., Kuo, T.-H., Cichy, A., Dey, S., Hays, C., Kateri, M., Logan, D.W., Marton, T.F., Spehr, M., et al. (2014). Murine Pheromone Proteins Constitute a Context-Dependent Combinatorial Code Governing Multiple Social Behaviors. Cell 157, 676–688.

Lee, H., Kim, D.-W., Remedios, R., Anthony, T.E., Chang, A., Madisen, L., Zeng, H., and Anderson, D.J. (2014). Scalable control of mounting and attack by Esr1+ neurons in the ventromedial hypothalamus. Nature 509, 627–632.

Lein, E.S., Hawrylycz, M.J., Ao, N., Ayres, M., Bensinger, A., Bernard, A., Boe, A.F., Boguski, M.S., Brockway, K.S., Byrnes, E.J., et al. (2007). Genome-wide atlas of gene expression in the adult mouse brain. Nature 445, 168–176.

Lin, D., Boyle, M.P., Dollar, P., Lee, H., Lein, E.S., Perona, P., and Anderson, D.J. (2011). Functional identification of an aggression locus in the mouse hypothalamus. Nature 470, 221–226.

Lister, J.A. (2011). Use of phage φC31 integrase as a tool for zebrafish genome manipulation. Methods Cell Biol. 104, 195–208.

Lu, J., Maddison, L.A., and Chen, W. (2011). PhiC31 integrase induces efficient site-

specific excision in zebrafish. Transgenic Res. 20, 183–189.

Luo, L., Callaway, E.M., and Svoboda, K. (2008). Genetic dissection of neural circuits. Neuron 57, 634–660.

Morgan, C.W., Julien, O., Unger, E.K., Shah, N.M., and Wells, J.A. (2014). Chapter Eight - Turning ON Caspases with Genetics and Small Molecules. In Methods in Enzymology, J.Y. and J.A.W. Avi Ashkenazi, ed. (Academic Press), pp. 179–213.

Nagel, G., Szellas, T., Huhn, W., Kateriya, S., Adeishvili, N., Berthold, P., Ollig, D., Hegemann, P., and Bamberg, E. (2003). Channelrhodopsin-2, a directly light-gated cation-selective membrane channel. PNAS 100, 13940–13945.

Osakada, F., and Callaway, E.M. (2013). Design and generation of recombinant rabies virus vectors. Nat Protoc 8, 1583–1601.

Osakada, F., Mori, T., Cetin, A.H., Marshel, J.H., Virgen, B., and Callaway, E.M. (2011). New rabies virus variants for monitoring and manipulating activity and gene expression in defined neural circuits. Neuron 71, 617–631.

Ou, H., and Lei, T. (2013). A novel strategy for conditional gene knockout based on ΦC31 integrase and Gal4/UAS system in Drosophila. IUBMB Life 65, 144–148.

Sohal, V.S., Zhang, F., Yizhar, O., and Deisseroth, K. (2009). Parvalbumin neurons and gamma rhythms enhance cortical circuit performance. Nature 459, 698–702.

Stachniak, T.J., Ghosh, A., and Sternson, S.M. (2014). Chemogenetic Synaptic Silencing of Neural Circuits Localizes a Hypothalamus→Midbrain Pathway for Feeding Behavior. Neuron 82, 797–808.

Sternson, S.M., and Roth, B.L. (2014). Chemogenetic Tools to Interrogate Brain Functions. Annual Review of Neuroscience 37, 387–407.

Swanson, L.W. (2003). The amygdala and its place in the cerebral hemisphere. Ann N Y Acad Sci 985, 174–184.

Unger, E.K., Burke Jr., K.J., Yang, C.F., Bender, K.J., Fuller, P.M., and Shah, N.M. (2015). Medial Amygdalar Aromatase Neurons Regulate Aggression in Both

Sexes. Cell Reports 10, 453–462.

Veening, J.G., and Coolen, L.M. (1998). Neural activation following sexual behavior in the male and female rat brain. Behav Brain Res 92, 181–193.

Veening, J.G., Coolen, L.M., de Jong, T.R., Joosten, H.W., de Boer, S.F., Koolhaas, J.M., and Olivier, B. (2005). Do similar neural systems subserve aggressive and sexual behaviour in male rats? Insights from c-Fos and pharmacological studies. Eur J Pharmacol 526, 226–239.

Wall, N.R., Wickersham, I.R., Cetin, A., Parra, M.D.L., and Callaway, E.M. (2010). Monosynaptic circuit tracing in vivo through Cre-dependent targeting and complementation of modified rabies virus. PNAS 107, 21848–21853.

Wickersham, I.R., Lyon, D.C., Barnard, R.J.O., Mori, T., Finke, S., Conzelmann, K.-K., Young, J.A.T., and Callaway, E.M. (2007). Monosynaptic Restriction of Transsynaptic Tracing from Single, Genetically Targeted Neurons. Neuron 53, 639–647.

Wietek, J., Wiegert, J.S., Adeishvili, N., Schneider, F., Watanabe, H., Tsunoda, S.P., Vogt, A., Elstner, M., Oertner, T.G., and Hegemann, P. (2014). Conversion of Channelrhodopsin into a Light-Gated Chloride Channel. Science 344, 409–412.

Williams, W.P., Jarjisian, S.G., Mikkelsen, J.D., and Kriegsfeld, L.J. (2010). Circadian Control of Kisspeptin and a Gated GnRH Response Mediate the Preovulatory Luteinizing Hormone Surge. Endocrinology 152, 595–606.

Wu, M.V., Manoli, D.S., Fraser, E.J., Coats, J.K., Tollkuhn, J., Honda, S.-I., Harada, N., and Shah, N.M. (2009). Estrogen masculinizes neural pathways and sex-specific behaviors. Cell 139, 61–72.

Yang, C.F., Chiang, M.C., Gray, D.C., Prabhakaran, M., Alvarado, M., Juntti, S.A., Unger, E.K., Wells, J.A., and Shah, N.M. (2013). Sexually dimorphic neurons in the ventromedial hypothalamus govern mating in both sexes and aggression in males. Cell 153, 896–909.

Zhang, F., Wang, L.-P., Brauner, M., Liewald, J.F., Kay, K., Watzke, N., Wood, P.G., Bamberg, E., Nagel, G., Gottschalk, A., et al. (2007). Multimodal fast optical interrogation of neural circuitry. Nature 446, 633–639.

Chapter 7

Conclusions

Summary

It was previously known that estrogen and therefore aromatase is responsible for establishing male-specific patterning and wiring in the male brain during development. I have refined this understanding, showing that aromatase is produced and acts within the brain during this time. In addition I have explored the consequences of development in the absence of any sex hormones, and found that the default state of the brain is in fact female. The presence or absence of aromatase during the critical period is the single deciding factor in the development of a masculinized or a feminized brain.

The role of aromatase in adulthood, however, is far less prominent. Current understanding in the field emphasizes the importance of estrogen in mediating male behaviors, yet I find that in males lacking aromatase or ERa after the critical period are behaviorally indistinguishable from their control littermates. Even females lacking aromatase in their entire nervous system show no reproductive deficits at all. Wu et al. showed that estrogen is essential during development, while Juntti et al. showed that testosterone is responsible for modulating the intensity of male behaviors. Perhaps these two ideas form more or less the whole picture. There is likely to be more subtle modulation by estrogen, to biologically justify its continued production, but the estrogen is clearly not as influential as previously believed.

While estrogen itself may not be doing much in adulthood, I did show that the neurons that express aromatase are functional within circuits that control male- and female-specific behaviors. In the medial amygdala (MeA) ablation or inhibition of aromatase+ neurons leads to a subtle but significant decrease in aggressive behaviors, both in males, and in females. The fact that this effect is present in females further underlines the decreased importance of aromatase function in these neurons, given that testosterone is undetectable in the bloodstream and ovary-derived estrogen is already high. Nonetheless, aromatase expression marks neurons that function within a circuit to produce aggressive behaviors.

I further find that the MeA is comprised of two separate subregions, although I was not able to parse their individual functions.

Thus aromatase is responsible for establishing male or female-specific patterning of the brain during development and then aromatase+ neurons are responsible for executing the appropriate sex-specific behaviors in adulthood.

A discussion of gender

Genetic sex is a reasonably simple concept. In mammals sex is determined by the composition of sex chromosomes, with some variations involving aberrant numbers of sex chromosomes, and the presence or absence of the gene Sry. The idea of gender, on the other hand, is complicated and nuanced. Many believe that gender is a social construct, for which there is a continuous spectrum. While it is true that the spectrum is continuous, there is clearly also a genetic and hormonal basis for gender. Gender is a mental state, but I have shown that genetics and hormones play an important role in establishing that state. It is also not hard to see how it would be possible for small differences in hormone titer or ratio, or even hormone receptor sensitivity, could lead to larger effects that manifest as natural variation within a population. By basing gender on the presence or abscence of a single hormone, it is surprising that evolution has produced so many successful species.

The evolutionary costs and benefits and aggression

Obviously one of the major goals of life is to reproduce and ensure the continued survival of your genetic material, albeit in a slightly altered form. One method for proving the worthiness of your genetic material is merely to stay alive (survival of the fittest). However reproduction is expensive, so for many species, especially (though not limited to), mammals and birds, simply managing to live to reproductive maturity is not sufficient to ensure reproductive success. For many species sexual selection plays a large role in determining

the next generation. For some, this means elaborate courtship displays, for others, fierce competitions for dominance between members of the same sex. These displays are costly, either spending countless hours perfecting a song or carrying cumbersome or flashy physical attributes that may attract a predator or encumber movement, or by engaging in risky and potentially fatal aggressive acts. A species that routinely pits its most fit members against one another in violent displays is not one that overall has the best chance of success. This strategy is only successful for species whose lifespan includes only one chance at mating. Otherwise, the animals who may be genetically most fit, may become injured or die, or subject to predation, and not get another chance to pass on their genes. In addition, competition is not solely amongst same-sex members of their own species; there is also competition for food, territory and other resources between species. Removing or handicapping the most fit members of a species will overall hinder the success of that species.

However, aggression does have its place. Both intra- and interspecies disputes over territory and food sometimes must be resolved with aggressive displays, as well as protection of young from predators, not to mention predation itself, which is often violent. Clearly the aggression circuit remains intact in nearly all animal species despite its high cost, indicating that it continues to serve a vital evolutionary purpose.

But is this still true? Perhaps the latest evolutionary trends suggest a shift towards non-violent communities. Many bird species now choose their mates based on elaborate songs or the best-built nest. Some non-human primates choose their mates based on how often they share their food or groom one another. Even some spiders, who are vicious predators themselves and cannibalistic as well, opt for a courtship dance instead. 65 million years ago, those who dominated the Earth were large and muscular, with powerful jaws and sharp teeth and claws. Now however, the top predators are smaller (primarily due to the changing climate) and smarter, and work together to hunt their prey. Lions, wolves, killer

whales, all hunt in coordinated packs. They also live in communities, and while they are definitely aggressive towards members of their own species, evolutionary trends appear to be favoring intellect over musculature.

Aggression in human society

While aggression may have served its purpose in getting us to where we are now, it surely has no place in modern human society. The success of our species in recent times can be attributed to cooperation rather than the fitness of any one individual. No individual could ever have achieved what we, as a community, as a species, have achieved together. Cooperation is undoubtedly the key to our success, and aggression, in all of its forms, undermines that success. While it may result in short term gains for an individual, those gains are ephemeral at best, and come at the cost of much greater gains for the whole community.

And yet we still have the circuit for aggression, with no real outlet for it. Instead we turn to sports, such as boxing and American football and hunting, and sometimes it explodes out in the form of road rage, gang violence, domestic abuse, and war. And not all forms of aggression are physical. Any sport or action that is designed to causes harm to another individual is a detriment to society. In evolutionary terms, I predict that these traits will not continue to exist. The success of our species depends on it.

Final remarks

Throughout my thesis I have followed aromatase through development, into adulthood, and finally to what the neurons themselves may be doing during sex-specific behaviors. Rather than adhering to a single idea, I have allowed the results of the previous experiment to direct the hypothesis of the next, and in so doing, have been taken on a far more interesting journey than I could have imagined. It is my sincerest hope that we can all

continue this model of true scientific curiosity and inquiry, because it is the surest path to groundbreaking insight and practical understand.

Publishing Agreement

It is the policy of the University to encourage the distribution of all theses, dissertations, and manuscripts. Copies of all UCSF theses, dissertations, and manuscripts will be routed to the library via the Graduate Division. The library will make all theses, dissertations, and manuscripts accessible to the public and will preserve these to the best of their abilities, in perpetuity.

Please sign the following statement:

I hereby grant permission to the Graduate Division of the University of California, San Francisco to release copies of my thesis, dissertation, or manuscript to the Campus Library to provide access and preservation, in whole or in part, in perpetuity.

Elizabeth Unger

Author Signature

3/30/2015

Date